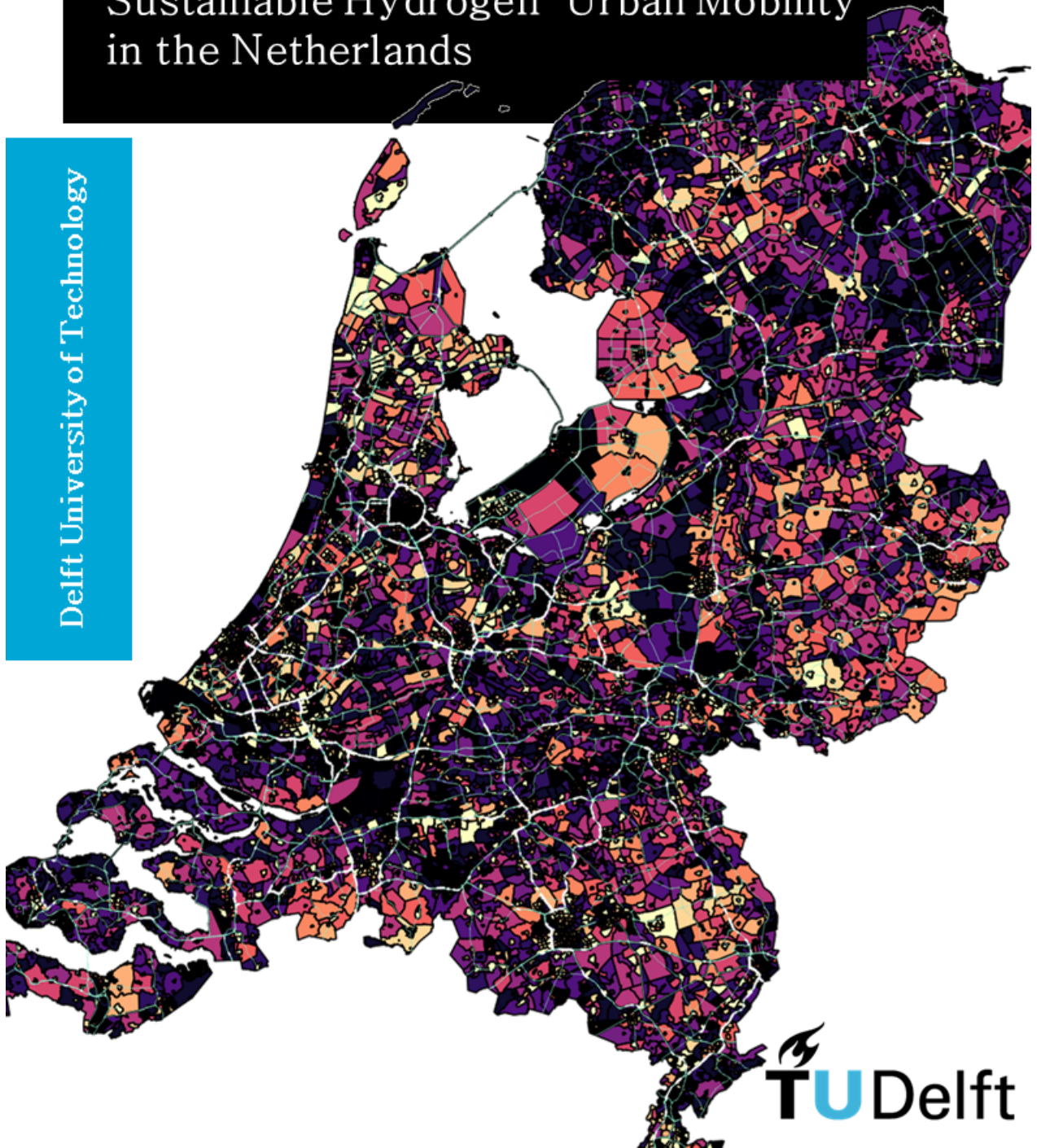


Energy Wall with Hydrogen Refueling Stations for Fuel Cell Scooters

An approach to Decentralized Sustainable Hydrogen Urban Mobility in the Netherlands

Delft University of Technology



ENERGY WALL WITH HYDROGEN REFUELING STATIONS FOR FUEL CELL SCOOTERS

AN APPROACH TO DECENTRALIZED SUSTAINABLE
HYDROGEN MOBILITY IN THE NETHERLANDS

by

Anna Petrakos

in partial fulfillment of the requirements for the degree of

Master of Science

in

Sustainable Energy Technology

at the Delft University of Technology,

to be defended publicly on Monday June 29, 2020 at 1:00 PM.

Supervisor: Prof. dr. Ad van Wijk
Daily Supervisor: Ir. Nikolaos Antsos-Chrysochoidis
Thesis committee: Prof. dr. ir. Zofia Lukszo
Dr. Linda Kamp

An electronic version of this thesis is available at <http://repository.tudelft.nl/>.



ABSTRACT

This project investigates the feasibility of hydrogen refueling stations using photovoltaic systems for fuel cell scooters.

The aim was to identify the solar electricity generation potential of noise barriers in the Netherlands and the connection between this and future theoretical hydrogen demand for fuel cell powered two wheelers (scooters or mopeds). Noise barriers block noise from inhabited areas, which is also where mopeds and their owners reside. Noise barriers retrofitted with solar panels, or Energy Walls, coupled with a hydrogen production, storage and dispensing system is proposed. This system would enhance sustainable, carbon neutral mobility as well as contribute renewable energy to the grid electricity mix. Particulate matter, greenhouse gases and noise pollution are reduced with electric drive vehicles such as fuel cell powered two wheelers.

A case study of a noise barrier on the A20 in Rotterdam Noord was modeled; other suitable locations were identified as well, such as Amsterdam or Delft. The characteristics of the barrier in Rotterdam provided a lower levelized cost of PV electricity and was thus chosen to simulate specifically. A range of electrolyzer capacities was also simulated to understand the effect of the electrolyzer capacity and the final cost of hydrogen to the user.

The demand base case was 100 scooters which traveled 2.5 km/day each on average. Provided a single metal hydride canister has a range of 25 km and capacity of 45 g_{H₂}, this demand configuration means 0.45 kg_{H₂}/day needs to be produced for the users. An hourly simulation of the energy production was modeled using two control strategies, which focused on maximizing the Energy Wall input and the use of the electrolyzer respectively. The second strategy had higher electricity costs as compared to the first, however the cost of the electrolyzer was minimal regardless of the number of panels.

The cost of hydrogen depends on the size of the Energy Wall and the electrolyzer capacity; for the lowest cost setup the price of hydrogen ranged between 14.3 and 7.2 €/kg_{H₂}. The cost per kilometer traveled by fuel cell scooters was found to be between 2.57 and 1.4 ¢/km. Battery electric vehicles are still much cheaper to operate in this aspect, driving at a cost mileage of between 0.3 and 0.6 ¢/km, however gas powered scooters had the highest cost per kilometer (3 - 5¢/km).

This model finds that the operational costs of a hydrogen fuel cell scooter are lower than its gas scooter counterpart, but not low enough to compete with battery powered scooters. The one advantage of gas scooters is the range on one refuel, however with their relatively high operational costs and emissions, electric drive engines become favorable. Battery electric have a good cost efficiency. Fuel cell scooters are quickly recharged with canisters, and are mid-cost range to operate compared to the other two technologies.

ACKNOWLEDGMENTS

So this journey ends. Its been a long and fruitful time. To those who were kind, those who were present, those who were there for some of it, and those who were there for all of it. To those who were. Thank you.

To the academics, Ad for your patience and guidance, Nikos for the discussions and support, and the lecturers who engaged in making lessons and transmitting their knowledge in a supportive, clear, and thoughtful manner.

To the positive minded and good vibed, for sharing the attitude. To the friends and chosen family, the Greek ghetto, the snowtrippers, the snowcallers, delftenaars, tershcellingers, mijn nederlandse vrienden, and the determined SETies of all ages.

To the beboppers, for the good times.

To the initiatives & movements, Conscious Kitchen, Foodsharing, Tinyhouse communities, XR, thank you for your work. I'm with you.

To the musicians, Jams with Benefits, the buskers, the bebop live sessions, OL24A. Thank you for the sessions that turned nothing into something, that allowed for a creative outlet that helped in so many ways.

To the (acro) yogi community, for the everlasting and continuous learning experiences of our balance, movements, connections, and communication.

To the Oostpleiners, for growing with me through the years of fun, banter, BBQs and late night kitchen sessions. Through all the good times and the bad, I love you guys.

To Melissa, Barry, and soon-to-be big brother Arlo, for all the joy you've brought just through your presence.

Finally, to the brother for the endless talks into all subjects and reality checks. To the mother, for being the best listener and giver of advice, and your never-ending worrying (but I don't blame you). And to the father, for the endless bestowment of knowledge, experiences, support, and your unconditional tough loving; I appreciate it more than I might show.

And to all the rest, who made me smile in good times and through the bad.

To all of those above, for the lessons in life.

And to mother nature, for life itself.

To the future of decentralized local systems.

CONTENTS

Abstract	iii
Acknowledgments	v
List of Figures	xi
List of Tables	xiii
1 Introduction	1
1.1 Research Questions	2
1.2 Motivations	3
1.2.1 Energy in Holland: Current Situation & Future Objectives	3
1.2.2 Hydrogen Economy	5
1.3 The Energy Wall	6
1.4 Scooter Use in The Netherlands	7
1.5 Research Questions	8
1.6 Overview of Report Structure	8
2 Literature Review & Preliminary System Design	9
2.1 Renewable Energy Generation Components	9
2.1.1 PV Working Principle [1, 2]	9
2.1.2 PV System Components	10
2.1.3 Types of Solar Panels [3, 4]	10
2.2 Hydrogen Technology Components	12
2.2.1 Hydrogen Production: Electrolysis	12
2.2.2 Types of Electrolyzers	13
2.2.3 Overview of Commercially Available Electrolyzers	15
2.2.4 Storage Options	16
2.3 Water Treatment	19
2.4 Scooters (a.k.a Mopeds)	20
2.4.1 Battery Powered Electric Scooters	21
2.4.2 Hydrogen Fuel Cell Scooter Situation	21
2.4.3 Key Differences between Battery, Fuel Cell and Gas Scooters	22
3 Noise Barrier, Scooter, and Geographical Analysis	25
3.1 Scooter Distribution	26
3.1.1 Scooters in Europe	26
3.1.2 Province Level in the Netherlands	28
3.1.3 Municipal Level Distribution	30

3.2	Noise Barriers (as Energy Walls)	32
3.2.1	Noise Barrier Suitability Filters & Criteria	32
3.2.2	Material Filter	33
3.2.3	Tilt Direction Filter	34
3.2.4	Summary of Noise Barrier Filtering	35
3.3	Noise Barrier and Scooter Distributions Coupling	35
3.3.1	Top Municipalities & Scooters	36
3.3.2	Noise Barriers in Top Municipalities	36
3.3.3	Coupling	37
3.4	PV Energy Yield Estimations	37
3.4.1	Nationwide Potential	41
3.4.2	Potential of Selected Municipalities	41
3.5	Comparison of Potential to Scooter Demand	42
4	Energy Wall Fuel Cell Hydrogen Refueling Station: A Case Study	45
4.1	Scooter Demand	46
4.2	Location Choices and Characteristics	49
4.2.1	Rotterdam	49
4.2.2	Amsterdam	49
4.2.3	Delft	50
4.3	Energy Production Model & Sizing	51
4.3.1	Noise Barrier Physical Aspects & PV capacity	51
4.3.2	PV Sizing Limitations	52
4.3.3	Modular Energy Wall Segments	53
4.4	Energy & Hydrogen Production Control Strategy	53
4.4.1	CS1: Maximum use of renewable energy	54
4.4.2	CS2: Operate electrolyzer at full capacity	54
4.5	Hydrogen Production	55
4.6	Model Iterations	55
4.7	Model Findings	56
4.7.1	PV Capacity Factors	56
4.7.2	Energy Wall Utilization & Contribution	57
4.7.3	Electrolyzer Capacity Factor	59
4.7.4	Demand Satisfaction & State of Charge	60
4.7.5	Avoided emissions	61
5	Costs: Modeling & Findings	63
5.1	Methodology	64
5.2	Electricity Cost Parameters	64
5.2.1	Energy Wall	64
5.2.2	Grid	65
5.2.3	Cost of Electricity to Electrolyzer	66

5.3	Hydrogen Cost Parameters	67
5.3.1	Production: Electrolyzer Costs	68
5.3.2	Production: Electricity	68
5.3.3	Buffer Storage Costs	69
5.3.4	Levelized Cost of Hydrogen to User	69
5.4	Cost Model Findings	69
5.4.1	Levelized Cost of Electricity of four locations	69
5.4.2	Contributions to LCOH	70
5.4.3	Comparison of Cost per Kilometer Between Different Types of Scooters	77
6	Results and Conclusions	79
6.1	Geographical Feasibility of Noise Barriers as Energy Walls with Hydrogen Production for Scooters in the Netherlands	80
6.2	Design & Simulation of Energy Wall Coupled with Hydrogen Production and Storage Units	82
6.3	Economic Feasibility of an Energy Wall H ₂ Refueling System	85
6.4	Evaluation of H ₂ Refueling Station for Scooters System in the Netherlands	87
6.5	Future Work	89
	Bibliography	91
A	Windleaf specifications and working principle	99
B	Electrolyzer Overview	103
C	Water Purification Additional Content	105
D	More Maps of Municipalities	107
E	Case Study Detailed Information	115
F	Cost Literature Review Notes	119
G	Grid Connection Costs	123
H	Additional Material for Scooters	125
I	Battery Powered Electric Scooter Review	127

LIST OF FIGURES

1.1 Sources of Primary Energy Supply and Electricity Generation for the Netherlands 2018 [5]	3
2.1 Physical Appearance of Monocrystalline-Si (left) and Polycrystalline-Si (right)	11
2.2 Variation of MPP with Temperature and Irradiance	11
2.3 Working principle of electrolyzers	13
2.4 Hydrogen Storage Methods and Energy Density of Various Fuels [6]	16
2.5 Pictures of Storage Units Envisioned	18
3.1 Number of Scooters [7] and corresponding population densities in European countries	27
3.2 Graphical Representation of Total Scooters and Scooters per 1000 Residents	28
3.3 Total and per Capita distribution of scooters in the provinces of the Netherlands	29
3.4 Municipalities containing over 4,000 scooters in the Netherlands	31
3.5 Roads and Noise Barrier Entities in the Netherlands	33
3.6 Barrier tilt & position characteristics	35
3.7 Distances from noise barriers in selected municipalities to nearest neighborhood	38
3.8 Correction factors on orientation and tilt as demonstrated by [8]	39
3.9 Noise Barrier Orientations	40
3.10 Electricity Demanded by Scooters and Noise Barrier Potential	43
4.1 Flowchart of Components of Case Study System	46
4.2 Noise barrier along A20 in North Rotterdam	49
4.3 Amsterdam Noise Barriers	50
4.4 Noise barrier along N470 in Delft	51
4.5 Schematic of PV Panels on Noise Barrier	53
4.6 Pressure flow in Hydrogen System	55
4.7 Model Iterations Schematic	56
4.8 Utilization of Energy Wall for Rotterdam	57
4.9 Contribution of Energy Wall to Hydrogen Production for Rotterdam	58
4.10 Comparison of Control Strategies in terms of Electricity Exchange (3 kW Electrolyzer, 4 NB Segments)	59
4.11 Hourly Electrolyzer Input and Grid Pattern for 1 kW Electrolyzer	59
4.12 Electrolyzer Capacity Factors for Both Control Strategies	60
4.13 Daily State of Charge Levels for Different Electrolyzer Sizes	61

5.1	Breakdown of LCOH Contributions	71
5.2	Levelized Cost of Electrolyzer	72
5.3	Total Gross Cost of Electricity for CS1 & CS2	73
5.4	Gross Cost of Electricity by Source for CS1 & CS2	74
5.5	Overall LCOH of Configurations	76
6.1	Trend of $LCOH_{Elec}$ and CF_{Elec} with increasing Electrolyzer Capacity	83
6.2	State of Charge of 1kW and 2 kW Electrolyzers using CS1	84
6.3	Overall LCOH of Configurations	86
A.1	Example of a Power Curve	100
D.1	Neighbourhood proximity to NBs in top 25 municipalities	108
D.2	Groningen	109
D.3	Cluster of Municipalities	110
D.4	Alkmaar and Zwolle	110
D.5	Amsterdam, Haarlem, Zaanstad and Haarlemmermeer	111
D.6	Den Haag, Rotterdam, Zoetermeer, and Alphen aan den Rijn	112
D.7	Utrecht, Amersfoort, Ede, Arnhem and Apeldoorn	112
D.8	Emmen and Enschede	113
D.9	Tilburg, Breda, 's-Hertogenbosch and Eindhoven	114
E.1	Details of Amsterdam Noise Barrier Locations	115
E.2	Delft and Rotterdam Noord Noise Barriers	116
E.3	Noise barrier along N470 in Delft	116
E.4	Noise barrier along A20 in North Rotterdam	117
F.1	[9]	120
F.2	Individual Component Cost out of total system cost for PV, 2017 [10]	121
H.1	Charging station diagram	125

LIST OF TABLES

1.1	NREAP Targets and Progress for the Netherlands [11]	5
2.1	Cathode and Anode half reactions of Alkaline and PEM electrolysis	14
2.2	Comparison between PEM and Alkaline Electrolyzers [12]	15
2.3	Overview of Suitable Commercial Electrolyzers	16
2.4	Metal Hydride Canister Properties [13]	19
2.5	ASTM Type II Demineralized Water Properties	20
2.6	Key differences between different types of moped scooters	23
3.1	Top 25 Municipalities in terms of total scooters (>4,000)	30
3.2	Unsuitable (Removed) Noise Barrier Characteristics and Lengths	36
3.3	Selected municipality data about scooters, electricity demand, noise barrier length & potential electricity generation	44
4.1	Scooter Demand Assumptions [7]	47
4.2	Summary of Characteristics of Chosen Locations, Noise Barriers & Scooters	51
4.3	PV Capacity Factors of Selected Locations	57
5.1	Summary of Parameters Used in the Cost calculations	63
5.2	Operational and Capital Costs of PEM Hydrogen Production from Renewables [14]	68
5.3	Base Case LCOE _{PV} of each Case Study Location	70
5.4	LCOH for 3 kW-CS1 Configuration for a Range of EWM, *50km range assumed	76
5.5	Summary of Scooter Operating Costs, *50 km range assumed for FC Scooter	77
6.1	Noise Barrier Filtering Characteristics and Lengths	81
6.2	Selected municipality data about scooters, electricity demand, noise barrier length & potential electricity generation	82
6.3	Summary of Scooter Operating Costs, *50 km range assumed for FC Scooter	86
6.4	Fuel Cell Scooter Cost Scenarios	87
6.5	Comparison of different hydrogen production methods, reproduced from [15]	88
6.6	Estimated Avoided Annual Emissions of 100 FC Scooters	89
E.1	Only Module Cost Survey	119
G.1	One-off Grid Connection Costs [16]	123
G.2	Annual Grid Connection Costs, OPEX _{Grid} [16]	124
I.1	Battery Electric Scooter Selection Overview	127

1

INTRODUCTION

Climate change is the one of the most important and critical challenges that this generation faces. Rising temperatures, melting ice caps, rising sea levels, and changes to the water cycles all result from the increased emission of carbon dioxide and other greenhouse gases (GHG) into the atmosphere. A multitude of resources are available which explain the effects and consequences of climate change. Fossil fuels have been the dominant source of energy for most applications, and the idea of transitioning away from them is challenging and concerning from a technology, financial and social point of view but also extremely necessary for a viable future on this earth.

Sustainable energy technologies are at this point readily available for this transition. Renewable energy generation units have been around for years, and are now cheap enough to compete with their traditional fossil fuel counterparts. Wind, water and the sun are some of the most popular and widespread implementations of renewable energy. In 2019 the cumulative capacity of wind energy was over 600 GW, solar installations were close at 580 GW, and hydropower, one of the oldest forms of renewable energy was over 1.1 TW. [17].

Technology, demand, awareness and the willingness towards environmental solutions and policies has accelerated the implementation of renewable energy and consequently the cost of these technologies has decreased significantly. Energy storage and grid development are progressing rapidly, dealing with any intermittency issues faced in the past. While batteries have been the leader in the storage field, hydrogen is progressively becoming a viable seasonal storage solution.

This thesis is concerned with the generation of green hydrogen in a decentralized manner for use in fuel cell electric mobility. The question then rises:

What is the feasibility of a hydrogen fueling station for scooters, powered by solar energy at a noise barrier?

1.1. RESEARCH QUESTIONS

Hydrogen applications in the mobility sector are starting to emerge commercially, which will be one of the anchor points of this thesis. In order to make the hydrogen production sustainable, renewable electricity generation from the sun will be coupled with an electrolysis unit for the production of hydrogen. The mobility application chosen was scooters, as these are quite prominent in the Netherlands and are significant contributors to air quality and GHG emissions. In this context, The Energy Wall is the concept of using existing noise barrier infrastructure to implement renewable electricity production modules. The project was guided by the following objectives:

Sustainable Mobility Transition in the form of fuel cell scooters, with green hydrogen and water as the only operational emission

Emissions Reduction in terms of greenhouse gases, as well as particulate matter and noise.

Geographical Considerations identifying locations with suitable noise barriers, sufficient scooter populations, and potential for coupling the two through a local H₂ refueling station.

System Design of a configuration which includes the following elements: electricity generation by the solar panels, DEMI water supply for electrolysis (bought externally or purified on-site), an electrolyzer unit for hydrogen production, pressurized buffer storage tanks, and a dispensing subsystem which consists of metal hydride canisters used by the scooters.

Small Scale System Simulation of on-site solar electricity generation and hydrogen production through electrolysis for use in hydrogen powered scooters using renewable energy sources.

Secondary Electricity Source such as the grid or batteries for added reliability of hydrogen production

Economic Feasibility Analysis of a case study system, using the levelized cost of the components in each process step from the electricity to the stored hydrogen. and the cost per unit distance driven for comparison to conventional scooters.

Scooter Performance Comparison in terms of the cost of operation between gas, battery electric, and fuel cell electric two wheelers.

In effort to answer the main research question and address the above objectives, the following sub-research questions were asked:

1. In terms of usable noise barriers, how many are feasible to be coupled with a hydrogen supply and canister refueling station in the Netherlands?
2. In technical design terms, what would the Energy Wall with hydrogen production look like?
3. How economically feasible is it to supply hydrogen canisters to scooter users?
4. What are the technical barriers or benefits of this type of system in the Netherlands?

1.2. MOTIVATIONS

The motivations stem from the current energy sources, transition status and progress, and the prospect of a hydrogen economy in the Netherlands. These elements are discussed in the subsections below.

1.2.1. ENERGY IN HOLLAND: CURRENT SITUATION & FUTURE OBJECTIVES

The Netherlands is the second largest producer of natural gas in Europe after Norway [5]. Figure 1.1 shows the energy supply and electricity generation by source for the Netherlands in 2018. Of the Total Primary Energy Supply (TPES), 91% is derived from fossil fuels (Natural Gas, Oil, and Coal).

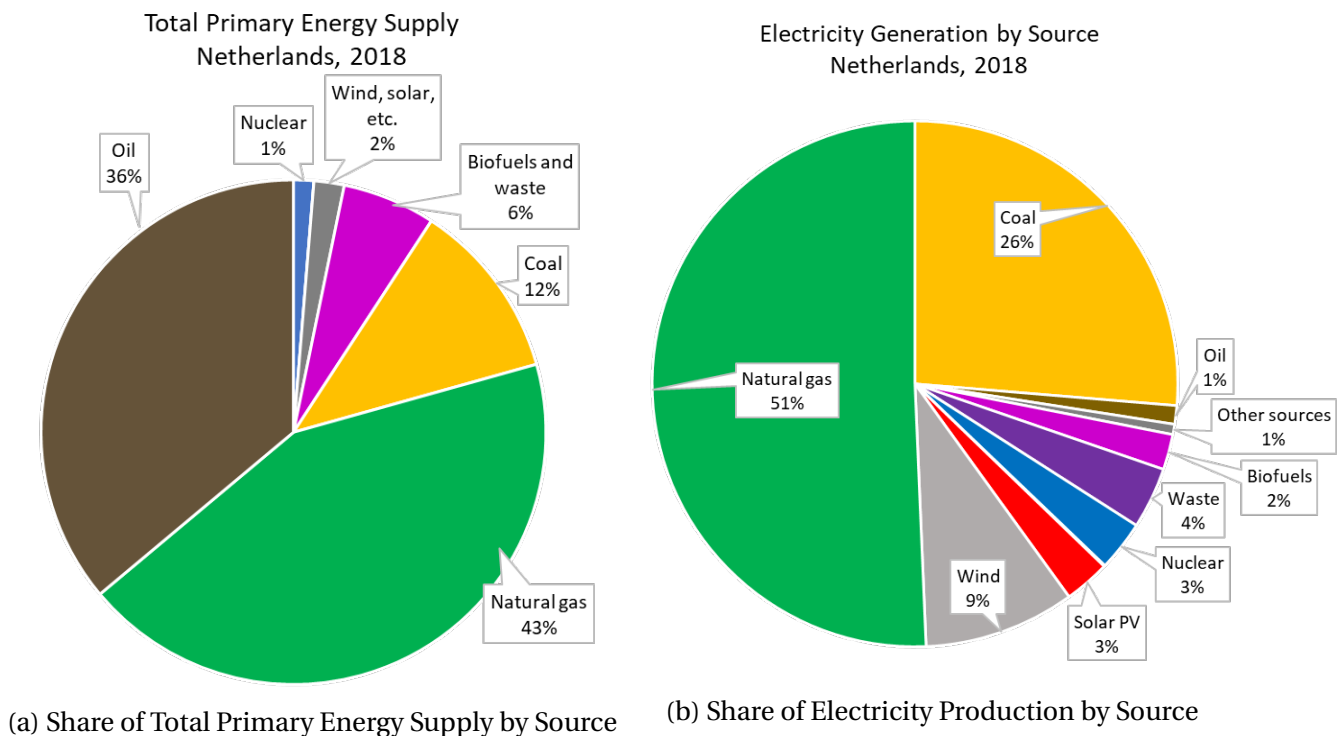


Figure 1.1: Sources of Primary Energy Supply and Electricity Generation for the Netherlands 2018 [5]

TRENDS IN ELECTRICITY

Transport vehicle engines were designed from their beginning to use fossil fuel sources; these remain the predominant fuels of road transport today. However this is not necessarily the case when it comes to electric powered mobility. In terms of electricity production sources a reduction in the fossil fuel sources is possible and necessary. As seen in figure 1.1b more than half of electricity production in the Netherlands was from natural gas and more than a quarter was from coal in 2018. Thus in cases of electric vehicles, although there are no direct emissions from the vehicle operation, there are significant emissions in the production of electricity.

Between 1990 and 2018 there has been an 8.6% increase in the amount of electricity produced by coal. Although the nationwide amount of electricity production has increased (27%) and the share of coal in the total electricity production mix has decreased (due to the addition of renewable electricity sources), it does not seem that our dependence on coal has decreased as it should.

Looking forward for the next 10 years, the electricity generation by coal (and other fossil fuels) should be *replaced* rather than supplemented, by renewable sources.

TRANSPORTATION ENERGY & EMISSIONS

Of the total consumption of the Netherlands, the transport sector accounts for 24% of the final energy consumption, while industry took 30% and other sectors such as services, households and agriculture accounted for 45%. A Sankey Diagram in [18] shows energy flows from production to consumption, as well as the sector in which it is consumed. Transport consumption consisted of: 95.5% by road, 3% by aviation, and 2% by rail. In terms of energy sources consumed, the majority (93%) came from oil and petroleum (O&P) products; renewable energies account for 5% and electricity for 2%. The total energy consumed for transport was 10.8 Mtoe.

Road transport was heavily dependent on fossil fuel energy, with 95% of the energy consumption attributed to O&P products, while the rest (5%) came from renewable energies. Electricity usage in the road transport sector was 46 ktoe, or $\leq 1\%$. Rail transport used mainly electricity (85%), while the rest came from O&P and renewables. [18] Emissions from transport applications were 31.6 Mt CO₂ in 2017 for the Netherlands, 95% of which were attributed to road transport. The transport sector as a whole was accountable for 20% of the total CO₂ emissions of the Netherlands. [19]

It becomes apparent that the reliance on- or rather reduction of- fossil fuels for road transport is an area which needs urgent action. The end goal is to reduce CO₂ emissions, hence by focusing on the sector which is responsible for one-fifth of these is a reasonable approach.

FUTURE TARGETS & PROGRESS IN RENEWABLES

Various agreements and summits have been held with the focus of setting transition targets and planning on how to achieve these. In the 2015 Paris climate agreement, the EU and its member states committed to a 40% reduction of GHG by 2030 [20].

In the Climate Agreement passed by Dutch parliament in 2019, a 49% reduction target in GHG emissions by 2030 as compared to 1990 levels was set. In the longer term, by 2050 the Netherlands aims to reduce its GHG emissions by 95% while producing 100% of its electricity from renewable energy. [5]

The National Renewable Energy Action Plan (NREAP) outlines a set of targets regarding the share of Renewable Energy Sources (RES) in the total gross consumption (RES-Share) and the sectors of Transport (RES-T), Electricity (RES-E), and Heating & Cooling (RES-H&C) for each member of the European Union. Europe has set a target of 20% share of energy from renewables for 2020 [11]. For the Netherlands the targets for 2020 and progress up until 2018 are shown in table 1.1. As of 2018, the progress for the share of renewable energy

sources and the electricity production from renewables was around half of the 2020 target. In contrast, the H&C and transport categories were much closer to the defined targets.

Category	Target 2020	Status 2018
RES Share	14.5%	7.38%
RES-T	10.3%	9.59%
RES-E	37%	15.12%
RES-H&C	8.7%	6.13%

Table 1.1: NREAP Targets and Progress for the Netherlands [11]

The overall share of gross energy consumption from renewable sources was given at 7.4% for 2018, while the 2020 target was set to 14% for the Netherlands; it was ranked last in the share of renewable energy consumption in the EU [21]. The share of renewables in the electricity production can be seen in figure 1.1b; the mix of renewable electricity consists of 9% from wind, 4% from waste, 3% by solar, and 2% from biofuels.

The Netherlands needs rapid transformation to catch up with the rest of the EU member states. Although good prospects in the wind energy field are prevalent, a larger share of the renewable energy consumption needs to be achieved in order to progress towards the above stated targets.

1.2.2. HYDROGEN ECONOMY

Hydrogen has become increasingly available and its applications as an energy carrier are slowly becoming apparent. The Hydrogen Council makes clear that it has important roles in the energy transition, such as de-carbonizing the transport industry, distributing energy across sectors and regions, increasing system resilience by acting as a buffer, and enabling large scale renewable integration and power generation. The last point is critical to reducing energy related emissions. One ambitious proposition in the Netherlands is to use multi-megawatt wind farm installations to produce hydrogen offshore [22].

Barriers to the hydrogen mobility sector are firstly the limited hydrogen refuelling infrastructure, and secondly the high risks associated with investment in hydrogen infrastructure. This limits the enablement of end users. The capital and operational costs of hydrogen infrastructure such as generation, transmission & distribution, and refueling stations are still relatively high [23].

During the deployment phase of fuel cell electric vehicle (FCEV) technology, it is expected that the hydrogen infrastructure will be underutilized, initially not returning enough profit on the investments made [24]. Therefore, a transition phase is needed before investments for large scale deployment of facilities are made [25].

By implementing small scale hydrogen production systems, hydrogen is introduced in the market as a possible means of clean energy. This stimulates the use of hydrogen in consumer applications and create a user base, therefore preparing the market for the roll-out of large scale hydrogen infrastructure and supply. This project identifies itself as part of the transition phase enabling consumers to directly use small scale hydrogen infrastructure

systems.

The idea of having citizens invest in hydrogen-powered vehicles means that an increasing demand for hydrogen will already exist by the time the large-scale hydrogen production is commercialized. While large scale production systems cater mainly to industrial applications, it will also assist the societal/community scale applications and social transition to sustainable mobility.

It is therefore strongly supported that cleaner moped vehicles in dense cities would greatly contribute to the health and wellbeing of the residents of the Netherlands.

1.3. THE ENERGY WALL

The *Energy Wall* is a concept whereby highway noise barriers are retrofitted as energy producing units by installing solar panels and micro wind turbines on them. The idea is that these existing structures are given more than the sole purpose of blocking noise from neighbourhoods or sensitive areas. Some ideas and concepts have been explored in [8, 26]. For the purpose of this project, an Energy Wall is used to produce renewable energy which is used by the hydrogen production unit to supply fuel cell electric scooters.

In a study by [8] it was found that there are 590 km of noise barriers with the potential to become 'Energy Wall' units. The retrofitting of a noise barrier into an Energy Wall was a test trial project at the Technical University of Delft in collaboration with Province of South Holland [27]. The potential of using highways to fuel the electric mobility sector was explored in [28], although this focused on large scale wind turbines, while the focus here is small scale electrolysis using photovoltaic systems.

This project aims to design a hydrogen refueling point which uses the Energy Wall as the electricity source, coupled with an electrolyzer on site to provide hydrogen to fuel cell scooters. Noise barriers have the objective of blocking noise from areas which are inhabited or sensitive to the noise of highways. Therefore, an advantage is presented to the scooter users of these inhabited areas since they will not be far from the hydrogen production points. The localized production also allows for little to no transport of the hydrogen, hence decreasing the costs of the overall system.

In summary, an electrolyzer can be placed near a segment of noise barriers that have been retrofitted with solar panels and/or wind turbines. The output of the electrolyzer will be pressurized hydrogen, which will be stored in compressed buffer storage tanks, which will then be scheduled to refill the hydride canisters used by the scooters. The tanks act as a buffer storage system before the refueling of the canisters. Considering cabling and associated losses, the hydrogen station should be located as close to the Energy Wall as possible, for these to be minimized.

This project investigates various aspects of the Energy Wall such as the cost of the energy, sensitivity to parameters including as the orientation of the walls, the material of which they are made, etc. For the economic feasibility of the system, the utilization of the hydrogen must be as high as possible. These aspects are further investigated in chapter 3.

1.4. SCOOTER USE IN THE NETHERLANDS

Scooters are a popular form of transport in the Netherlands. The country is characteristically flat and consists of excellent cycling infrastructure. Bicycles are the main form of day to day transport, but scooters are also popular.

A scooter (or moped) in this context is defined as a powered two wheeled vehicle, with two passenger spots. Scooters are useful for longer commutes within cities, commutes between and within cities, or for traveling from rural areas to urban areas. Small scooters (≤ 50 cc) are commonly allowed to drive in the same lanes as bicycles. Car congestion can be a problem in cities bringing some places in the Netherlands to have adopted car-free city centers. The only motorized vehicles allowed are taxis, limited mobility vehicles, and scooters. Scooters are also convenient as they consume less fuel per kilometer, take up less space in traffic, and are lighter than cars.

Since this project is focused on delivering hydrogen to scooter users, the next chapters provide more information regarding technical aspects, their relevance and use in the Netherlands.

AIR QUALITY & HEALTH

The quality of air in the major cities is indicated by the amount of particulate matter (PM) per unit volume of air. PM10 or PM2.5 denote matter with diameters of $10 \mu\text{m}$ and $2.5 \mu\text{m}$ respectively. PM is produced from sources such as traffic, livestock farms, (industrial) combustion processes and natural sources (such as salt) [29].

Mopeds release relatively large amounts of hydrocarbons, accounting for almost a quarter (13%-24%) of the total hydrocarbon emissions emitted by road traffic [30]. Their contribution to PM10 is 1-4%, while the carbon monoxide (CO) contribution is 4-10%. Mopeds have higher CO, hydrocarbon and PM emissions /km, while cars have higher CO₂ emissions /km. On the other hand, the share of moped contribution to the total of all traffic emissions is small.

Moped emissions can be reduced by either reducing the burning of harmful fuels (i.e. switching to zero emission fuels) or by engine optimization measures such as reducing fuel consumption by using fuel injection or transitioning from 2 stroke to 4 stroke engines to emit fewer particulates [30]. 2 stroke engines were deemed asymmetric polluters, constituting a small portion of the fleet but with emission factors up to thousands of times higher than other vehicles [31].

The health effects of the current air pollution as compared to the case of no air pollution are estimated as a 9 month reduction of life expectancy (an estimated 11% of lung cancer deaths are also attributed to air pollution) [32].

A map of the PM10 and PM2.5 can be seen at <https://arcg.is/151P04>. The major cities such as Amsterdam, Den Haag, Rotterdam and Utrecht are all mostly above the $20 \mu\text{g}/\text{m}^3$ level, the recommended limit suggested by the World Health Organization (WHO), creating more opportunity and need for fewer conventional scooters and more zero emission vehicles.

1.5. RESEARCH QUESTIONS

The overall objective of this thesis is to develop a model which simulates and controls a small-scale hydrogen production, storage, and dispensing system powered by solar energy sources. In addition, the feasibility of implementing a refueling station for scooters nearby the Energy Wall is desired. This poses the following research questions:

1. In terms of usable noise barriers, how many are feasible to be coupled with a hydrogen supply and canister refueling station in the Netherlands?
2. In technical design terms, what would the Energy Wall with hydrogen production look like?
3. How economically feasible is it to supply hydrogen canisters to scooter users?
4. What are the technical barriers or benefits of this type of system in the Netherlands?

1.6. OVERVIEW OF REPORT STRUCTURE

Chapter 2 is a literature review providing an insight into the working principles of the components which make up the Energy Wall with hydrogen production system. The relationship between noise barriers and scooter distribution in the Netherlands is analyzed in chapter 3. The model developed to understand the relationship between the energy resource and hydrogen production is detailed in chapter 4, where the specifics of the control strategies and method of simulation of the cases is given. The economic methodology and findings are provided in chapter 5. Finally, chapter 6 gives an overview of the findings, final conclusions and recommendations for further work.

2

LITERATURE REVIEW & PRELIMINARY SYSTEM DESIGN

This chapter lays out the foundation, identifies relevant literature and describes the concepts associated with the objectives of this project. Section 2.1 describes the renewable energy generation technology which is employed on the Energy Wall. The components associated with hydrogen generation and storage are discussed in section 2.2. In the same section background information about electrolysis is provided and a review of the two most feasible types of electrolyzers presented. Purified water options are given in section 2.3. Finally, technical information is provided about the electric and fuel cell scooters in section 2.4.

2.1. RENEWABLE ENERGY GENERATION COMPONENTS

The basis of this project is to provide clean renewable energy in order to produce hydrogen. This section discusses the energy generation components considered in the model of the Energy Wall. These are namely solar panels; micro wind turbines have the potential to be employed, but as found in [26] these are not economically viable yet, therefore omitted from this system. It should be noted that the Energy Wall is a distributed generation platform, meaning the energy generating components are placed nearby the load they serve, unlike centralized generation. This helps reduce the losses in transmission of electricity as well as offer some added independence to the location and its users [33]. The following sections aim to cover the working principle of photovoltaic (PV) technologies, i.e. the process of converting light to electricity as well as some of the most common materials used to fabricate these modules and the differences between them. The components of a full PV system are also outlined.

2.1.1. PV WORKING PRINCIPLE [1, 2]

Solar energy is harvested from the sun using modules which are made of a semiconductor material, converting sunlight into electricity. The principle which is applied to make this

conversion is called the *photovoltaic effect*, being: the generation of a potential difference at the junction of two materials in response to electromagnetic radiation.

The light from the sun is made up of particles which contain energy called photons. When photons hit the surface of the PV cells found in a module, they are absorbed. If the energy in the photon is enough it can excite an electron from an initial energy level into a higher one. Once this electron has been excited to the higher energy level, it leaves behind a void, otherwise known as a hole which has a positive elementary charge. The electron and hole are referred to as charge carriers. The electron-hole pair is able to recombine, but it can also be separated into the positive and negative junctions of the cell.

Once the electron-hole pair has been generated, the two charge carriers can be separated and collected through an external circuit. When electrons are transferred through the external circuit they are transformed into electrical energy. In this process current and voltage are generated, hence power. Individual solar cells are quite small but when grouped together to form solar modules their cumulative electricity production becomes significant.

Silicon is the most commonly used semiconductor material in solar applications. Pure silicon contains 4 valence electrons, which are covalent bonds forming a crystalline structure. This is quite a stable configuration and hence pure silicon behaves like both a conductor and insulator, thus the name semi-conductor. In order for electrons and holes to travel through these junctions, impurities are added to the silicon to make the material more, or less negatively charged, depending on which charge carriers it must convey. This process is called doping, whereby the positive side is doped with elements of 3 valence electrons such as Boron, and the negative side with elements of 5 valence electrons such as Phosphorus. This allows for the movement of holes and electrons through the semiconductor material.

2.1.2. PV SYSTEM COMPONENTS

Other than the electricity generating panels, a complete photovoltaic system includes other components which are essential for its operation. These are commonly referred to as Balance of System (BOS) components and they include converters, inverters, cabling, storage, controllers, and mounts. It is important to consider these components since they significantly contribute to the total cost. The BOS components may also vary depending on what type of system is being designed (e.g. grid connected or stand-alone).

2.1.3. TYPES OF SOLAR PANELS [3, 4]

There are several types of solar panels which differ in technology, cost, and performance. The most conventional types of solar panel materials are mono-crystalline (mono-Si), polycrystalline (poly-Si), and amorphous silicon (A-Si) cells.

Monocrystalline cells are more structured. They are the most efficient of the types mentioned above with values around 20%. They have a relatively longer lifetime than their counterparts and deal well with elevated temperatures, but come at a higher cost than other types of panels. Polycrystalline silicon cells are cheaper and easier to manufacture since the silicon is less structured, but are disadvantaged in terms of their efficiency which

is slightly lower at 15%. In addition their lifetime is lower and they have less tolerance to high temperatures. The physical appearance of these two can be seen in figure 2.1.

The choice of monocrystalline over polycrystalline is strongly case dependent. In cases where space is limited and power output has to be maximized, monocrystalline would be preferred at a higher cost. Alternatively, if space is not a limiting factor then a lower cost option of polycrystalline panels would be suitable.

Finally, amorphous silicon cells, also known as thin film, are the least efficient of the listed types of cells, but have the advantage of flexibility. They are cheap to produce and can be placed on a multitude of locations, however they have the shortest lifespan and efficiency of all the options mentioned so far.

For the case study system, polycrystalline solar modules are assumed.

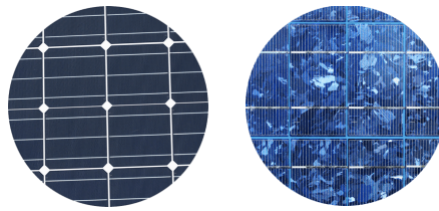


Figure 2.1: Physical Appearance of Monocrystalline-Si (left) and Polycrystalline-Si (right)

PV POWER OUTPUT

The maximum power point (MPP) is the current-voltage combination which yields the highest power. Typically systems have an MPP tracker which adjusts the voltage according to the current, resulting in the optimal combination. The current and voltage of a PV panel are subject to their operating conditions. A common way to illustrate the performance characteristics of panels is the I-V curves, which plots current against voltage. The MPP is the point at which the current-voltage product is maximized.

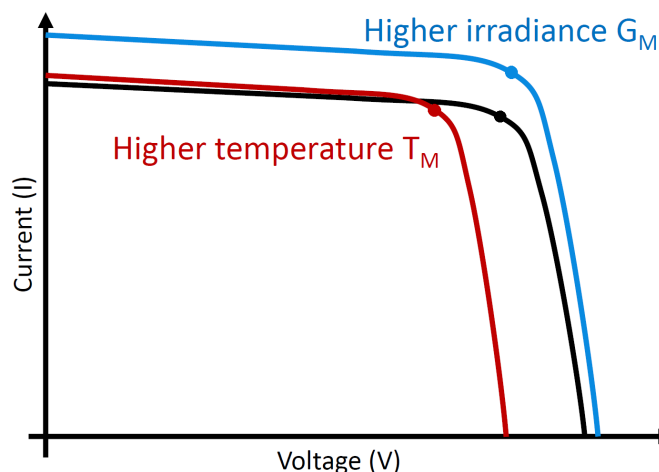


Figure 2.2: Variation of MPP with Temperature and Irradiance

The main influences of the power output of a PV panel are the temperature and irradiance at the site. These determine the operating capabilities of the PV system. When a

module operates in high temperature conditions the voltage of the module decreases due to heat losses, hence the MPP is also lower. The opposite stands for irradiance, whereby at higher irradiance values the power output increases since there are more photons exposed to the surface of the module. Figure 2.2 shows the effect on the current and voltage due to higher temperatures or irradiance; the same figure shows the shift in the MPP.

2.2. HYDROGEN TECHNOLOGY COMPONENTS

The components of hydrogen processing consist of production, storage, transport and re-conversion back into usable electricity. Production aspects such as the working principle of electrolysis, types of electrolyzers and considerations to the working environment of electrolysis are discussed in sections 2.2.1 and 2.2.2. A list of commercially available electrolyzers is then provided in section 2.2.3. A review of types of storage available is given in section 2.2.4, including content on both compressed (buffer) storage and metal hydride technologies (used by the scooter). Finally, information about sustainable scooter mobility is provided in section 2.4.

2.2.1. HYRODGEN PRODUCTION: ELECTROLYSIS

"The implementation of the Hydrogen Economy has been, since its first statement, disrupted by the fact that hydrogen does not exist in its molecular structure in nature." - Marcelo et al. [34]

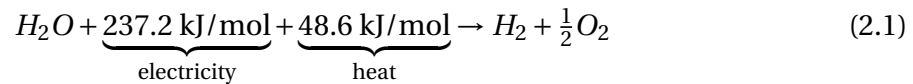
Hydrogen is classified depending on how clean the production processes used are:

- Green H₂: when there are no greenhouse gas emissions during the process
- Blue H₂: when there are emissions of greenhouse gases, but carbon capture processes are used to curb or balance the net greenhouse gas emissions
- Grey H₂: when hydrogen production emits greenhouse gases without prevention of greenhouse gas emissions

Steam reforming, which is the dominant method of hydrogen production, produces blue or grey hydrogen. It works by reacting water vapour with natural gas, propane, methanol or other fossil fuels in the presence of a (usually nickel) metal catalyst to produce hydrogen. Other than the harmful greenhouse gas emissions associated with this method, the purity of the produced hydrogen would not be adequate for the end application of the designed system, thus more energy must be used to further purify the gas. [35]

Electrolysis was chosen as the production method since it does not produce any greenhouse gas related by-products during its operation. In addition, by using sustainable energy the electricity source is also carbon neutral. It should be noted that in the case of a grid connection for back up power, a quantity of associated greenhouse gas emissions is possible due to the energy mix which the grid utilizes.

Hydrogen production occurs in the electrolyzer. This is a device which splits water to its elemental form, hydrogen H_2 and oxygen O_2 . The process is described in equation 2.1 with the additional electrical and heat energy per mole required [34]. In theory, 1.28V is the minimum voltage required to split one molecule of water, in laboratory conditions. In practice higher voltages are used for a higher rate of hydrogen production. [35]



The basic structure of an electrolyzer are two electrodes (an anode and a cathode), an electrolyte between them, and an external circuit to conduct electricity; electrolyzer schematics are shown in figure 2.3. The types of electrolyzers available for this setting are described in the following section.

2.2.2. TYPES OF ELECTROLYZERS

Electrolyzers are differentiated based on the type of electrolyte they use, which determines the intermediate water splitting reactions. There are three main types of electrolyzers, namely the Solid Oxide (SO), Alkaline, and Proton Exchange Membrane (also known as Polymer Electrolyte Membrane, PEM). The latter two are considered for this project since they operate at low temperature ranges. The SO electrolyzer, although quite efficient, only operates at very high temperatures ($\sim 1000^\circ\text{C}$).

The difference between Alkaline and PEM electrolysis is the electrolyte, as seen in figure 2.3. Since they have different electrolytes, the half reactions at the electrodes are also different; Alkaline conducts OH^- while PEM conducts H^+ . A schematic of Alkaline and PEM electrolyzers can be seen in figures 2.3a and 2.3b respectively. The reaction equations at each of the electrodes of both types are given in table 2.1.

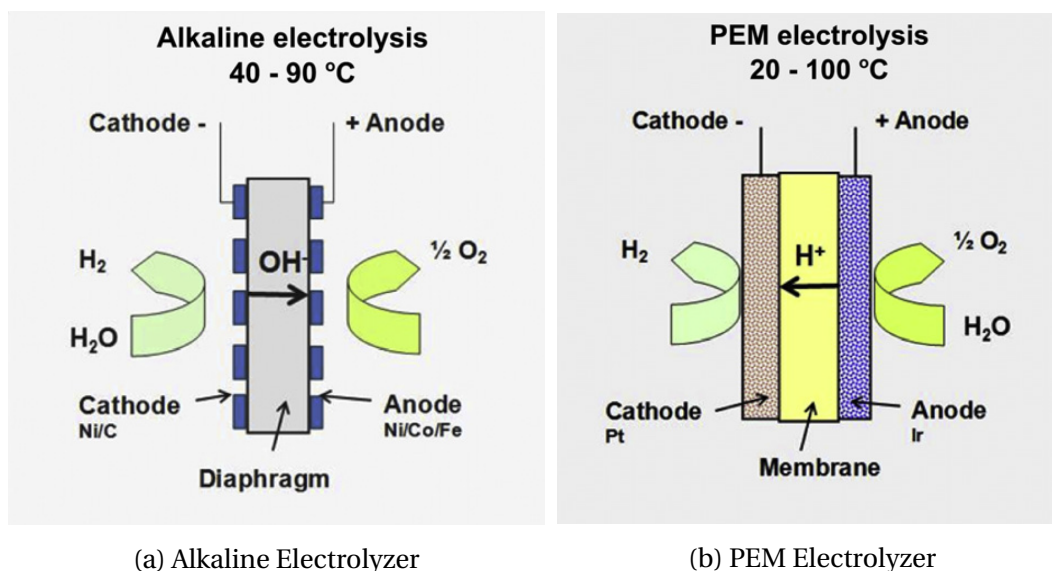


Figure 2.3: Working principle of electrolyzers

	Cathode	Anode
Alkaline	$2\text{H}_2\text{O} + 2e^- \rightarrow \text{H}_2 + 2\text{OH}^-$	$2\text{OH}^- \rightarrow \frac{1}{2} \text{O}_2 + 2\text{H}_2\text{O} + 2e^-$
PEM	$2\text{H}^+ + 2e^- \rightarrow \text{H}_2$	$\text{H}_2\text{O} \rightarrow \frac{1}{2} \text{O}_2 + 2\text{H}^+ + 2e^-$

Table 2.1: Cathode and Anode half reactions of Alkaline and PEM electrolysis

ALKALINE BENEFITS AND DRAWBACKS

Alkaline electrolysis is what electrolysis itself began with in the 19th century, thus the technology is well matured and established. Hence it has the advantage of lower cost than its PEM counterpart.

The electrolyte is a liquid, which brings certain disadvantages compared to a solid electrolyte. Three main disadvantages are named in [34], which are the low partial load range, a limited current density and low operating pressure. The diaphragm, as depicted in figure 2.3a does not completely separate the hydrogen and oxygen streams, allowing diffusion to occur.

Due to the liquid electrolyte and porous diaphragm, ohmic losses in alkaline electrolyzers are high. With higher current densities there are higher losses and thus the efficiency of the electrolyzer decreases. The operating current density range in [25] is given from 200 - 500 mA/cm² for alkaline electrolyzers; for comparison purposes in the same paper the range for PEM is 1500 - 2000 mA/cm². Finally, the electrolyte does not allow for high pressures making the design of alkaline electrolyzers quite bulky and not compact.

PEM BENEFITS AND DRAWBACKS

PEM electrolysis is comparative to alkaline since both operate at low temperatures. A key difference between the two is the electrolyte: PEM uses a solid electrolyte as compared to the liquid electrolyte used by alkaline. The solid electrolyte is more dense allowing it to be thinner and hence making the design of the electrolyzer more compact. The thinner electrolyte also reduces the ohmic losses associated with the ionic transfer.

The problems of alkaline electrolysis are eliminated by PEM, as stated by [25]. The solid electrolyte allows the electrolyzer to load follow since the operation can be dynamic and the range of current density operation is large. PEM electrolyzers can operate with safe pressure differential due to the solid electrolyte. The ability to have a pressure differential means that the process doesn't require pressurized oxygen to operate. Therefore oxygen can be taken out of the ambient air. The risk is therefore minimized, and the required safety equipment is reduced, ultimately reducing the capital cost. Ambient temperature of oxygen allows for low-cost plastic tubes rather than high pressure piping. Achievable current densities of ≥ 2 A/cm² are reported by [34], which is higher than those in alkaline systems.

Some of the drawbacks of PEM systems are the high cost of catalysts. Due to the highly acidic environment, the catalysts for the reaction are limited to noble metals. Impurities are a problem in PEM electrolysis since they can stick to the solid electrolyte and reduce the conductivity and consequently the efficiency. In liquid electrolytes the effect of impurities is not so significant.

SUMMARY OF PEM & ALKALINE

Until recent years, alkaline electrolysis has been used much more commercially, however PEM electrolysis has started becoming equally as favourable due to its advantages. There were only a handful of companies which worked with PEM electrolysis, two of the most notable were Proton and General Electric which have been mentioned in various sources. Recent developments and research have made PEM electrolysis competitive to alkaline electrolyzers [36].

Table 2.2 gives a summary of some of the most important aspects of each electrolyzer discussed. In summary, the main advantages of PEM over alkaline are higher efficiencies, higher purity of the output hydrogen gas, and compact mass volume characteristics [37]; they are easy to start up, making them attractive for coupling with renewables.

Technology	PEM	Alkaline
Status	New; Partially established	Old; Well established
Electrolyte	Solid	Liquid and corrosive
Cost	High cost of components	Cheapest and effective
Catalyst Type	Noble	Noble
Durability	Comparatively low	Long term
Stacks	> MW range	MW range
Efficiency		70%
Status	Commercialization is in near term	Commercialized
Pressure		Low operational pressure
Load Range	good partial load range	low for partial load
Dynamic operation	High	Low
Purity of Output	High gas purity	Low (crossover of gases)
Current Density	High	Low

Table 2.2: Comparison between PEM and Alkaline Electrolyzers [12]

2.2.3. OVERVIEW OF COMMERCIALY AVAILABLE ELECTROLYZERS

PEM electrolyzers are still in an early commercial stage, thus their price is high relative to alkaline electrolyzers but expected to fall [14]. The aim of this section is to identify a selection of small scale electrolyzers in order to better understand how the available models compare with each other and to find the key operational characteristics of each. A review of a number of small scale commercial *PEM* electrolyzers is shown below, with key characteristics of each summarized in table 2.3. More detailed explanations of each electrolyzer can be found in appendix B.

Model	Output [Nm ³ /h]	Energy Consumption [kWh/kg]	Water Intake [L/Nm ³]	Output Pressure [bar]
GreenHydrogen P1	1 - 4	61.2	5	50
H ₂ GEN E-Series	5 - 120	63.4	< 2	35
NEL H-Series	2/4/6	81.2/77.9/75.7	0.92	15
NEL S-Series	0.53/1.05	74.5	0.89/0.9	(or 30)
HyLYZER	1/2	74.5	1	0-7.9
HPAC 10	0.7	55.6	N/a	15
HPAC40	2.81	53.4	N/a	15

Table 2.3: Overview of Suitable Commercial Electrolyzers

2.2.4. STORAGE OPTIONS

Hydrogen can be stored in various ways, all of which have their benefits and disadvantages. The methods by which hydrogen can be stored are shown in figure 2.4a; this is useful to see how many different types of technology exists, with options for different applications of varying complexities. Figure 2.4b shows different fuels and their position in terms of gravimetric and volumetric energy content, providing an understanding of how hydrogen competes with conventional fuels in terms of energy content.

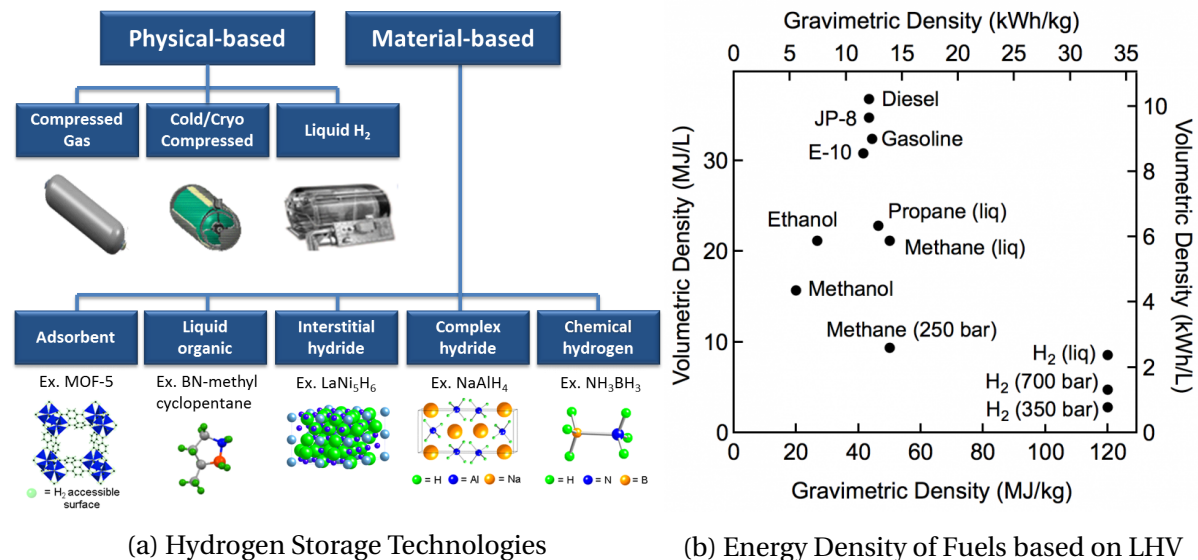


Figure 2.4: Hydrogen Storage Methods and Energy Density of Various Fuels [6]

The objective is to make the system as efficient and low cost as possible. The option of liquid hydrogen was considered too complex for a small scale system such as this one. The process of liquefying hydrogen is energy intensive since the gas must be cooled down to its extremely low boiling point of 20.28 K (-252.9 °C). Suitable insulation is also required to avoid boil-off effects, which are ultimately energy losses. Although liquid hydrogen has the highest gravimetric density (see figure 2.4b) the trade-off between energy density and cost is not sufficient to supply this system.

The main challenge with storing hydrogen stems from the size of the particles. The storage material must be able to block the particles from escaping through the pores. The strength of material must be adequate since hydrogen is usually stored above atmospheric pressure, thus the structure should be able to withstand elevated pressures. The two main storage technologies considered in this project are:

1. Compressed Gas: Storage of H₂ gas directly after electrolysis
2. Interstitial Hydrides: H₂ stored in hydride form ready for use by the fuel cell (FC) scooter

For the first option, the purpose is to store the hydrogen in bulk as it is produced. The second is transferring the hydrogen from the compressed buffer storage tanks to the metal hydride canisters used by the scooters. The refiling process is assumed to occur in one time-step. These storage technologies are discussed in the following sections.

COMPRESSED BUFFER STORAGE

Compressed gas storage has been the most common way of storing pure hydrogen. The density of hydrogen increases with increasing pressure, therefore more energy can be stored in a fixed volume when it is pressurized.

Compressed storage tanks are usually cylindrical and the material is determined by the conditions of storage. For pressures up to 200 bar, steel cylinders are adequate. Technological advancements in materials have allowed for pressures up to 800 bar using lightweight composite materials. When compressed to this pressure, the volumetric density is nearly half that of liquefied hydrogen. [38]

When compressing hydrogen, a certain amount of energy is required to push the gas into a smaller volume. This can be viewed as a percentage of the energy content of the hydrogen that is being stored. For pressures in the 800 bar range, it can take up to 13% of the energy content of the hydrogen just to compress it. [38]

For this system, low pressure systems are preferred in order to use the energy efficiently. Pressures of 800 bar are where the limits of technology have reached, however this system aims to be simple so that its implementation is not hindered by expensive and high tech components. Hence in efforts to make the cost of this system as low as possible and use energy efficiently pressures of 50 bar or lower are simulated.

There are several companies which manufacture tanks for hydrogen storage. Many manufacturers offer mainly high pressure storage. One notable storage tank manufacturer is Mahytec, which specialize in a range of storage applications: high pressure tanks, low pressure tanks, and hydride material products. Mahytec is also a distributor of the Green-Hydrogen electrolyzers. [39]

One Mahytec low pressure storage tank is capable of holding 4.2 kg of hydrogen at 60 bar. This tank is made of composite materials, making it considerably lighter than its steel counterpart. This tank can be seen in figure 2.5a. For the system in question, the tanks can be mounted onto the wall, possibly in an enclosure to protect against theft and extreme weather conditions. [40]



(a) MAHYTEC Buffer Storage Tanks [40]



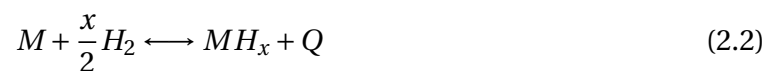
(b) APFCT Scooter Canister [41]

Figure 2.5: Pictures of Storage Units Envisioned

METAL HYDRIDE CANISTERS

Metal hydrides are a form of solid storage of hydrogen. Hydrogen enters the metal hydride environment, where it dissociates from H_2 atoms into its atomic form at the surface of the metal or metal alloy material. In the case of interstitial metal, after the hydrogen splits, it diffuses into the atomic structure of the host metal.

The equation showing the reaction of reversible hydrides is shown in equation 2.2. M is the metal or alloy, H is the hydrogen, x is the stoichiometric coefficient, and Q is the associated energy with inserting hydrogen or releasing it from the metal material. The process of inserting hydrogen is called hydriding, and removing it is dehydriding. When hydrogen is exposed to these metals, after dissociation, it acts as a metal and forms inter-metallic compounds. [38]



Metals and hydrogen have a higher entropy than the metal hydride, therefore during the formation of a hydride, energy is released and the reaction is exothermic. In releasing the hydrogen from the metal hydride it is the opposite: the reaction is endothermic and energy must be supplied to the hydride. In other words, when the hydrogen is to be released heat must be supplied. In practical applications the heat (enthalpy) associated with hydriding and dehydriding can prove critical to the heat management and thermal operating range of the application. The enthalpy also determines the stability of the hydride. The higher the (absolute) value of enthalpy, the higher the temperature at which hydrogen is released becomes. [38]

Metal hydrides are safer than other forms of storage such as compressed gas and liquefied hydrogen. The capacity of hydrogen stored in hydrides is measured either by the atomic content of hydrogen to metal ratio (H/M), the weight percent (wt%), or the volumetric terms. Since the hydrogen is bonded with the metals, rather than compressed in its molecular form, higher densities can be achieved. Disadvantages of metal hydrides are their sensitivity to impurities. These can cause reversible damage, but also irreversible

damage depending on the hydride-impurity combination. Thankfully, the hydrogen in this case is of high purity since it is produced by electrolysis which itself requires high purity water. [38]

The cost of alloys used in metal hydride applications comprises of the raw materials, melting and annealing, metallurgical complexity costs, profit, and the degree of precision of the pressure-composition-isotherm required for the application. [38]

The canisters that the scooter uses are metal hydride canisters, which allow for relatively large quantities of hydrogen to be stored at low pressures. The properties of the canisters are given in table 2.4. Each canister is able to hold 45 grams H₂, which is 1.1% of the total weight of the canister. [13]

Property	Value
Storage capacity	45 gH ₂ /canister
Canister material	Aluminium 6061-T6 alloy
Canister diameter	76mm
Canister length	365 mm
Metal hydride material	AB5 alloy
H ₂ purity requirement	>99.99%; O ₂ , CO, S <1 ppm
Weight	4.4 kg ± 0.1 kg
Charging pressure	140 psig (9.65 bar) @ 10-20 °C
H ₂ Discharge rate	>45 gH ₂ /canister > 39gH ₂ /canister

Table 2.4: Metal Hydride Canister Properties [13]

2.3. WATER TREATMENT

Electrolysis uses purified water for its operation. Spring water usually contains minerals, which are safe to drink. For applications where these minerals are harmful, there are many types of processes which demineralize water, also known as DEMI water.

The electrolyte is highly vulnerable to impurities and this can cause reductions in the efficiency. If the catalysts become contaminated, less surface area is available for the electrode reactions with the feed in gases to occur, thereby reducing the amount of hydrogen produced and hence the efficiency.

PEM electrolyzers require purified water, commonly of at least ASTM Type II purity, the characteristics of which are given in table 2.5. The purity standard specifies a maximum level of certain impurities, such as chlorides or organic compounds.

The options for obtaining purified water for the electrolyzer operation is either by buying purified water directly or by connecting a water purifier to a local tap water connection and purifying it on-site.

Methods to purify water are described in appendix C, including the processes of distillation and reverse osmosis which are the most effective at removing the undesirable contaminants. For ultra pure (Type I) water, UV radiation is also employed, but for the purpose

Property	Value
Electrical Conductivity @ 25°C	< 1 $\mu\text{S}/\text{cm}$
Electrical Resistivity @ 25°C	$\geq 1.0 \text{ M}\Omega\text{-cm}$
Total Organic Carbon	< 50 $\mu\text{g}/\text{L}$
Sodium (Na)	< 5 $\mu\text{g}/\text{L}$
Chlorides (Cl)	< 5 $\mu\text{g}/\text{L}$
Total Silica	< 3 $\mu\text{g}/\text{L}$

Table 2.5: ASTM Type II Demineralized Water Properties

of this study this is not required. The option of having readily purified water delivered to the site was dismissed. The main reason was to allow the system to be able to self-sustain itself. In addition, it is not yet reasonable to assume that the trucks delivering the water are net zero in terms of their emissions. Thus, in light of trying to have a sustainable, clean system the option of purifying the water on site was chosen.

Some electrolyzers, such as the *H₂GEN* described in section 2.2.2, include water treatment units in their systems, therefore an external purifier is not necessary. The only requirement for these type of systems is a tap water connection.

Commercially available purifier units were explored but their cost was very low compared to the rest of the system components, thus the cost of the purification system and water use was assumed negligible.

2.4. SCOOTERS (A.K.A MOPEDS)

Powered two wheelers can be categorized based on the size of their engine and drive mechanism. A big distinction between scooters is made based on the engine drive system, being powered by gas or electricity. The latter is predicted to grow as the means to reducing GHG emissions in transport applications, while the former is mentioned purely for comparison purposes.

In the Netherlands the so-called bromfietsen and snorfietsen are the most popular types of scooters for daily commuting. Bromfietsen are scooters which have a maximum speed of 45 km/h, with an internal combustion engine of no larger than 50 cm³ or an electric motor of 4 kW. Snorfietsen are smaller with a maximum speed of 25 km/h and no specific limits on the size of the engine; bicycles with a motor are included in this category [42]. Snorfietsen are also used more commonly in urban areas, while bromfietsen are used for commuting in sparse areas or in rural areas for transportation to urban centers. In this context, the term scooter denotes either of the two mentioned.

In 2016, 4.9% of the total number of registered scooters in Europe was in the Netherlands. Over one fifth (21.7%) of the scooters purchased in Europe in 2017 was in the Netherlands, indicating that the market for scooters is growing. [7].

Electric scooters are two-wheeled vehicles which are propelled by electronic actuators and do not consume fossil fuels. They offer advantages such as zero greenhouse gas emissions, reduced noise and air pollution. As stated by [43], electronic motors are direct drive

mechanisms, avoiding the use of gearboxes, clutches, and auto transmission systems. The maximum torque is when the vehicle is not moving, allowing for quick accelerations to move away for example. It is also common to maintain a nearly constant torque until reaching top speed (which is electronically limited), contrary to conventional scooters. Noise reduction offered by any electric motor is especially valuable in cities.

Fuel Cell Electric Vehicles (FCEV) are also electric vehicles, however most conversations are currently around Battery Electric Vehicles (BEV). Non-emitting mopeds have been gaining popularity in recent years, and BEVs have become commercial products. An overview of commercially available electric scooters with the range, charging time and price is provided at <https://electricscooters.eu/>.

2.4.1. BATTERY POWERED ELECTRIC SCOOTERS

Increasing use of electric vehicles in the Netherlands is evident as the number of non-fossil fueled vehicles increases each year, as well as electric charging stations now being a not-so-rare occurrence. In 2015 there were 2,197 electric scooters sold in the Netherlands, accounting for 3.5% of the total sales that year [44]. In 2017 this number rose by to 2,529 (up by 332) but only represented 3% of the total purchases that year [7]. Each year the number of electric scooter sales is between 3% and 6% of the total sales, which shows a prospective market for alternative vehicles and thus the possibility of hydrogen integration.

Battery powered vehicles offer advantages such as zero emissions of GHGs and PM. The capability to charge at home overnight or at the place of employment, with more and more charging stations appearing, is viewed as a plus.

Besides the zero emission operation of these vehicles, there are still some inherent disadvantages to batteries. Batteries can be made using abundant resources, but more advanced battery technologies tend to use rare natural resources such as lithium; complex mechanical structures of some batteries results in challenges when reclaiming these materials. There is also a high rate of energy and water use associated with battery manufacturing [45]. Batteries cannot store energy for prolonged periods due to high discharge rates, as compared to fuels. The battery capacity is sensitive to temperature and depth of discharge. This is detrimental to the performance of the scooter, especially in places where temperature fluctuates or reaches extremes. It should also be recognized that when a battery is charged by electricity which has been produced from fossil fuel generation units, it is still accountable for the end use emissions of that source. Despite the disadvantages, battery powered applications are still an approach to using fewer fossil fuels and hence reducing the greenhouse gas emissions and the health effects associated with fossil fuel vehicle operation.

2.4.2. HYDROGEN FUEL CELL SCOOTER SITUATION

The technology status of fuel cell vehicles is at its early commercialization stage, with much ongoing development and testing still taking place. To date, only a handful of commercial hydrogen two-wheeler vehicles exist. The fuel cell scooter model presented by Asia Pacific Fuel Cell Technologies (APFCT) seems to be the most developed, with their 10+ years

breadth of experience in fuel cells. The scooter uses two metal hydride canisters, which can be replaced when they run out resulting in minimal refueling time. Hydrogen does not scale proportionally with the weight and volume of its container, and the gravimetric energy density is higher than that of batteries.

A case study was performed where the scooter was offered to drivers in an area of Taiwan in order to obtain real driving data [46]. The case study aimed to record data such as temperature, speed, elevation, as well as give users an experience riding the scooter and receive user feedback on the performance of the vehicle. The key findings stated that users were happy with the speed, range and handling of the scooter, as well as the ease of changing the canisters. The 80 scooters that were deployed covered a total of 245,446 km and consumed 453 kg of hydrogen. Although the (highway mode) range stated is 80 km, this figure assumes steady speed and limited accelerations/decelerations. The more realistic range for city mode is closer to 50 km [13].

According to the Hydrogen Council, which investigated the commercialization of fuel cell electric vehicles, it is estimated that on average 20-25% of the vehicles in 2050 would be FCEVs, but this was mainly regarding larger vehicles such as trucks, cars, and buses. They estimate 10% for small cars, and less than 10% for 2 or 3 wheeled vehicles [47].

Hydrogen as fuel for FCEVs can make a significant contribution to the low-emission fulfillment of the transport requirement for people and goods. Hydrogen and fuel cell vehicles combined with batteries offer the potential for full electrification of all road traffic. In addition to the reduction of GHGs in the air, the health hazards due to emissions of NO_x , SO_2 , and PM and noise pollution are all drastically reduced.

2.4.3. KEY DIFFERENCES BETWEEN BATTERY, FUEL CELL AND GAS SCOOTERS

Although electric scooter technology is beneficial over the gas powered counterpart in terms of emission-less transport, battery and fuel cell technologies have their differences which are summarized here. The APFCT scooter is taken as the FC model; the battery scooter used for comparison is the Niu: NQi Sport model, since the engine size is comparable. A wider range of electric light scooter models is given in appendix I. For the gas scooter, AGMs iCON50 was used for comparison to the electric drive systems. The commonalities between these three scooters are their engine size (all around 1.8 kW) and the top speed which is 45 km/h in this case.

The weight of the energy carriers of FCEV and BEVs are comparable. The battery contains one 10kg battery, while the metal hydrides weigh 4.5 kg each; one scooter fits two therefore the carriers weigh 9kg. The gas scooter uses a 5 L tank which weighs around 5 kg, half the weight when compared to the electric drive examples.

The energy content of a metal hydride canister was given as 45 gH₂. The energy content of hydrogen ranges between 33.3 kWh/kgH₂ and 39.4 kWh/kgH₂, depending on whether the Higher or Lower heating value is taken. Hence, a fully charged pair of canisters contain between 3 and 3.5 kWh of energy. The actual output will depend on the efficiency of the scooter fuel cell. The energy content of the batteries was given as 29 Ah; given the 60V operational voltage of the BEV the capacity is found to be 1.74 kWh. This is around half of

that of the fuel cell scooter.

The energy density of the carriers is provided in [48]. The energy density of a Lithium-ion battery was given as 125 Wh/kg. The energy density of metal hydrides was much higher at 400 Wh/kg.

The range of any vehicle depends on the driving style of the user. The electric scooters have a comparable range at 50-80km. The gas scooter is at a clear advantage in this aspect since its range is between 200-250 km on one tank. The range is given as 50km/L in [49], assumed to be the maximum achievable range.

One advantage of the metal hydrides over the rest of the energy carriers is their plug&play mechanism, whereby the user needs to replace the empty canister with a full one to refuel, which takes 1-2 minutes. Battery scooters have started using the concept of swappable batteries (see Gogoro) although this is not very common, yet. The battery charging time given by the manufacturer was between 6 and 7 hours, although semi-charging is also possible. The refuel time of a gas scooter is roughly 5 minutes.

In conclusion, the main advantage of FCEVs is the charging time, especially for users who are unable to wait long periods between charge cycles. The range of both the FCEV and BEV are comparable, and both depend on the driving style of the user, but are both inferior to the range provided by the gas scooter. This advantage is provided at the cost of operational emissions. A comparison of the cost to drive each of these scooters is given in section 5.4.3.

Description	FCEV [13, 41]	BEV [50]	Gas [51]
Model	APFCT	Niu NQi Sport+	AGM:iCON 50
Engine Size	1.8 kW	1.8 kW	1.8 kW (49cc)
Top Speed [km/h]	45	45	45
Energy Carrier	MH Canisters	Li-ion Battery	Gas Tank
Weight of 1 Energy Carrier	2×4.4 kg ±0.1 kg	10 kg	~ 5 kg
Capacity of Full Energy Carrier	90 gH ₂ 3 - 3.5 kWh	29Ah @60V 1.74 kWh	5L 46.5 kWh
Range at full charge	50-80km	50-80 km	200-250 km
Energy Density of Carrier [48]	400 Wh/kg	125 Wh/kg	
Refueling Time	1 min	6-7 hrs	5 mins
Scooter Weight [kg]	115	95	90

Table 2.6: Key differences between different types of moped scooters

3

NOISE BARRIER, SCOOTER, AND GEOGRAPHICAL ANALYSIS

The Netherlands has more than other European countries, which goes to show that there is already a market for hydrogen refueling stations. A possibility would be to implement the proposed system near already existing H₂ stations.

Geographic Information Systems (GIS) are a powerful tool which can be used in many fields and applications. In addition to the geography of a region, information about the geographic entities is provided. The specific GIS software used for this project was QGIS 3. GIS datasets were used to understand the scooter distribution in the Netherlands, and their geographical relation to noise barriers which have the potential of being used as Energy Wall units.

This chapter aims to show how scooters are distributed in relation to noise barriers, supporting the idea that scooters (namely *snorfiets*) and noise barriers are both found in urban centers.

Information is openly available about attributes at the neighborhood, district, and municipality level, from the Centraal Bureau van de Statistiek (CBS) [52]. The available information includes the number of (*snorfiets*) scooters, land area, population, energy use, births, deaths, and more. A data set from the Rijkswaterstaat was obtained by request on behalf of the University, which provided information about noise barriers in the Netherlands, including the length, material, orientation, tilt, and other properties.

The Energy Wall is defined as noise barriers which run along highways to create a renewable energy production system utilizing already existent infrastructure. The aim is to reduce the cost of the energy production system as well as explore alternative pathways to sustainable mobility implementation. Noise barriers have the primary purpose of blocking highway noise created by fast or heavy vehicles from noise-sensitive residential areas. By retrofitting noise barriers with energy production units, namely solar panels and/or wind turbines, another function is added to the infrastructure unit. Populating the barrier with energy generating units adds significant value to it, transforming the barrier from a noise prevention civil structure to a combined energy generation unit.

By understanding the proximity of- and quantitative relationship between- scooters and noise barriers, the potential of Energy Walls as hydrogen refueling stations for scooters in the Netherlands can be assessed. The aim of this chapter is to identify regions where suitable noise barriers exist, areas in the Netherlands that have a high density of scooters, and eventually couple these two factors to find the regions with both suitable noise barriers and a scooter-rich characteristic. This concept can be applied to a nationwide, provincial, or municipal level in terms of the scooter distribution.

It should be noted that although this study considers the total number of scooters, sustainable scooter mobility is, at present, not a majority of the market share of scooters. Unless driven by legislation or otherwise, the transition to sustainable mobility will gradually grow and the share of (fuel cell) electric vehicles will increase. This can be driven and accelerated by the recognition of feasible locations, low cost stations, and low emission vehicles.

For the purpose of this project, GIS is used to establish the feasibility of using noise barriers to extend the renewable energy network. This has used nationwide data to establish the premise, however, in future work a more in-depth analysis of this data can be used to illustrate the specifics of the photovoltaic or wind energy potential of the noise barriers nationwide.

Scooter data and their distribution are analyzed in section 3.1, starting from a European level and narrowing down to national provinces and municipalities. Municipalities which seem attractive in terms of the number and density of scooters are identified. Section 3.2 concerns the *noise barriers* in the Netherlands, and their suitability to become Energy Walls based on stated suitability criteria. Once the scooter dense regions and suitable noise barriers are identified, the two are coupled in section 3.3. The methodology and estimation of the potential photovoltaic electricity production of all the noise barriers is given in section 3.4. Finally a comparison between the demand of the scooters in the vicinity of the noise barriers and the electricity potential is made in section 3.5 to understand what can be supplied and what the expected demand might be.

The findings of this chapter aim to present information about provinces and municipalities which might be worth examining in more depth concerning their potential to have Energy Wall units implemented and coupled with sustainable mobility systems.

3.1. SCOOTER DISTRIBUTION

The assessment of scooter distributions is taken from a broad European perspective and progressively narrows down to a select number of attractive locations. The number of scooters is the main metric used to identify suitable areas but in cases where interest exists, the land area, population or density of scooters relative to these attributes is also examined.

3.1.1. SCOOTERS IN EUROPE

The number of scooter registrations in Europe is available in [7]. The Netherlands is ranked 6th highest. A closer look at the land area and populations of the countries with the highest numbers of scooters shows that the Netherlands has the smallest area of the 5 predecessors,

as well as a relatively high population. The population density of the Netherlands is the highest making the country very attractive in terms of implementing a sustainable mobility project for urban scooters.

Figure 3.1 shows the number of scooters for all European countries as well as the population density for the ten countries with the highest numbers of scooters. From the figure it becomes obvious how much higher the population density of the Netherlands is as compared to other European countries. Combined with the high number of scooters, it is not unreasonable to consider the Netherlands as one of the nations where implementation of such a system looks promising.

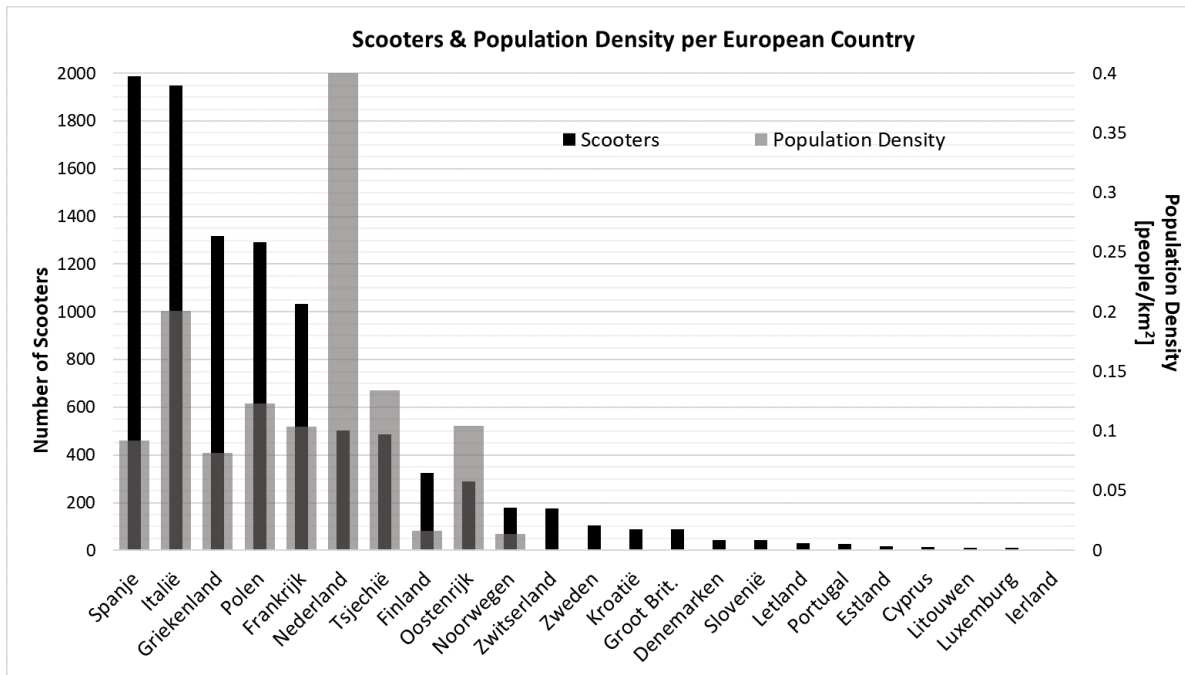


Figure 3.1: Number of Scooters [7] and corresponding population densities in European countries

One limitation of using the total land area is that countries other than Holland may have cities which are densely populated and countryside which is sparsely populated. This could be mis-characterized by the nationwide population density. Other countries may also have more sparsely populated countryside or mountainous regions, accounting for their higher land area. For example, in Greece around half the population lives in the capital, and the other half is in other cities or towns.

Hence, implementation of a hydrogen refueling station should be based on the GIS data of major urban centers in Europe rather than country-wide data. A more accurate study can be carried out for the major urban centers of Europe, however this requires a collection of GIS data for each one of these and this has been deemed out of the scope of this project; it is definitely an interesting point for future work. The purpose of a European country level comparison was to verify whether the Netherlands was a feasible choice, and it seems to be so. In conclusion the benefits of having sustainable refueling stations for scooters implemented in the Netherlands are the short distances, small land area, and high population density.

3.1.2. PROVINCE LEVEL IN THE NETHERLANDS

The Netherlands is split into 12 provinces. After establishing that the Netherlands is a suitable choice for implementation in terms of number of scooters and population density at the European level, some aspects about the provincial distribution of scooters are studied.

Two metrics were looked at, namely the total scooters and the number of scooters per 1000 residents. Figure 3.2 shows the value of these metrics for each province. Desirable provinces are identified as those which have high values of total and per capita number of scooters. A high value of both is desirable since it implies that the province has both a high number of total scooters and that there are many people who are scooter owners.

South Holland demonstrates high values for both metrics, followed closely by North Brabant and North Holland. It should be noted that Amsterdam is found in North Holland, while Rotterdam and the Hague are in South Holland; these are three of the most populous cities of the country. Therefore, it is worthwhile looking into these three provinces for barriers suitable to retrofit as renewable energy generation units.

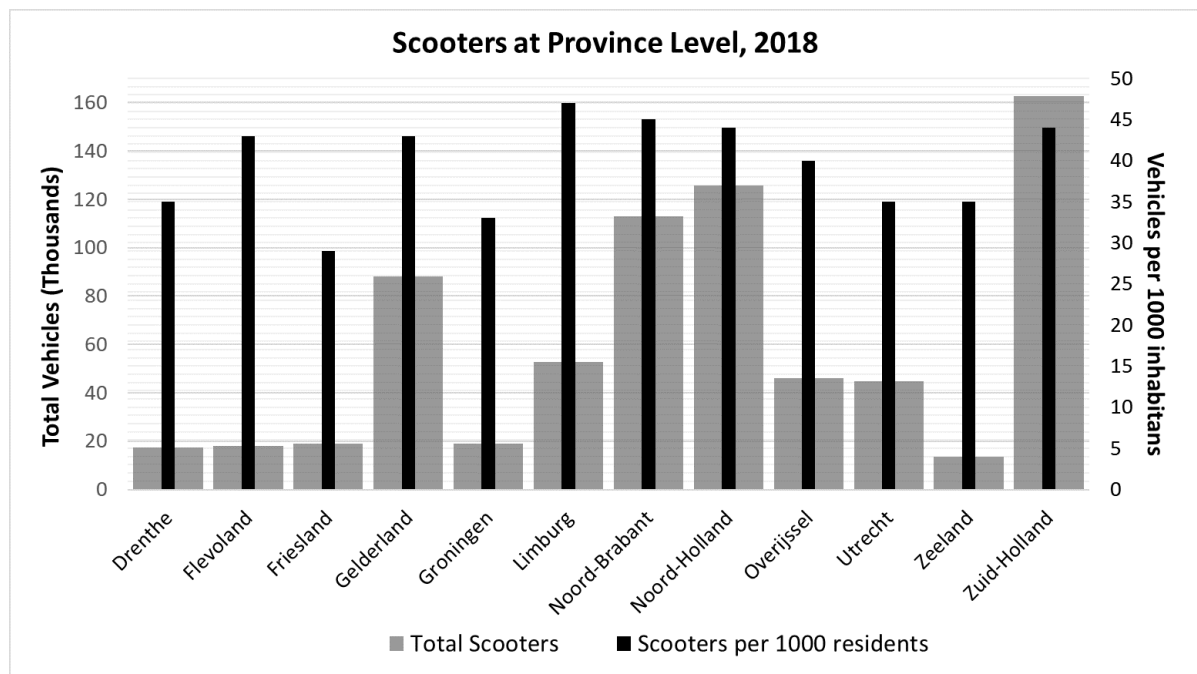
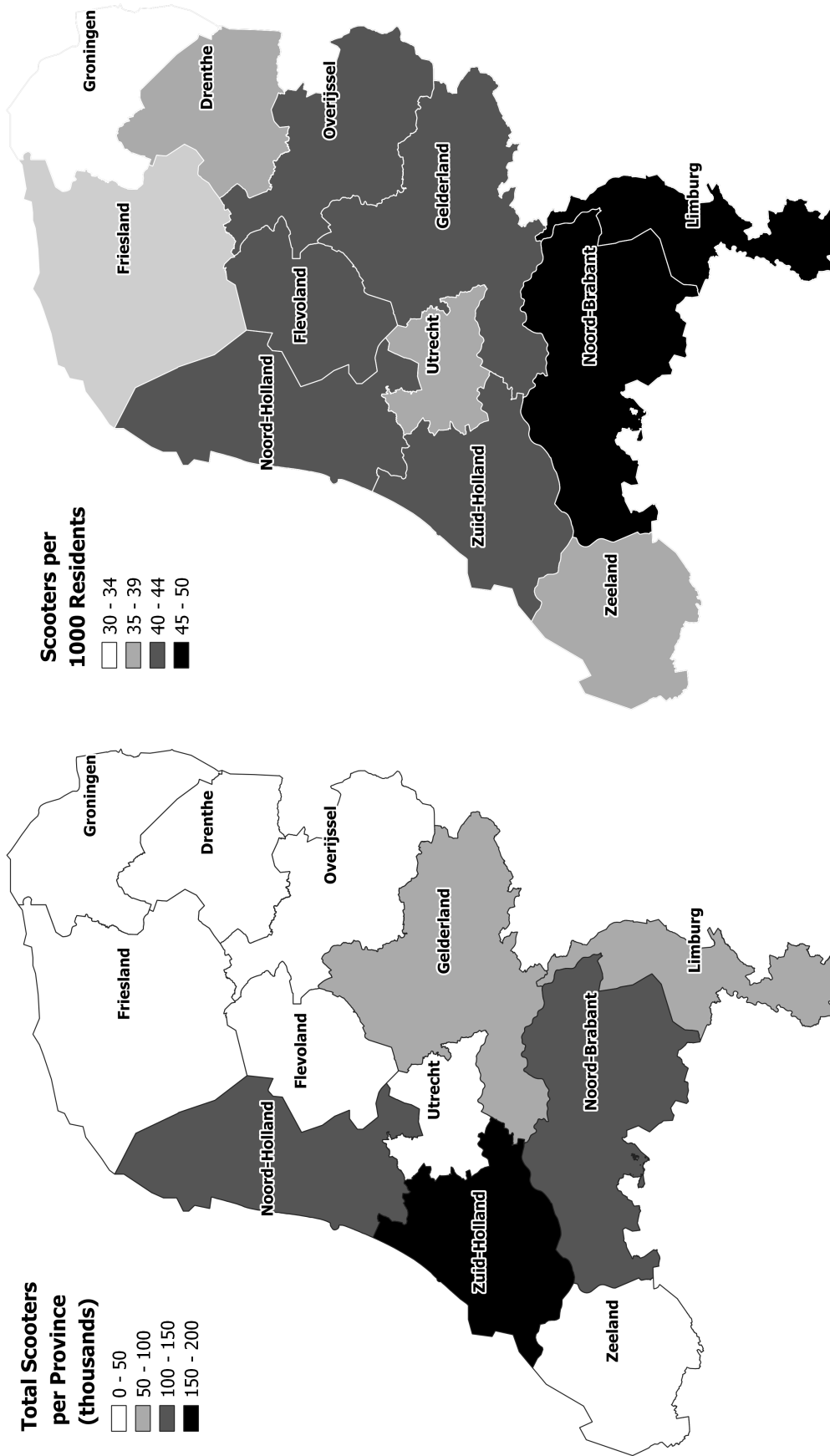


Figure 3.2: Graphical Representation of Total Scooters and Scooters per 1000 Residents

The distribution of the total number of scooters per province is shown in the map of figure 3.3a. The provinces with the highest values were South Holland, North Holland and North Brabant respectively. Figure 3.3b shows the scooters per 1000 residents for each of the provinces within the Netherlands. Limburg and North Brabant are in the highest category with 47 and 45 scooters per 1000 residents respectively. North Holland and South Holland follow with 44 scooters per 1000 residents each. This metric concludes that there is a high number of scooter users out of the entire population.



(a) Total Number of Scooters in each of the Dutch Provinces (b) Scooters per 1000 residents in each of the Dutch Provinces

Figure 3.3: Total and per Capita distribution of scooters in the provinces of the Netherlands

3.1.3. MUNICIPAL LEVEL DISTRIBUTION

The municipal level provides a smaller size of regions and thus a better understanding of where the majority of scooters are concentrated. Amsterdam, Rotterdam and the Hague have a disproportionately higher number of scooters than the rest of the municipalities, which is reasonable given they are the three most populous cities of the Netherlands. They have over 10,000 scooters each.

The municipalities with lower than 4,000 scooters were excluded from this study as the likelihood of a successful implementation of a hydrogen scooter mobility project may not be economically attractive at this point due to the low number of scooters and their potential sparseness in the area, both of which ultimately lead to low system utilization.

Table 3.1 lists the municipalities with over 4000 scooters, the scooter density per area, and the per capita value. These are also shown on the map in figure 3.4. The area around the noise barriers within these municipalities is what will be investigated in the latter sections.

Ranking	Municipality	Total Scooters	Scooters per km ²	Scooters per 1000 residents
1	Amsterdam	18750	85	22
2	Rotterdam	12280	38	19
3	's-Gravenhage	10325	105	20
4	Utrecht	7640	77	22
5	Almere	6950	28	35
6	Zaanstad	6915	83	45
7	Apeldoorn	6830	20	43
8	Eindhoven	6820	77	30
9	Haarlemmermeer	6655	36	46
10	Tilburg	6365	53	30
11	Breda	5705	44	31
12	Amersfoort	5595	88	36
13	Haarlem	5320	166	33
14	Groningen	5305	52	26
15	Enschede	5250	37	33
16	Emmen	4975	14	46
17	's-Hertogenbosch	4625	39	30
18	Zwolle	4515	38	36
19	Alphen aan den Rijn	4510	34	41
20	Nijmegen	4495	78	26
21	Alkmaar	4450	38	41
22	Ede	4405	14	39
23	Arnhem	4350	43	28
24	Zoetermeer	4065	110	33
25	Westland	4040	45	38

Table 3.1: Top 25 Municipalities in terms of total scooters (>4,000)

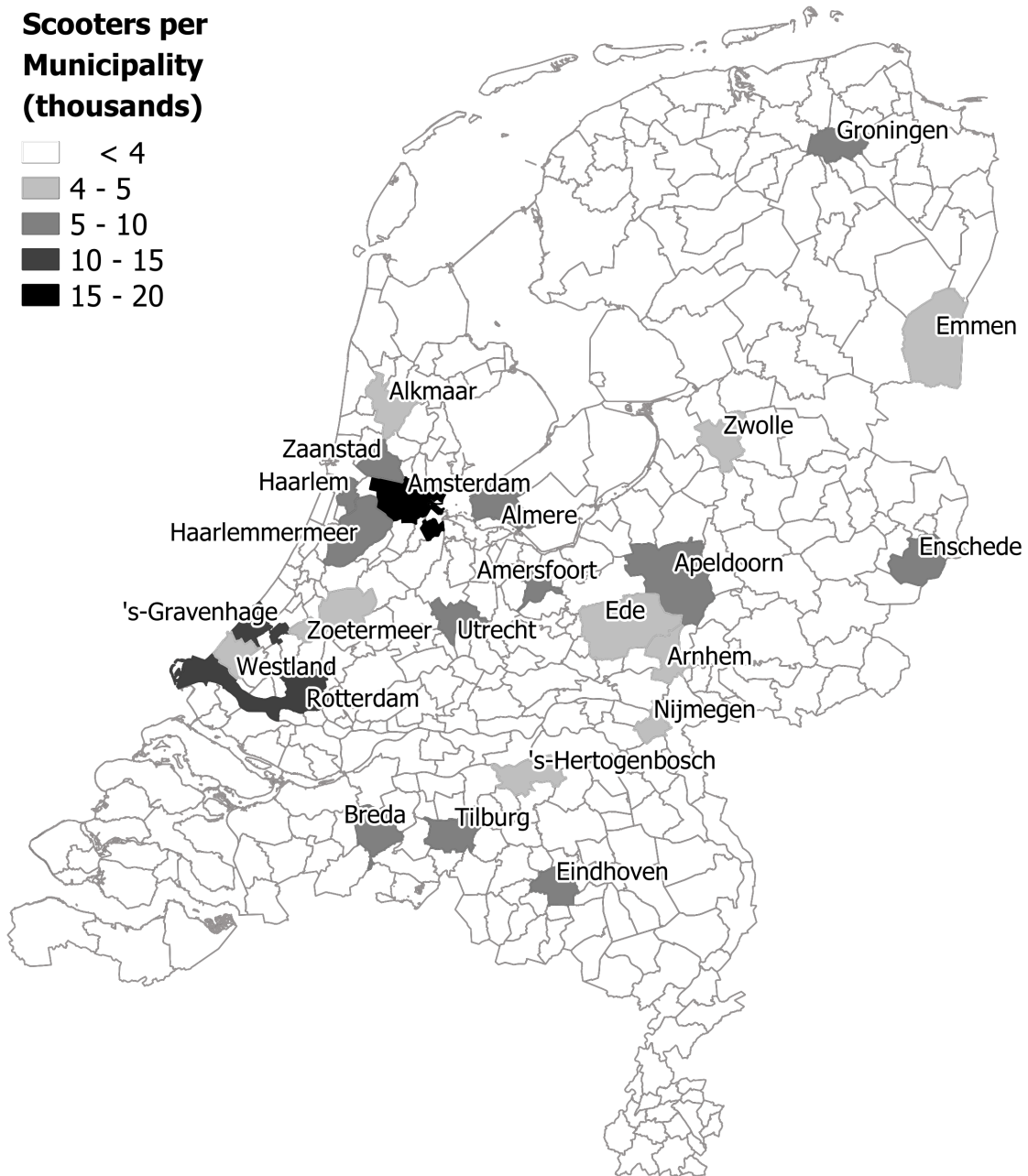


Figure 3.4: Municipalities containing over 4,000 scooters in the Netherlands

3.2. NOISE BARRIERS (AS ENERGY WALLS)

Research has been conducted around the idea of using noise barriers as structures for renewable energy components. In [53] an extensive overview of implemented examples is given. One notable example is from the Netherlands, of a bi-facial PV system which was implemented well before renewable energy was an attractive investment.

The idea is certainly not new, but not widely implemented either. A list of photovoltaic noise barriers installed in Europe as early as 1989 is given in [54]. A specific system was installed in Switzerland and produced roughly 100 MWh annually. A system in the Netherlands was also implemented not long after that, yielding 176 MWh annually. Since then, various projects have taken off in Europe, especially Switzerland, Germany and Italy. The system sizes range from tens of kilowatts to a few megawatts. The largest system listed in [54] is 2.65 MW along the A3 in Germany (Aschaffenburg) which was installed in 2009.

The ministry of Infrastructure and Water Management of the Netherlands (Rijkswaterstaat) is also active in implementing the "solar highways" concept by using photovoltaic panels as the building material itself rather than add them on to the structure; this project is partnered with TNO and SEAC [55, 56].

There has not been much research in the field of decentralized micro wind turbines, possibly due to their high current cost, the limited power output, and the difficulties in predicting or modeling the site conditions due to the structure and vehicle activity. The province of South Holland has set up a series of innovative concepts, outlined in [27]; the Energy Wall is included in these concepts. Experimentation was carried out on a noise barrier in South Holland, under the initiative of TU Delft, whereby wind turbines were added to the barrier [57] and the characteristics of wind flow around the barrier was observed.

Solar energy at this point is deemed a more suitable option for the retrofitting of noise barriers. The next subsections focus on defining the suitable range of noise barriers which can be converted into Energy Walls. First the suitability criteria are defined and then the filtering process is described for each criterion. A summary of the remaining noise barriers is provided in the last subsection. This data set will move on to be coupled with scooter rich municipalities.

3.2.1. NOISE BARRIER SUITABILITY FILTERS & CRITERIA

The following sections focus on the filtering and removal of unsuitable noise barriers based on material and tilt direction. The aim was to obtain a data set of suitable noise barriers to analyze further by estimating the potential energy yield (section 3.4). Although more detailed filtering criteria may be applied, using the aforementioned filters allows for the available noise barriers to be narrowed down significantly for the purposes of this project.

For consistency with previous related projects, a **segment** is defined as "a length of noise barrier along which the attributes are the same" and an **entity** is defined as "a length of noise barrier where the properties such as height or material may vary". Multiple connected segments form one entity.

The total length of noise barriers in the Netherlands is 1071.4 km, made up of 6138 segments. A map of the total (unfiltered) noise barriers is shown in figure 3.5.

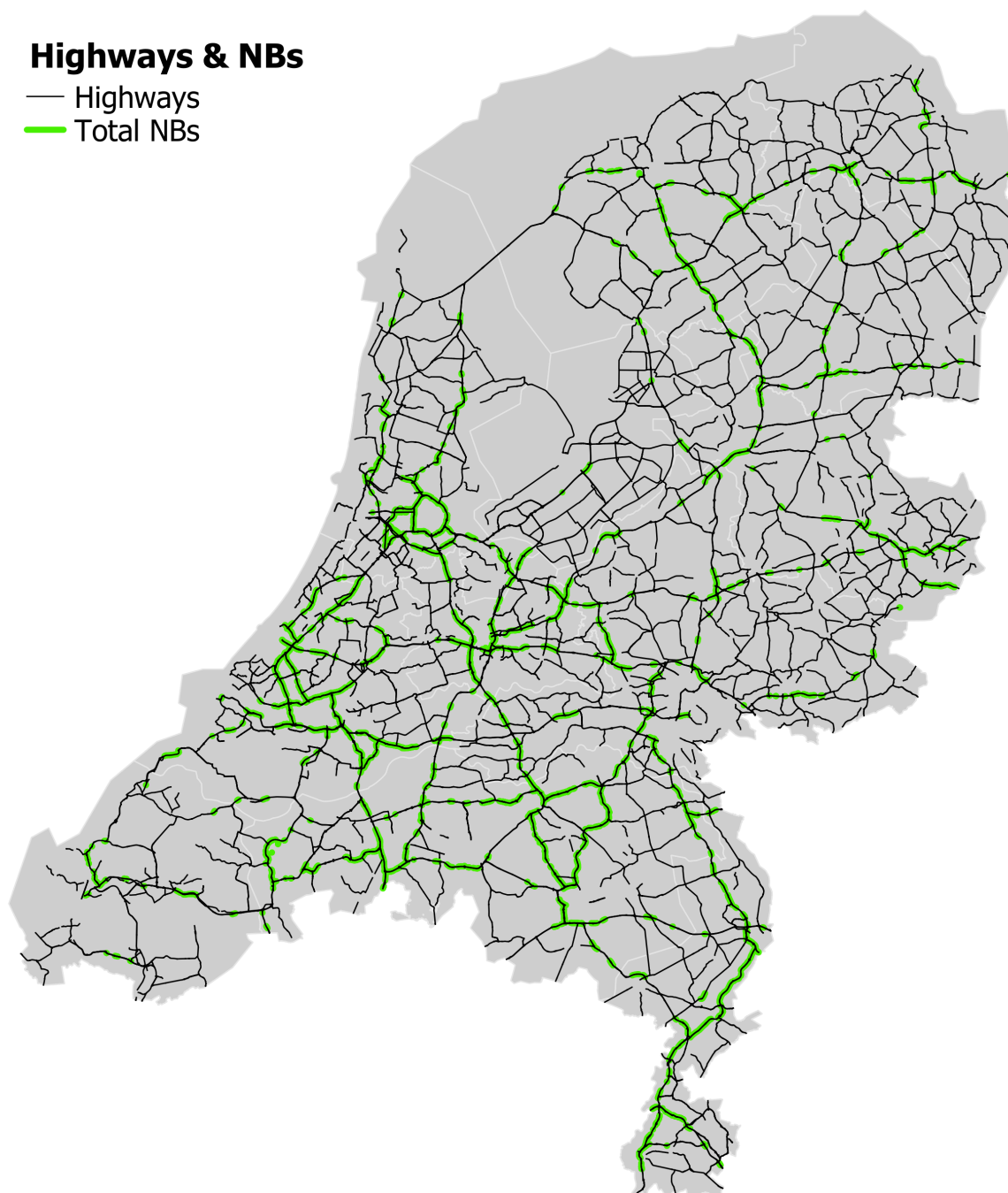


Figure 3.5: Roads and Noise Barrier Entities in the Netherlands

3.2.2. MATERIAL FILTER

Noise barriers are made of various materials ranging from concrete to plastic, metal, wood, or earth embankments. Previous studies argued that some noise barrier materials were deemed unsuitable to be turned into Energy Wall units [8]. This was on the basis of material strength or likeliness of vegetation growth on the noise barrier material. A length of 577 km, or 53.8% of the total length of noise barriers was removed from the data set due to their unsuitable material. This left 494 km of suitable noise barriers.

3.2.3. TILT DIRECTION FILTER

The tilt of noise barrier affects both the suitability of a barrier to become an Energy Wall and the energy potential that the barrier may offer, however the latter is discussed in section 3.4. The suitability of a barrier is affected by the tilt when the barrier wall leans towards unfavorable directions. Of the material-filtered dataset, 58.4% are tilted in some direction, while the rest are simply perpendicular to the ground.

NON-TILTED BARRIERS

The barriers with no tilt were all deemed more or less suitable. The ones which were facing South were the most favourable, however if the orientation was North it is assumed that PV panels can be placed on the South facing side since the barrier is perpendicular to the ground. For the barriers which were oriented facing East or West, although it is not always the most favourable orientation, these noise barriers can potentially be bi-facially fitted and therefore their energy output per unit meter of barrier increases.

TILTED BARRIERS

The attributes which characterize the tilt are firstly, the angle of tilt which ranges from 10°-30° and secondly, the tilt direction, characterized by the data set as one of the following two categories:

- Forwards towards the road, figure 3.6a
- Backwards away from the road, figure 3.6b

The convention of forwards or backwards does not explicitly tell in which direction the barrier is tilted, therefore using the position of the barrier with respect to the road, one can understand the direction of tilt. The position is given in terms of 0, North, South, East, or West. The first, "0", describes barriers which are curved around road bends, in between roads, or other peculiar circumstances; Thus they have more than one or a variable position with respect to the road. The convention of the latter noise barrier positions is visualized in figures 3.6c & 3.6d, specifically for the North and South positions.

Barriers which are on the South side of roads should tilt forward towards the road for them to be suitable; likewise barriers which are on the north side of the road should tilt backwards away from the road. There may be some cases where the noise barrier is tilted *towards the South*, which is unfavorable. If the panel would be placed on the South face of a South-tilting barrier, self-shading occurs, even more-so when the sun reaches high altitudes; if it is placed on the North side, the energy yield is bound to be low and therefore the economic attractiveness and practicality of such an investment decreases. Therefore, the barriers with the following combination of tilt characteristics were removed:

- **Forward** tilting barriers on the **north** side of the road
- **Backward** tilting barriers on the **south** side of the road

This step in the filtering process removed 124 km (11.6% of total length) of the available barriers, leaving 370 km of suitable noise barrier length, which is rather significant.

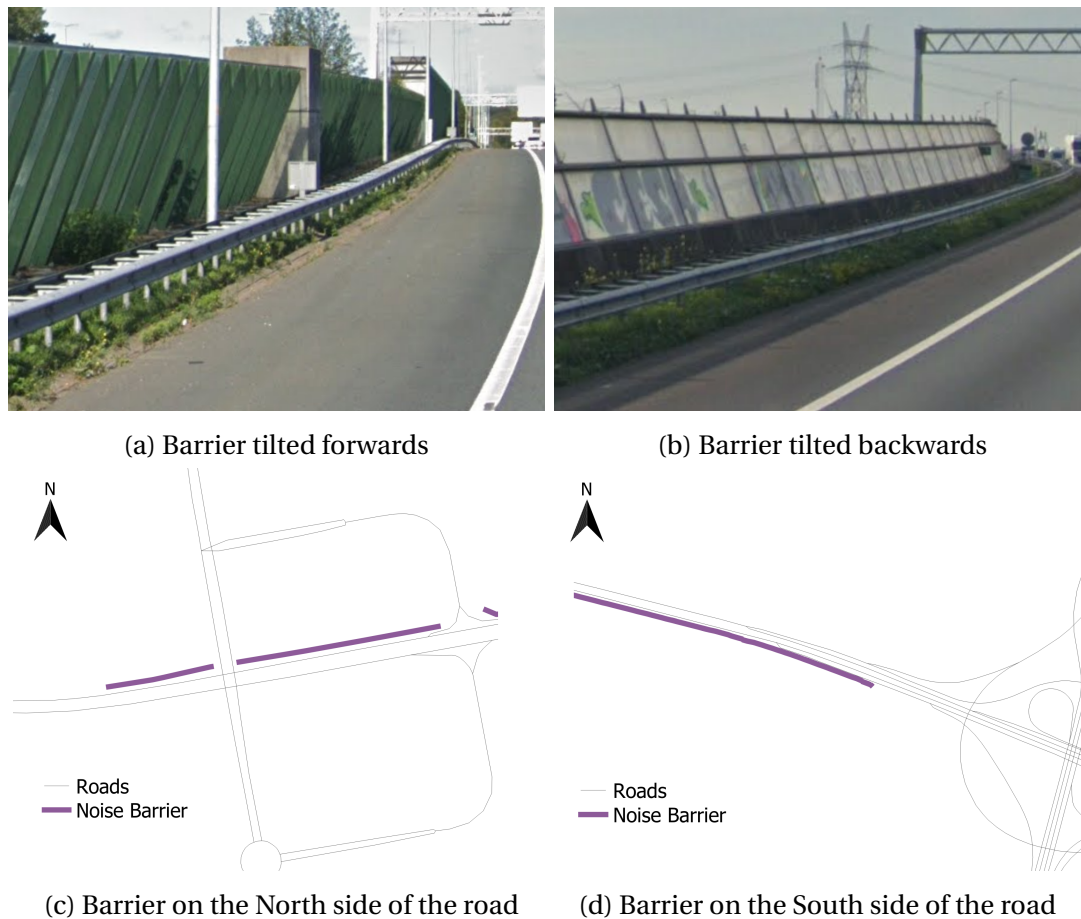


Figure 3.6: Barrier tilt & position characteristics

3.2.4. SUMMARY OF NOISE BARRIER FILTERING

From the total number of noise barriers, 65.5% were removed as they were deemed unsuitable to be turned into Energy Wall units. The percentages and lengths of the removed noise barriers are shown in table 3.2, with a breakdown of the categories within the encompassing filtering criteria.

Over half of the noise barriers were deemed unsuitable through this filtering process. Had a more in-depth methodology and filtering process been employed, it is expected that even more would have been filtered out. This process left **370** km of noise barriers (34.5% of total) that were suitable.

3.3. NOISE BARRIER AND SCOOTER DISTRIBUTIONS COUPLING

In order to find which areas would most likely succeed with the proposed hydrogen refueling station, scooter dense regions were coupled with suitable noise barriers. Figure 3.7 shows every municipality considered; the reader is kindly asked to refer to appendix D for more detailed figures of the top municipalities defined in section 3.1.3.

Filtering Criterion	Length [km]	Share of Total NBs
Unfiltered (Total) Barriers	1071.4	100%
Material	-577	-53.88%
Earth	399.6	37.31%
Wood Fiber Concrete	99.7	9.30%
Wood	50.7	4.73%
Growth Screen	11.3	1.05%
Stone	7.0	0.65%
Gabion	4.8	0.45%
Others	4.1	0.38%
Tilt	-124.4	-11.61%
Forward Tilt - North of Road	5.2	0.48%
Backward Tilt - South of Road	119.2	11.13%
Remaining Suitable Barriers	370	34.53%

Table 3.2: Unsuitable (Removed) Noise Barrier Characteristics and Lengths

3.3.1. TOP MUNICIPALITIES & SCOOTERS

The municipalities with the highest number of scooter registrations were identified in section 3.1.3 and listed in table 3.1. There were 25 municipalities which each had over 4,000 scooters; 15 with over 5,000; and 3 with over 10,000, each.

The 25 top municipalities contained 161,135 scooters in total. The top 15 contained 116,705 scooters. The top 3 contained 41,355. In terms of share of the total number of scooters, these values correspond to 24.6%, 17.8%, and 6.3% of the total scooter population respectively.

In conclusion, almost a quarter (24.6%) of the entire scooter population is found within 25 cities. There are over 40,000 scooters in 3 municipalities. Considering a scenario where 1% would be converted to hydrogen powered scooters, the 414 scooters would require roughly 37.3 MWh/year to produce the hydrogen to power their annual average distance.

3.3.2. NOISE BARRIERS IN TOP MUNICIPALITIES

Using the data set of filtered noise barriers (based on the criteria defined in section 3.2.1), the noise barriers which were found within these municipalities were singled out.

The total length of the barriers located within the top 25 municipalities is 156 km, which is 14.56% of the total length of noise barriers. This methodology was employed as these barriers are likely to have a significant and sufficient number of scooters within a close vicinity, and thus would benefit from a hydrogen production system aimed at scooters. Figure 3.7 shows the barriers in orange.

Of the municipalities listed in table 3.1, Nijmegen and Almere did not contain any noise barriers. The potential of the barriers within each municipality group is presented in table 3.3.

3.3.3. COUPLING

After coupling the municipalities with suitable noise barriers, the smaller divisions of land could be examined. The division of area after the municipal level is the district (wijk) and then the neighbourhood (buurt).

The distance between the selected noise barriers and neighbourhoods was calculated through the NNJoin plugin available in the QGIS software. The NNJoin plugin assumes the center point of the entities it analyzes, in this case the noise barriers and neighbourhoods. The result of this method is the number of scooters, and consequently theoretical hydrogen demand, around the selected noise barriers.

The distances considered acceptable depend on the distance a scooter would be "willing" to travel to refuel. The daily average distance a scooter drives is 2.5km, as explained in section 4.1. Figure 3.7 shows the distance between each neighborhood and the closest noise barrier entity. The white parts indicate the neighbourhoods within 2.5 km of the noise barrier; distances higher than this are shown in a grey gradient as denoted in the legend of the figure.

Using the methodology to estimate the PV energy potential as described in section 3.4 the same estimation can be carried out for the noise barriers found within the 25 municipalities. This way, the energy potential can be compared to the energy required to supply the scooters within these municipalities, and to understand what relation the two have.

The overall findings of the coupling process showed the following:

- The number of scooters in the top 25 municipalities is 161,135 (24.6% of total)
- The number of scooters in neighbourhoods within 2.5 km of the noise barriers is less: 135,370. This is a difference of 25,765 scooters.
- There are three municipalities which contain no noise barriers (Almere, Westland, Nijmegen). The number of scooters in these municipalities is 15,485.

The number of scooters in the neighbourhoods within 2.5 km of the NB are shown in the 2nd column of table 3.3 (found at the end of this chapter). The 3rd column shows the equivalent electricity demand for each group.

In view of the above the yield of noise barriers is estimated for the scooters presented in these municipalities.

3.4. PV ENERGY YIELD ESTIMATIONS

An initial PV yield estimation was carried out. This was done for the set of noise barriers deemed suitable in the entire Netherlands and for the set of noise barriers that were distinguished in section 3.3.2. The method of estimating the PV energy yield is by using correction factors to adjust the optimal energy yield of *one* PV panel according to the tilt and orientation characteristics of the barrier, and then multiplying this potential energy yield by the length of the barriers. The correction factors used are provided and explained below.

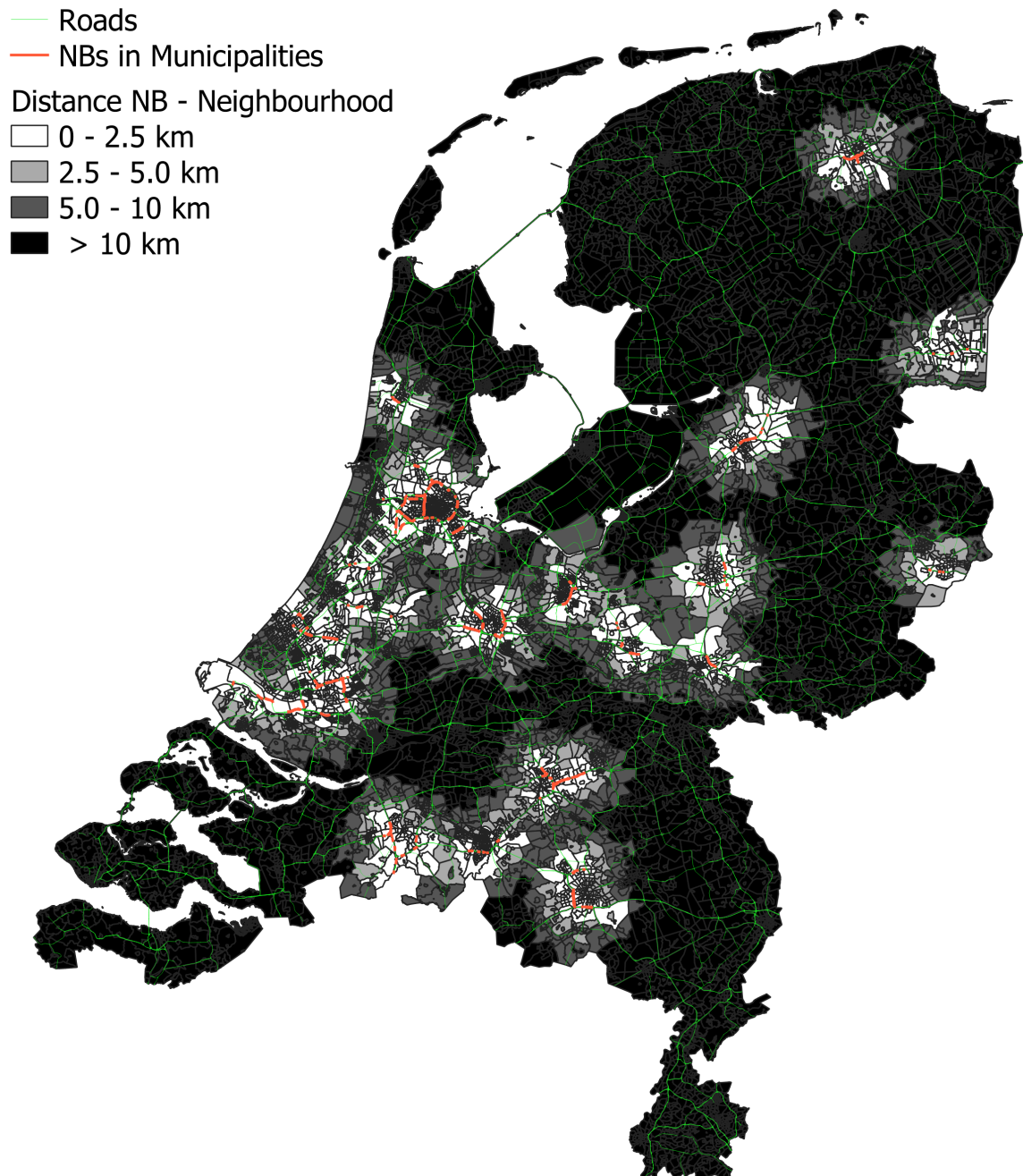


Figure 3.7: Distances from noise barriers in selected municipalities to nearest neighborhood

CORRECTION FACTORS

The tilt and orientation (t&o) are parameters which significantly affect the energy yield of the PV system and need to be taken into account during the process of estimating the energy potential of Energy Wall segments. This is accurately done on a location specific basis, however for the purposes of understanding the overall energy potential of the noise barriers, a simpler method of corrections is used rather than modeling every segment. The t&o

of the panels is inherently determined by the t&o of the barrier itself.

In [8] correction factors have been defined which adjust the optimal (maximum) energy yield according to the t&o of the PV panels. These have been reproduced in figure 3.8. The most appropriate orientation is towards the equator, i.e. south facing in the Netherlands. As discussed in [8] the effect of the orientation angle on the energy yield was more prominent as compared to tilt, which is also shown by the aforementioned figures. This approach gives an estimate of the solar energy potential, but the method is generalized in the sense that it does not take into account the differences in irradiation experienced in the different regions of the Netherlands or any obstructions to the horizon of the solar panel (such as tall buildings, trees, or other objects).

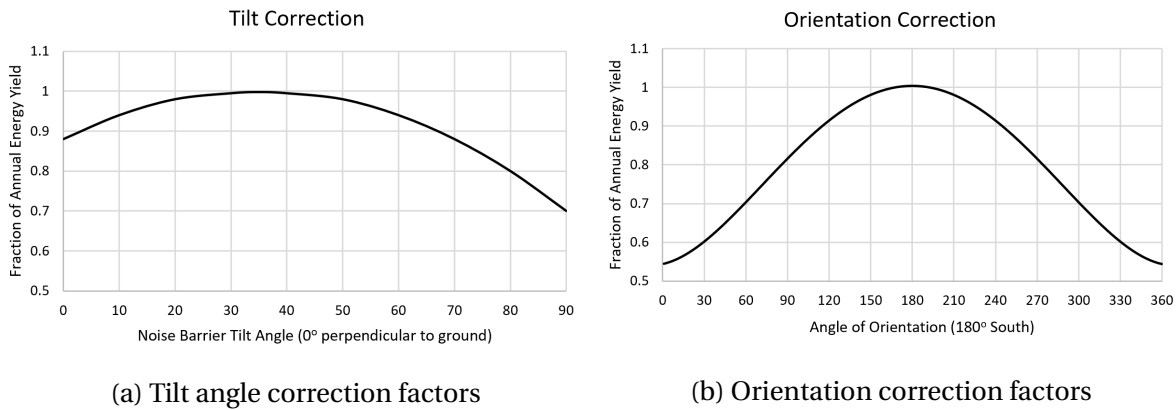


Figure 3.8: Correction factors on orientation and tilt as demonstrated by [8]

The tilt correction factor is expressed as η_{tilt} . The range of tilts that noise barriers experience are between 0° and 30° (corresponding to module tilts of 90° to 60°). For example, in Delft the optimal tilt angle is 38° (corresponding noise barrier angle of 52°), therefore the energy yield is likely to be between 70% and 90% of the optimal energy yield, according to figure 3.8a.

The orientation correction factor is expressed as η_{orient} . Figure 3.9 shows a map with the orientations, categorized between equal intervals of 45° . Concerning the orientation of the barriers, a range between 0° and 180° is provided by the dataset. North/South facing barriers are given 0° and 180° , while 45° and 135° are East/West. Figure 3.8b gives the value of η_{orient} according to the orientations seen in the map.

CALCULATION OF YIELD

The method of finding the annual electricity production, AEP_{NB-POT} , that can be potentially produced assuming the noise barriers are fitted with PV panels is shown in equation 3.4. The variables of this equation are explained below in order of appearance.

$$AEP_{NB-POT} = \eta_{NB} \times AEP_{PV-OPT} \times \frac{L_{NB} \cdot H_{NB}}{L_{PV} \cdot H_{PV}} \quad (3.1)$$

The first variable, η_{NB} is the overall correction factor of the noise barrier entity according to the tilt and orientation as described in the previous subsection. Using the data set

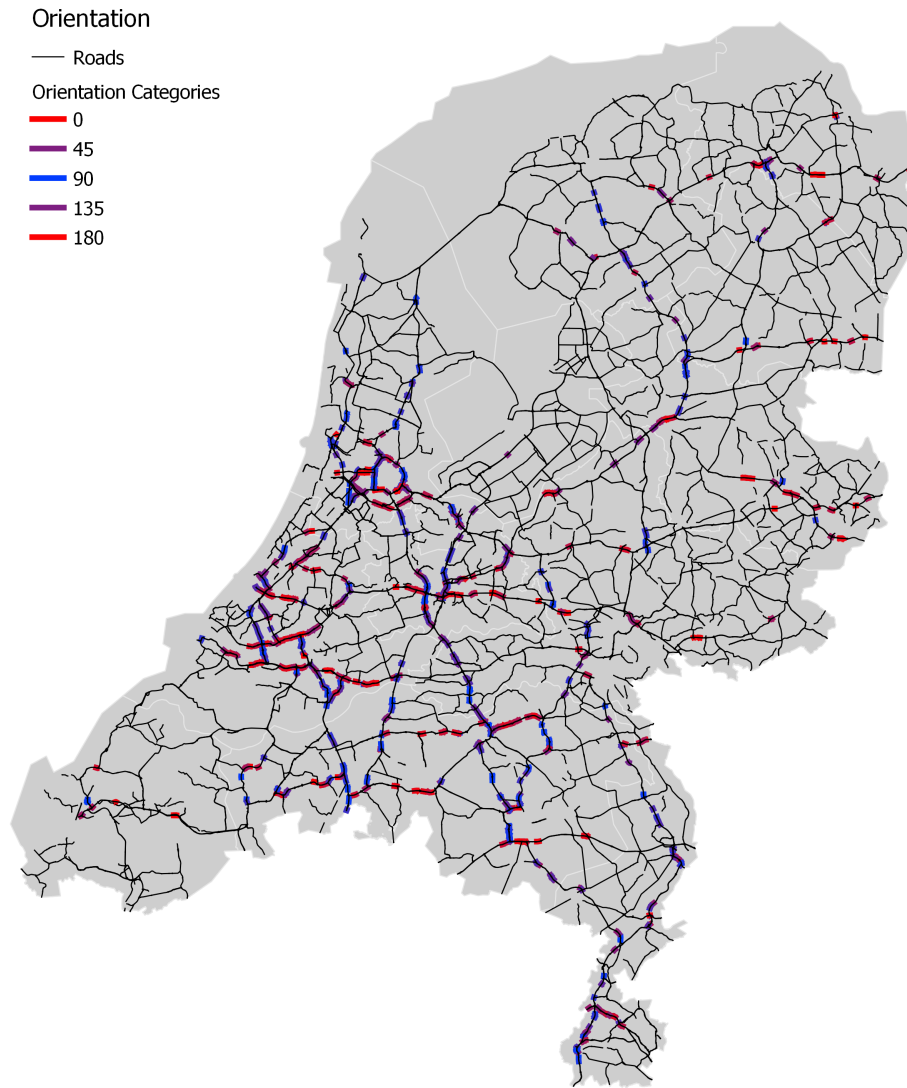


Figure 3.9: Noise Barrier Orientations

and lookup table functions, η_{tilt} & η_{orient} can be defined for every noise barrier entity. Therefore, the overall noise barrier correction factor is expressed as

$$\eta_{NB} = \eta_{tilt} \times \eta_{orient}$$

PVGIS [58] is a tool developed by the European Commission which gives information about photovoltaic characteristics, weather stations, and other handy tools used when designing a PV system. It provides the annual electricity production, AEP_{PV-OPT} , for optimally tilted and oriented PV panels. PV panel capacity ranges between 200 and 450 Wp, therefore the middle value of 325Wp was used; the dimensions assumed were $1 \times 1.6 \text{ m}^2$, a common size of commercial panels. The annual energy production of a 1-panel configuration changes according to the location. The middle value of the electricity generation potentials was used for this study, which was 275 kWh/panel/year.

The next step is to estimate the number of panels that can fit on the barrier. The length, L_{NB} is given by the data set, however the height is not. Noise barrier heights range between

1 and 10 m [59]. As this is a simplified study to understand the rough potential, the amount of usable height on the noise barriers, H_{NB} is assumed to be 2 m, allowing for 2 rows of solar panels to be placed on the barrier in landscape position.

The size of most standard industry panels is around $1.6 \times 1 \text{ m}^2$ ($L_{PV} \times H_{PV}$). If a safety factor of 1.2 (20% of the panel size) is taken into consideration, given there may be areas where panels cannot be mounted (such as the connection points between barrier entities) the effective area that panels require becomes 1.92 m^2 . Thus, a part of equation 3.4 can be simplified to: $\frac{H_{NB}}{L_{PV} \times H_{PV} \times 1.2} = \frac{2}{1.92} \approx 1$.

3.4.1. NATIONWIDE POTENTIAL

Using the above mentioned methodology to find the AEP of the suitable noise barriers, the noise barrier PV potential in the Netherlands was found to be

$$AEP_{NB-POT} \approx 60.1 \frac{\text{GWh}}{\text{year}}$$

This potential corresponds to a length of 370 km of barrier walls, and is corrected for the orientation and tilt. The barriers are assumed to have one side fitted with panels, however this value could potentially increase assuming the East or West oriented (non tilted) walls have both sides fitted with panels.

In [60] the potential along the noise barriers was also investigated for a number of European countries, and the Netherlands was included. In 2004, the time of writing of that paper, there were 475.9 km of noise barriers along highways and 444.6 km along railroads. The PV potential along these was found to be 91.8 GWh/year for the highway barriers and 65.6 GWh/year for the railroad barriers. The value calculated above is in the same magnitude range but lower than the values mentioned in [60]. However the value calculated is over a shorter length of barriers.

POTENTIAL PER UNIT LENGTH OF ENERGY WALL

Normalizing the energy per unit length helps compare the value calculated and the value presented in [60]. The potential calculated above per unit length of noise barriers was 162 MWh/year/km, given a length of 370 km.

The aforementioned paper [60] found that the potential per unit length was 193 MWh/year/km and 147 MWh/year/km for the highway and railway barriers respectively. The total length of noise barriers in the paper is also considerably larger. Nonetheless, the value calculated above is well between the range provided by the report in [60].

3.4.2. POTENTIAL OF SELECTED MUNICIPALITIES

Each municipality differs in size, therefore the potential of the NBs in each separate municipality is calculated. This is further cross checked with the number of scooters in each corresponding municipality group and the equivalent electricity demanded. Ultimately this will distinguish the regions where a hydrogen refuelling station would be feasible.

The municipalities, neighborhoods and noise barriers which were examined are shown in figure 3.7. There were cases where some neighbourhoods were close to two different bar-

riers, sometimes in different municipalities, such as the case of The Hague & Zoetermeer. Some of the municipalities overlap or border, therefore these were grouped. More detailed maps of the groups can be seen in appendix D. The potential of the noise barriers within each municipality (or group of municipalities) was calculated using the method described in section 3.4.

The total cumulative potential electricity generation for the NBs which are within the region of the top 25 municipalities was found to be $\sim 25.8 \text{ GWh/year}$. The NB length and corresponding potential for each municipality (group) is shown in table 3.3 (4th and 5th columns). The Amsterdam group had the highest potential, followed by Rotterdam and Den Bosch. The group of Den Haag and Zoetermeer were ranked 6th, preceded by Utrecht and Eindhoven. The NB energy potential is plotted in figure 3.10.

The potential per unit length was also calculated for the noise barriers. The values range between 117.8 and 212.6 MWh/km/year, with an average of 159.8 MWh/km/year. Higher values imply that the municipality in question has a higher number of barriers which may be south facing for example. A more suitable t&o barrier will have a higher yield per km. Zwolle has the highest yield per kilometer.

3.5. COMPARISON OF POTENTIAL TO SCOOTER DEMAND

The feasibility of a noise barrier refuelling station is assessed by comparing the electricity demanded to produce the hydrogen to fuel the scooters with the electricity production potential of the noise barriers in the proximity of these scooters.

DEMAND CALCULATION

In short, the method of calculating the electricity required per scooter is as follows: On average, a scooter drives 2.5 km each day [7], therefore covering 912.5 km annually. One hydrogen canister provides a 25 km range (city mode) with 45 g_{H₂} [13, 46]. Therefore, for one year a scooter would require 36.5 canisters, or 1.6425 kg_{H₂}. Assuming an electrolyzer efficiency of 55 kWh/kg_{H₂} [61], **one scooter needs 90.34 kWh/year** of electricity for hydrogen production to travel its average annual distance.

NATIONWIDE COMPARISON

In the Netherlands there are 655,965 scooters in the < 50 cc category (snorfiets). In the scenario where 100% of the scooters in the Netherlands were fuel cell powered, and using the assumptions above, the demand for energy would be $\sim 59.26 \text{ GWh/year}$.

The difference between the potential and demand was $\sim 800 \text{ MWh}$. Hence based on these assumptions and calculations the noise barriers could provide the base for a PV system which would satisfy the electricity demand for the current number of scooters.

MUNICIPAL COMPARISON

Narrowing down to the municipal level allows for the feasibility of more specific regions to be examined. The potential of the NBs within the top 25 municipalities was calculated in the preceding section. The neighbourhoods in close proximity to said noise barriers are shown in figure 3.7 (more detailed maps in appendix D). The number of scooters contained

within these neighbourhoods is also known. Hence, a value for the electricity demanded can be assigned to each municipality group.

Considering a distance of 2.5 km, the number of scooters nearby the NBs of each municipality is shown in the 2nd column of table 3.3, next to the equivalent electricity demanded for those scooters.

The total number of scooters considered here are 135,370 representing 20.6% of the total scooter population of the Netherlands. Cumulatively, these scooters would require 12.22 GWh/year. The cumulative potential of the noise barriers within the top 25 municipalities is 33.64 GWh/year which is more than double the demand requirement by the scooters in the municipalities. The reason for the individual municipal analysis is to understand which municipalities can supply the scooters in their vicinity.

The aim of this was to understand how many scooters or what percentage of scooters the noise barriers could provide for.

Figure 3.10 shows three values: the NB potentials annually in the top 25 municipalities (grey), the annual demand of the scooters within 2.5 km of these noise barriers (black), and the ratio between those two values (green).

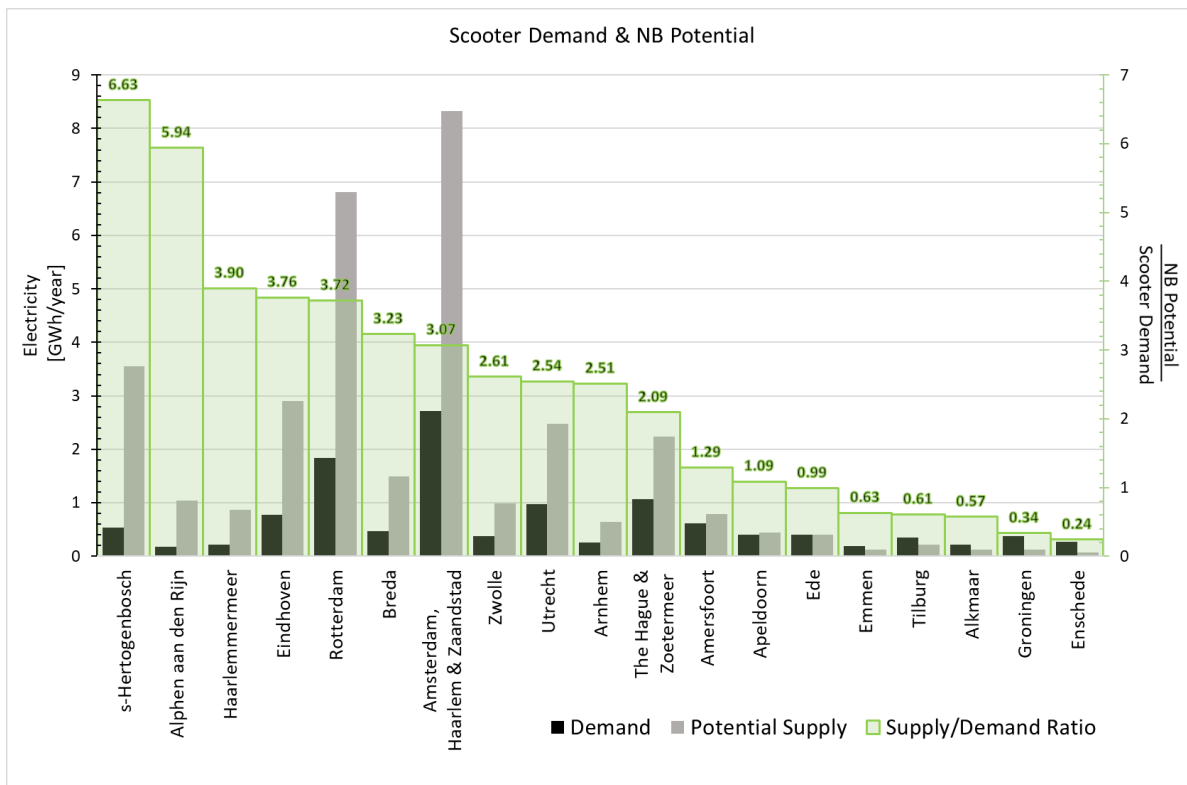


Figure 3.10: Electricity Demanded by Scooters and Noise Barrier Potential

In some cases there was a lower NB electricity production potential than the scooter electricity demand, namely in the last 6 municipalities shown in figure 3.10 (Ede, Emmen, Tilburg, Alkmaar, Groningen, and Enschede). The rest of the municipalities or groups had sufficient noise barrier potential to supply the *entire* fleet of scooters in the surrounding area. Based on the above analysis, there are sufficient lengths of noise barriers in close

proximity to scooter rich areas, which could provide the electricity to produce hydrogen to satisfy the demand these scooters may have. The choice of locations to proceed with in the detailed simulation of a case are areas which have a high NB potential to scooter demand ratio (at least ≥ 2).

Municipality Names	Scooters	Demand [GWh/year]	NB length [km]	NB Potential [GWh/year]	NB Potential to Demand Ratio
Amsterdam, Haarlem & Zaanstad	30015	2.71	48.82	8.33	170.6
Rotterdam	20280	1.83	41.92	6.82	162.6
The Hague & Zoetermeer	11865	1.07	16.93	2.24	132.4
Utrecht	10775	0.97	17.23	2.48	143.7
Eindhoven	8520	0.77	18.22	2.90	159.1
Amersfoort	6805	0.61	4.22	0.79	187.8
s-Hertogenbosch	5930	0.54	20.20	3.55	175.9
Breda	5130	0.46	8.21	1.50	182.4
Apeldoorn	4465	0.40	3.24	0.44	135.5
Ede	4465	0.40	2.77	0.40	144.3
Zwolle	4200	0.38	4.66	0.99	212.6
Groningen	4165	0.38	1.07	0.13	117.8
Tilburg	3940	0.36	1.41	0.22	153.3
Enschede	2980	0.27	0.46	0.06	140.2
Arnhem	2855	0.26	4.67	0.65	138.8
Haarlemmermeer	2450	0.22	4.56	0.86	189.0
Alkmaar	2435	0.22	1.07	0.13	117.8
Emmen	2150	0.19	0.70	0.12	176.2
Alphen aan den Rijn	1945	0.18	5.32	1.04	196.2

Table 3.3: Selected municipality data about scooters, electricity demand, noise barrier length & potential electricity generation

4

ENERGY WALL FUEL CELL HYDROGEN REFUELING STATION: A CASE STUDY

The objective of this study was to gain an understanding of feasibility and parametric relations between the system components of an energy wall with hydrogen production, storage and dispensing aimed for fuel cell scooter applications.

SYSTEM DESIGN

The entire system is visualized in figure 4.1, which is split into two main subsystems: electricity & hydrogen. This chapter aims to identify which factors influence the sizes, and consequently costs, of each subsystems parameters and final outputs. The objective is to produce hydrogen **reliably** and at a relatively **low cost**. The system is grid connected to assist in the intermittency issue of solar energy. The main assumptions that were made for the case study are:

- polycrystalline silicon PV panels
- constant number of scooters $N_{scooters}$ and hence hydrogen demand (HD) each day, week, month, year (D/W/M/Y)
- canister refiling done in bulk i.e. all the empty canisters are refilled at once

SYSTEM SIZE INFLUENCING FACTORS

When sizing such a system, there are various approaches which were considered. A few determining factors were identified, mainly being:

Number of scooters: this value was kept constant in order to compare the influence of changing the parameter sizes in the two subsystems. The demand was also assumed constant for each day and dynamic refilling was not taken into account. Rather, a quantity of hydrogen was required to refill a set number of canisters each day, week, month and year. The number of scooters assumed in this system is 100.

The **Energy Wall & electricity production** are determining factors since a significant part of the cost of hydrogen is the cost of electricity. Also, one of the desired characteristics

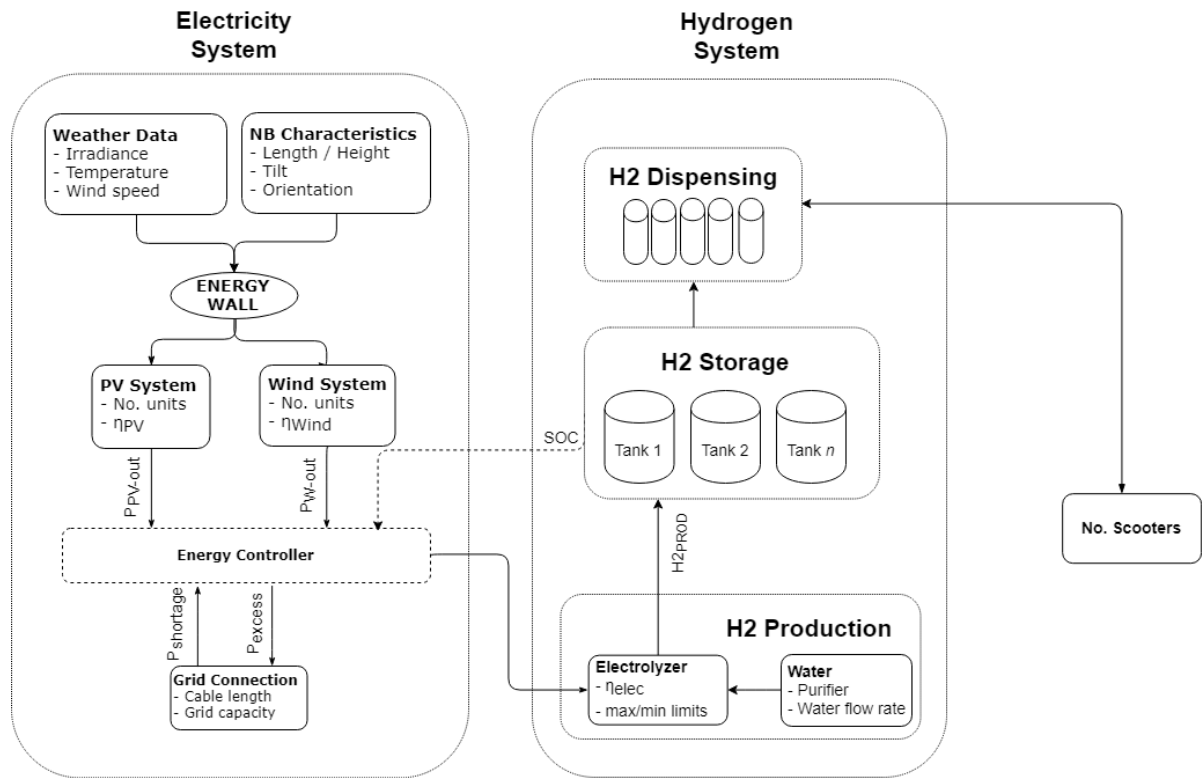


Figure 4.1: Flowchart of Components of Case Study System

of this system is to keep emissions associated with hydrogen production as low as possible. The electricity production is defined by the orientation and tilt of the noise barrier wall. The generation capacity is constrained by the length of the wall.

Finally, the **cost** of the system is what determines the feasibility of producing hydrogen for scooters using the proposed configuration. The cost modeling and results are examined in chapter 5.

4.1. SCOOTER DEMAND

Considering the scooters are the end users of this system, it is important to determine their daily hydrogen demand in order to size the electricity production system appropriately. The demand is proportional to the number of scooters in the case study. In this section the demand of one scooter is estimated.

The *daily* hydrogen demand of one scooter multiplied by the number of scooters gives the total daily hydrogen demand of the system. Similarly, it is assumed that the driving patterns of scooter users does not differ between seasons [], therefore the weekly and monthly demand are also constant throughout the year.

The hydrogen demand was estimated using two attributes:

1. Daily distance travelled per scooter, D_{Daily} [km/scooter]
2. Fuel efficiency of hydrogen, $\eta_{scooter}$ [kg/km]

D_{Daily}

Data was given on the distance per inhabitant per day and on the distance per inhabitant per year. The data was manipulated to find the distance per scooter per day and distance per scooter per year. The values are summarized in table 4.1. Values taken from literature are marked by a bold row number.

Row no.	Parameter	Value	Unit
1	Inhabitants	17,081,507	inh
2	Total scooters (2018)	1,076,443	sct
3	Total mileage by all scooters	939,000,000	km/year
4	Daily distance per inhabitant	0.16	km/inh/day
5	Annual distance per inhabitant	61	km/inh/year
6	Annual distance per scooter	872	km/sct/year
6	Daily distance per scooter	2.5	km/sct/day

Table 4.1: Scooter Demand Assumptions [7]

Provided the total number of scooters and annual total distance travelled (rows 2 and 3), the annual distance per scooter was found (row 6). The daily distance per scooter (last row) was then found accordingly. It was approximated as follows:

$$D_{Daily} = 2.5 \text{ km/scooter/day}$$

For the purpose of this project and due to a lack in weekly driving pattern data for scooters in the Netherlands, the daily hydrogen demanded has been assumed to be the constant each day of the week throughout the year. The driving patterns of scooters in the Netherlands does not seem to change through the seasons. [62]. Another assumption is that all scooters have the same driving patterns, which may not be the realistic case. However, it is assumed that the large distances travelled by some is balanced out by the occasional scooter users in any area. The value in table 4.1 for the number of scooters is both snorfiet and bromfiet; snorfiet are not commonly used for long distances however these are compensated by the journeys of bromfiet between urban centers.

 $\eta_{scooter}$

The driving distance that a pair of canisters can provide when operating in city mode is given as 50 km [13]. The city mode gives a conservative figure since it assumes many accelerations and decelerations. In highway mode, a driving pattern of fewer accelerations and decelerations and long hauls of constant speeds, the scooters range extends to 80 km. A full pair of canisters contains 90 g_{H2}. Therefore the fuel efficiency of the scooters was calculated as:

$$\eta_{scooter} = \frac{90 \text{ g}_{H_2}}{50 \text{ km}} = 1.8 \frac{\text{g}_{H_2}}{\text{km}}$$

 $N_{scooters}$

The number of scooters is one of the determining factors for the size of the hydrogen production system since this is sized to produce enough hydrogen to serve the surrounding

area. The option of producing surplus hydrogen and distributing it for other applications is also an option. On the other hand, producing less hydrogen than the set demand would mean the system is under-performing and consequently not meeting the objective of reliable production.

In this study a constant number of scooters was chosen to be modeled; the base case considers a fleet of 100 scooters. This is an arbitrary number and can be changed for sizing different systems and applications. Assuming this fleet size, the mass of hydrogen and electricity requirement to produce this is calculated below.

FINAL DAILY DEMAND PER SCOOTER

Considering the value of the average daily distance traveled by scooters (D_{Daily}) and the fuel efficiency of hydrogen model ($\eta_{scooter}$), the daily hydrogen production required can be found, shown in equation 4.1. The mass of hydrogen required daily per scooter, $DH_{scooter}$, is found to be $4.5 \text{g}_{H_2}/\text{scooter}/\text{day}$. The number of scooters is denoted by $N_{scooters}$, and is multiplied by hydrogen demand per scooter to find the total daily hydrogen demand (DH_{tot}). In this case the number of scooters is 100, therefore the total daily hydrogen production requirement is $0.45 \text{kg}_{H_2}/\text{day}$.

$$\begin{aligned} DH_{scooter} &= D_{Daily} \times \eta_{scooter} = 4.5 \frac{\text{g}_{H_2}}{\text{day} \cdot \text{scooter}} \\ DH_{total} &= DH_{scooter} \times N_{scooters} = 4.5 \times 100 = 450 \frac{\text{g}_{H_2}}{\text{day}} \end{aligned} \quad (4.1)$$

The electricity requirement to produce this hydrogen, assuming an electrolyzer conversion efficiency, η_{Elec} , of $55 \text{kWh}/\text{kg}_{H_2}$ (or Wh/g_{H_2}), the Electricity Demand (ED) is found in equation 4.2. For a fleet of 100 scooters the total daily electricity requirement is $24.75 \text{kWh}/\text{day}$.

$$\begin{aligned} EH_{scooter} &= DH_{scooter} \times \eta_{Elec} = 4.5 \times 55 = 245.7 \frac{\text{Wh}}{\text{day} \cdot \text{scooter}} \\ EH_{total} &= EH_{scooter} \times N_{scooter} = 24.75 \frac{\text{kWh}}{\text{day}} \end{aligned} \quad (4.2)$$

DISTANCE TO REFUEL

The distance that a scooter would travel to refuel was based on reasoning around the daily distance traveled. If the daily distance one travels is 2.5 km, it is not expected that that user would travel further than that *just* to refuel. Hence this is taken as one of the design constraints for the rest of the model set up.

The modularity of the canisters allows the possibility of transferring them to more convenient locations for distribution, such as super markets, gas stations, and local convenience stores frequented by scooter users. This concept would be particularly interesting to maximize the utilization of the station and its components. For the system to maintain the sustainability targets, the mode of transport which the canisters are moved with would also need to be carbon neutral, otherwise the purpose of reducing emissions in transport is somewhat defeated. One of the reasons this system was chosen to be small scale is to keep the overall capital costs low, and provide a localized, decentralized system available for the surrounding community.

4.2. LOCATION CHOICES AND CHARACTERISTICS

Chapter 3 presented an analysis of municipalities which seem attractive to install one of these systems. Locations with low NB potential to scooter electricity demand ratios (see figure 3.10) were not preferable for further study.

This section inspects the characteristics of a specific noise barriers located in three municipalities, two of which had high correlations between scooters and noise barrier potential as found in section 3.5. Meteorological data is highly site dependent therefore specific locations were chosen to examine as case studies in terms of their electricity and hydrogen production. Given a location, the irradiation profiles are more accurate as opposed to the generalized approach taken in the previous chapter. The chosen locations are provided below.

The simplification of a constant daily demand allows for the energy system influences to be examined independently (such as the orientation or size of Energy Wall). Barriers with desirable orientations are preferred.

4.2.1. ROTTERDAM

The extensive work by Nash [8] which focused on the Rotterdam Ring and given the scooter population in the municipality, Rotterdam is an interesting choice for this implementation. The chosen barrier is near the Rotterdam Noord train station, which could serve as a convenient location for people to exchange canisters. The chosen barrier is shown in figure 4.2.

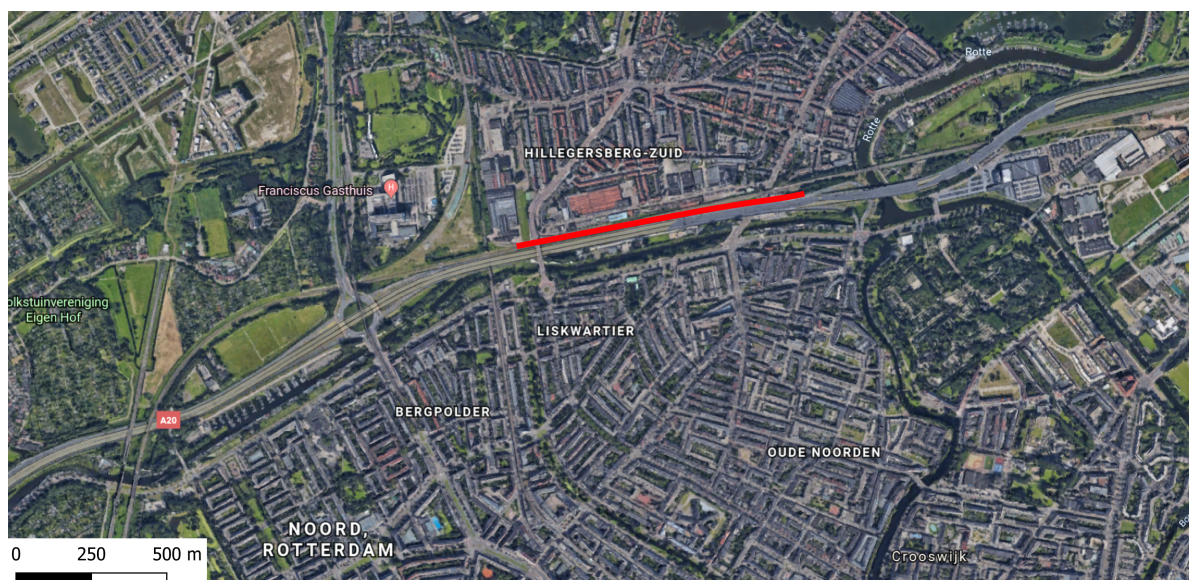


Figure 4.2: Noise barrier along A20 in North Rotterdam

4.2.2. AMSTERDAM

Being the most populated city in the Netherlands, Amsterdam offers ample opportunity for reduction of greenhouse gases, air pollution, and noise. Scooters are reportedly one of the

biggest nuisances in the city, often driving in designated cyclist paths (leading to the ban of mopeds on some cycle lanes in the city [63]). There is a ring road surrounding Amsterdam with sufficient length of noise barrier segments, pictured in figure 4.3. Two segments were deemed desirable, one in Amsterdam West and one in Amsterdam South-East (Zuid-Oost).



Figure 4.3: Amsterdam Noise Barriers

4.2.3. DELFT

Since this study is part of the TUDelft, and Delft is conveniently situated between two of the largest cities, Delft was also explored as a potential location for such a system implementation. Living here one notices a high number of (food) delivery scooters. This specific application would be interesting for further exploration. The noise barrier at the intersection of the N470 and the A13 highway, at the border between Delft and Pijnacker and close to the university would be a suitable choice for Delft, shown in figure 4.4.



Figure 4.4: Noise barrier along N470 in Delft

Location	Ams. West	Ams. Zuid-Oost	Rotterdam	Delft
Coordinates	52.3630 4.8424	52.3409 4.95268	51.9414 4.4778	51.9975 4.3936
Road	A10	A10	A20	N470
Length of Barrier	1021 m	771 m	952 m	498 m
Barrier Orientation (0° = North)	270°	150°	170°	170°
Barrier Tilt (0° = no tilt/perpendicular)	10°	10°	10°	10°
Max PV Capacity	347.1 kW	262.1 kW	323.7 kW	169.3 kW
Scooters in 1.5 km	2480	1145	460	1335
Scooters in 2.0 km	3635	1605	625	1680
Scooters in 2.5 km	4945	2470	1065	2290
Share of 100 scooters in 1.5 km	4%	9%	22%	7%
Share of 100 scooters in 2.0 km	3%	6%	16%	6%
Share of 100 scooters in 2.5 km	2%	4%	9%	4%

Table 4.2: Summary of Characteristics of Chosen Locations, Noise Barriers & Scooters

4.3. ENERGY PRODUCTION MODEL & SIZING

The energy model uses the location characteristics for irradiance and temperature over one year. The PV modeler used was PVGIS, an online free resource, which provides the power generation, irradiance (in-plane, diffuse and reflected), temperature, solar azimuth/altitude, and wind speed for a specific location. The annual hourly profile of a 1 kW panel was obtained through PVGIS, for a specific tilt and orientation according to the noise barrier characteristics.

4.3.1. NOISE BARRIER PHYSICAL ASPECTS & PV CAPACITY

The installed capacity of the Energy Wall depends on the number of panels (N_{panels}) which are placed on the NB. This value is limited by the physical size of the noise barrier, i.e. the length and height. This section shows how many panels can be placed on each of the case

study noise barriers. There are various types of modules, as explained in section 2.1.3, but it was established that the energy output does not increase in proportion to the price, hence polycrystalline modules are considered for this case.

The positioning of the panels on the Energy Wall were assumed flat in order to have high utilization of the surface area of the NB and save space. Were the panels to be tilted to the optimal slope, more space between rows would be required to avoid shading. The horizontal dimensions would also increase, which on a highway may not be possible due to passing vehicles.

To find the number of panels, N_{panels} , that fit on each noise barrier, equation 4.3 was used. It calculates the ratio between the size of NB surface to the size of the PV panels. A safety factor σ is taken into account for unusable space on the noise barrier such as the segment interconnections, or irregular surfaces where panel mounting is not possible. The length and height are denoted as L and H respectively, with the corresponding subscripts NB and PV where applicable.

$$N_{panels} = \frac{L_{NB} \times H_{NB} \times \sigma}{L_{PV} \times H_{PV}} \quad (4.3)$$

Panels are commonly rectangle shaped, with common dimensions being $1m \times 1.6m$. Therefore the denominator $L_{PV} \times H_{PV}$, is assumed as $1.6m^2$. The PV panels assumed are polycrystalline silicon, with an efficiency of 14%.

Noise barrier heights can range anywhere between 0.5 and 5 meters. For each case study, the barriers chosen were at least 2-3 meters high (verified using GoogleMaps StreetView). Therefore it is assumed that two rows of PV panels can be fitted on to the barrier. The configuration is shown in figure 4.5. The example takes a noise barrier section of 2 m length and at least 2 m high. Allowing a 20% safety factor for σ , equation 4.3 becomes:

$$N_{panels} = \frac{L_{NB} \times 2 \times 0.8}{1 \times 1.6} \approx L_{NB}$$

The power rating of solar panels varies depending on the technology used. Typically the rating ranges between 250 and 400 W_p per panel. A panel rating of 340 W_p is reasonable in this range; the rating per square meter (using a $1.6m^2$ panel area) is $212.5 W_p/m^2$. [64].

4.3.2. PV SIZING LIMITATIONS

The size of the Energy Wall electricity production system is limited by two main factors. The first, more active constraint is the size of the grid connection capacity. As discussed in section 5.2.2, in the interest of keeping the system cost low, the grid connection capacity should be kept under 175 kW. With the panel capacity given above as 340 W_p /panel, this limits the system to 515 panels. If a higher capacity such as 400 W_p were used, this would reduce the number of panels to 438 (77 fewer panels with 60 W_p /panel increase).

The second constraint is the physical size of the noise barrier. This is the maximum length that can be utilized to install solar panels upon. Given this, equation 4.3 and the length of the noise barriers, the maximum installable capacity is shown in table 4.2. The Rotterdam and Amsterdam barriers show capacities higher than the grid limit, therefore some of the barriers would not be fully retrofitted.

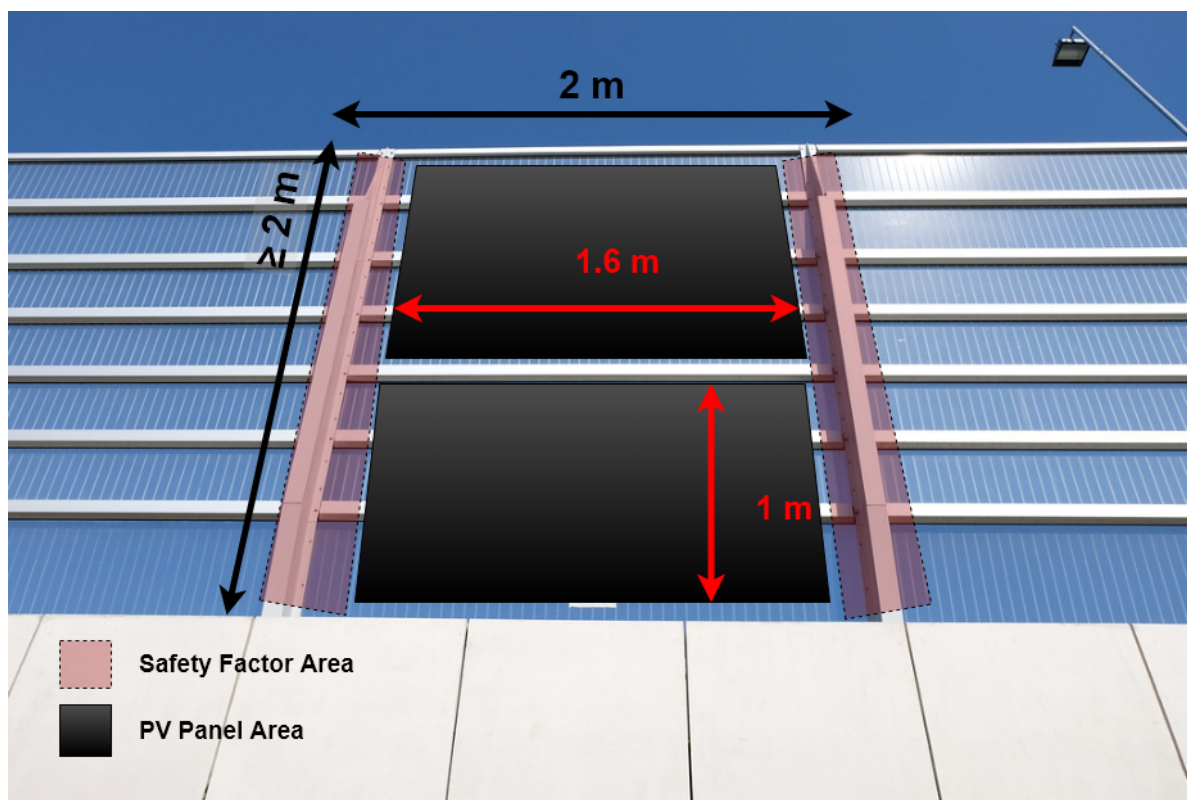


Figure 4.5: Schematic of PV Panels on Noise Barrier

4.3.3. MODULAR ENERGY WALL SEGMENTS

The concept of using modular Energy Wall segments, defined as a specific installed capacity on a set length of noise barrier, has been explored in previous studies.

In previous studies using the Energy Wall as a production site, the concept of modular Energy Wall segments was explored. Energy Wall modules are defined as a length of barrier with a fixed capacity or number of panels. The process of simulating modular Energy Wall segments (groups of PV modules) rather than individual modules reduces the number of iterations and simulation time.

In [26] one Energy Wall Module (EWM) had a length of 6 m and a height of 5.2 m, fitting 12 panels with a cumulative capacity of 4.08 kW_p per segment (340 Wp panels assumed). That study explored the possibility of a micro wind turbine as well but as it concluded, the cost did not outweigh the benefits; thus a wind turbine is not included in the present study.

For consistency, the number of modules was kept the same. One Energy Wall module in this study is a 12 m length of noise barrier with 12 solar panels, rated 4.08 kW_p each. The maximum allowable number of segments according to the 175 kW grid limit is 42 EWMs.

4.4. ENERGY & HYDROGEN PRODUCTION CONTROL STRATEGY

An interconnection between the grid, the Energy Wall and the hydrogen production system allows for reliable hydrogen production. At times where there is not enough energy from the Energy Wall, the grid acts as a back up source supplying the required energy. On

the other hand, when the tanks are full and there is still energy being produced by the Energy Wall, the surplus can be sold to the grid, avoiding curtailment and "greening" the grid electricity mix by using the sustainable energy produced.

Two main sizing methods were explored. The demand and buffer tank capacity was kept constant for both control strategies, while the size of the PV system and the electrolyzer were adjusted to understand their effect on cost. The hydrogen production is limited by the size of the tanks, as their maximum capacity is the daily demand. The two control strategies (CS) applied were:

1. CS1: Maximize the use of renewable energy
2. CS2: Use the electrolyzer at full capacity

4.4.1. CS1: MAXIMUM USE OF RENEWABLE ENERGY

In this strategy the utilization of renewable energy is maximized in effort to reduce dependence on the grid. The strategy acts so that when the sun is above the horizon, the electrolyzer is powered by electricity from the Energy Wall. Excess photovoltaic electricity is sent to the grid. When the sun sets, the grid supplies the electrolyzer at full capacity until the state of charge (SOC) of the buffer storage tanks is 100%.

The number of EWMs limits are the size of noise barrier and grid capacity category. It was established that the noise barriers have enough length, and hence space for PV panels to produce more than enough electricity to meet the demand of hydrogen. The electrolyzer operates from the Energy Wall during sunlight hours, and tops up from the grid at full capacity after sun set.

The rate of hydrogen production is variable through out the day and depends on the available electricity from the Energy Wall; it is limited by the electrolyzer capacity when the electricity produced in an hour is more than the capacity of the electrolyzer. The objective becomes to supply the required demand while utilizing most of the PV energy.

In some instances, the PV production in a given hour was higher than the electrolyzer capacity. In these cases, while the electrolyzer was operating at full capacity, there was still electricity being sent to the grid, indicating an underutilization of PV electricity. The renewable electricity was better utilized with larger electrolyzers.

4.4.2. CS2: OPERATE ELECTROLYZER AT FULL CAPACITY

The second CS works by operating the electrolyzer at maximum capacity. This means that as long as the tanks are not full, the electrolyzer will be producing hydrogen at full capacity using electricity from the grid and the Energy Wall. The grid and the Energy Wall supply the electrolyzer simultaneously so that it works at full capacity until the buffer storage tanks are full. When there is excess PV electricity, it is sent to both the electrolyzer and back into the grid (if the electrolyzer capacity is not large enough to use all the PV electricity). It is assumed that the price of hydrogen using this configuration will be higher since grid electricity has a higher price than the Energy Wall, however the reliability of the hydrogen production may be higher.

4.5. HYDROGEN PRODUCTION

The conversion efficiency of the electrolyzer, η_{Elec} is assumed to be 55 kWh/kg. This is calculated from the specifications of the GreenHydrogen electrolyzer, which is a small scale PEM unit [61]. The pressure drops throughout the process are shown in figure 4.6, illustrating the passive aspect of the design; additional components such as compressors are not included as a cost reduction strategy. It is important to state that there are losses along the way, such as heat losses in the process of refiling the canisters, but these are not considered as losses of the mass of hydrogen but rather as additional electricity needed to cool the refiling system.

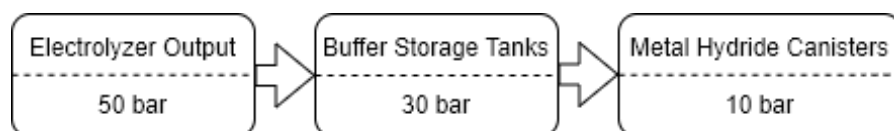


Figure 4.6: Pressure flow in Hydrogen System

By keeping the number of scooters to be served at a constant value of 100 scooters, the daily demand of hydrogen is equal each day of the year, and hence the electricity demand from the electrolyzer is also constant. Different electrolyzer sizes were simulated in the model, ranging from 1 kW to 5 kW capacity. The number of segments is also varied to understand the effect of a long or short Energy Wall system.

MATLAB was used to simulate the model and control strategies. The findings and observations are extensively discussed in the next sections and the end of the next chapter which is concerned with the cost model. The energy utilization from each source affects the final cost of hydrogen, hence the mix of electricity defines the feasibility of each system configuration.

4.6. MODEL ITERATIONS

The software used to simulate the parameters listed in this chapter was MATLAB.

The electrolyzer size range was from 1 to 5 kW installed capacity, in 1 kW steps. The maximum number of EWMs was limited to 42. The range simulated was in steps of 1 module from 1 to 20, and then in steps of 2 between 20 and 42 EWMs; this is steps in total. The step size changed to reduce the computing time. It was interesting to see the result of the maximum number of segments as well as the trend that the various parameters followed through the EWM size range.

This brings the number of iterations to 155. The entire loop was repeated for 2 control strategies, therefore the total number of iterations became 310. The results of multiple parameters of both control strategies in the model are explained in the cost findings (section 5.4). The main assumptions made and model flow is shown in figure 4.7.

The considerations of the model parameters and control strategies outlined in this chapter are carried over to the cost model found in the following chapter, to identify the cost results and feasibility of a hydrogen refueling system coupled with an Energy Wall.

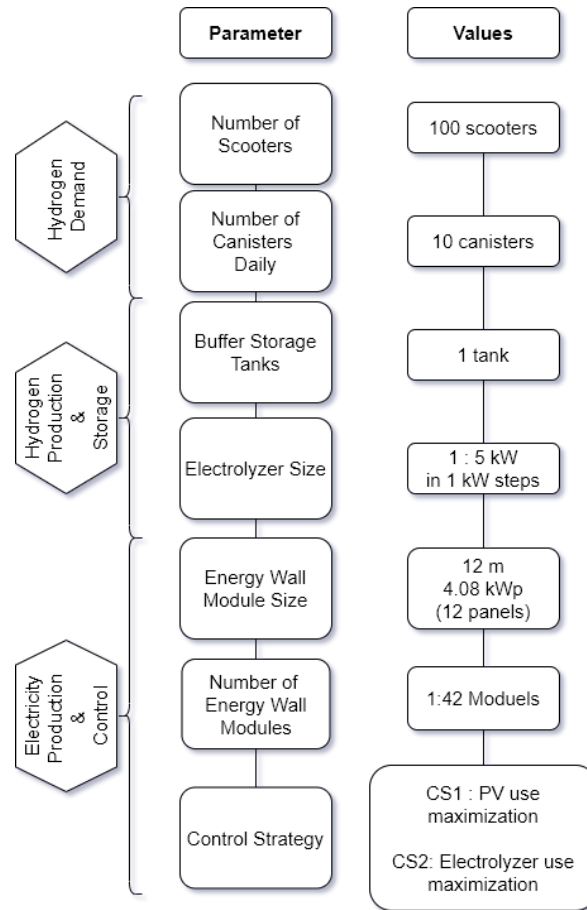


Figure 4.7: Model Iterations Schematic

4.7. MODEL FINDINGS

The feasibility of the system depends on its cost and functionality. Even though it is grid connected, the dependence on the grid should be kept low without compromising the ability to meet the demand. The energy flow between the Energy Wall (PV), the Grid (G) and the Electrolyzer (E) were given the following definitions:

- PV2E: Energy Wall to Electrolyzer
- PV2G: Energy Wall to Grid
- PG2E: Grid to Electrolyzer

The Energy Wall capacity factors are given first. Then the contribution and utilization of the Energy Wall is shown. A range of configurations was marked as unsuitable based on criteria.

4.7.1. PV CAPACITY FACTORS

The PV capacity factor is defined as the ratio between actual produced electricity and maximum full operation generation. The PV capacity factor (CF) is defined as the amount of

electricity produced compared to the electricity production capability in the case the system was operating all the time at full capacity. For each location the capacity factors are given in table 4.3. Rotterdam showed the highest capacity factor, therefore it is considered the base case for the rest of the results, unless otherwise indicated.

Ams. West	Ams ZO	Rotterdam	Delft
7.18%	8.78%	10.20%	9.20%

Table 4.3: PV Capacity Factors of Selected Locations

4.7.2. ENERGY WALL UTILIZATION & CONTRIBUTION

The share of electricity used from the overall PV generation for hydrogen production, as well as the share of PV electricity in the total electricity sent to the electrolyzer follows.

UTILIZATION

The *utilization*, U_{PV} , of the Energy Wall was defined as the ratio of electricity sent for hydrogen production, out of the total electricity produced by the Energy Wall, shown in equation 4.4. The utilization is plotted in figure 4.8 for the two control strategies and range of energy wall modules.

$$U_{PV} = \frac{PV2E}{PV2E + PV2G} \quad (4.4)$$

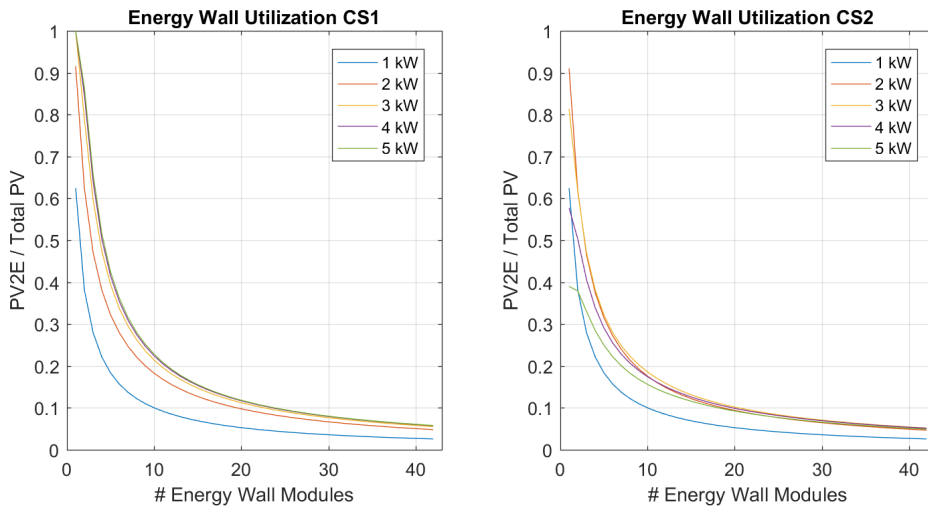


Figure 4.8: Utilization of Energy Wall for Rotterdam

For CS1 the utilization is generally higher as compared to CS2, meaning more of the PV energy is used for hydrogen production. Whatever is not sent to the electrolyzer is re-directed to the grid. The grid functions primarily as a back up source for the electrolyzer and secondly as a sink for the excess PV.

CONTRIBUTION

The *contribution* shows what percentage of electricity to the electrolyzer came from the Energy Wall, defined as CC_{PV} in equation 4.5. The contribution trends are shown in figure 4.9.

$$CC_{PV} = \frac{PV2E}{PV2E + PG2E} \quad (4.5)$$

The 1 kW electrolyzer sourced less than 50% of its electricity from the Energy Wall for the production of hydrogen, regardless of the number of Energy Wall modules for both control strategies, shown in figure 4.9. As the electrolyzer capacity increased, so did the contribution. CS1 has a higher CC_{PV} than CS2, and higher values are achieved sooner than CS2 configurations when increasing the number of Energy Wall modules.

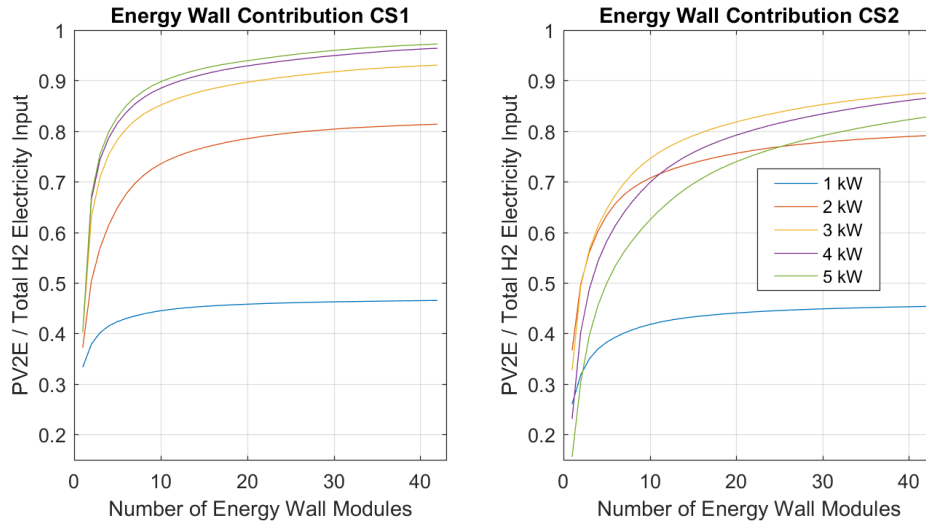
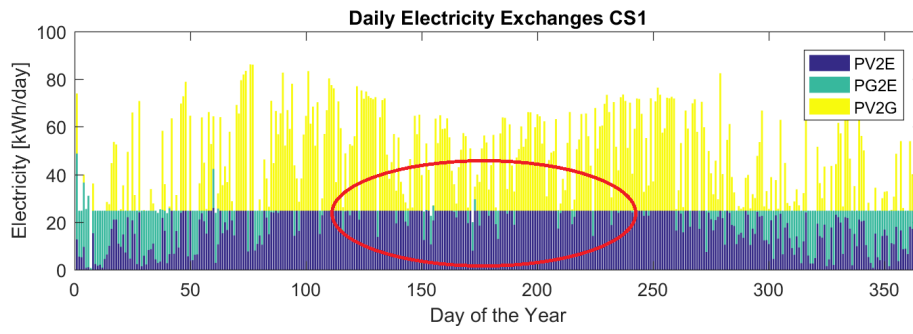


Figure 4.9: Contribution of Energy Wall to Hydrogen Production for Rotterdam

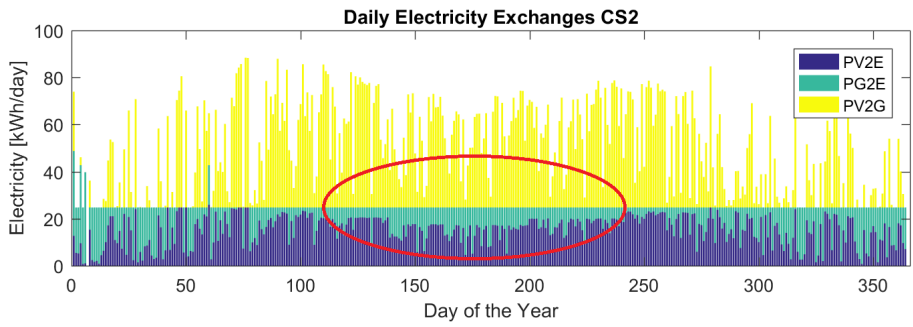
The difference between the two control strategies can be seen in the daily energy flows in figure 4.10. The configuration in shown is for a 3 kW electrolyzer with 4 Energy Wall modules. It is clear that CS2 uses more grid electricity compared to CS1. In the circled area in figure 4.10b, more electricity is directed from the grid to the electrolyzer, whereas in figure 4.10a the equivalent electricity is supplied by the Energy Wall. Another disadvantage of CS2 is that more PV electricity is sent to the grid, decreasing both the utilization U_{PV} , and more so the contribution CC_{PV} .

Figure 4.11 shows the hourly simulation results of a 1 kW electrolyzer, and where the electricity was sourced from for a day with high irradiance. It can be seen that even though there was sufficient PV electricity production, some of it was sent to the grid due to the small electrolyzer input capacity (1 kWh/h); later in the same day the grid was used to top up the hydrogen production. This is an inefficient way to use the electricity, since a portion of the PV generation is sent to the grid during the day for a low price, and bought back at a higher price when needed later in the day.

In conclusion, if the electrolyzer is too small, it will send more PV electricity to the grid, since the electrolyzer can only use 1 kWh each hour. This limits the amount of electricity from PV used. In addition, the daily demand is not fulfilled by the end of the PV production hours, therefore grid intervention is necessary to top up for the day.



(a) Renewable Electricity Maximization (CS1)



(b) Electrolyzer Maximization (CS2)

Figure 4.10: Comparison of Control Strategies in terms of Electricity Exchange (3 kW Electrolyzer, 4 NB Segments)

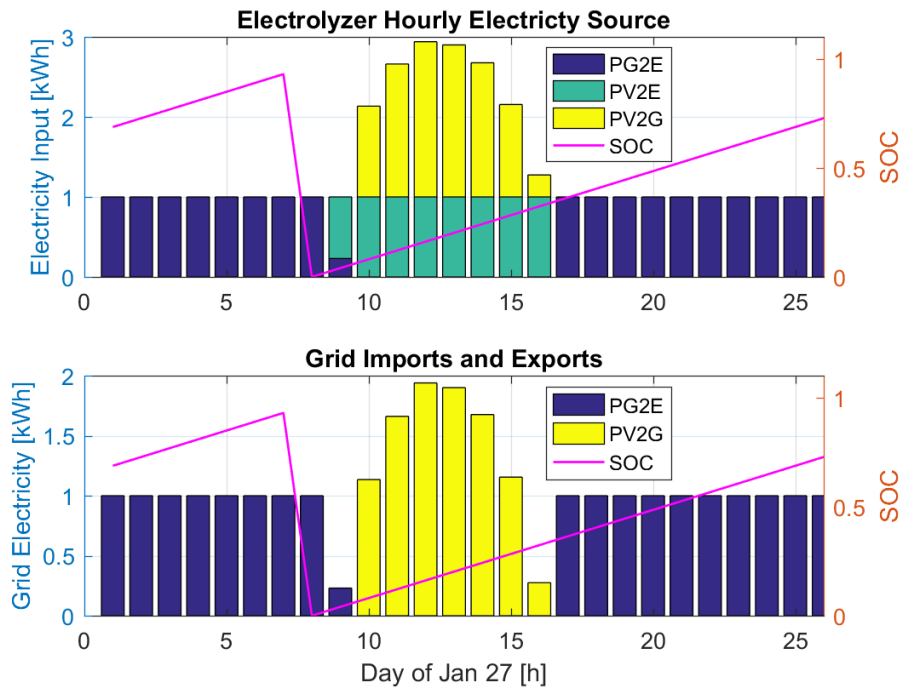


Figure 4.11: Hourly Electrolyzer Input and Grid Pattern for 1 kW Electrolyzer

4.7.3. ELECTROLYZER CAPACITY FACTOR

The capacity factor of the electrolyzer (CF_{Elec}) is defined as the ratio between the actual operating capacity of the electrolyzer over the maximum operating capacity achievable.

Figure 4.12 shows the capacity factor of different sized electrolyzers for the range of Energy Wall segments simulated.

Both control strategies had more or less a constant electrolyzer capacity factor; the only case in which this was not valid was for the 1 kW electrolyzer which had an increasing capacity factor with increasing number of Energy Wall segments. CS2 had a constant electrolyzer capacity factor as well as leveled cost of electrolyzer (discussed further in cost findings, section 5.4).

The tanks in this system were sized according to the daily expected hydrogen production. In the case that the tank size was variable, this could affect CF_{Elec} .

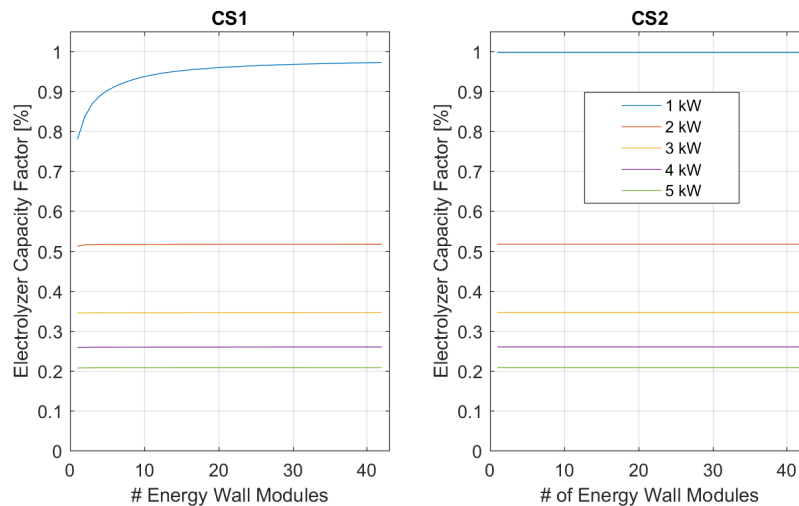


Figure 4.12: Electrolyzer Capacity Factors for Both Control Strategies

In conclusion, the CF_{Elec} is not affected by the change in number of Energy Wall modules. The differences noted between control strategies are not significant, except when the electrolyzer is small (i.e. 1 kW in this case). In that case CS2 is favored since the electrolyzer operation is kept high at the cost of a higher input electricity cost. The 1 kW electrolyzer CS1 case has an increasing CF_{elec} because it primarily uses PV electricity before topping up to the grid. The larger the number of EW modules, the higher CF_{elec} since it operates longer with PV electricity.

4.7.4. DEMAND SATISFACTION & STATE OF CHARGE

The demand is satisfied through means of supplying full canisters for empty ones to the scooter users, and was observed using the State of Charge (SOC) of the tanks at the end of the day for each configuration. The daily SOC was the level of charge of the tanks at the end of the day, at the point before the canisters are refilled. The number of days the daily SOC surpassed certain levels, namely 50%, 75%, 80%, 90%, and 95%, were measured; the values for CS1 are shown in figure 4.13. When the configuration is able to supply the full demand for most of the year it is considered reliable. There were configurations, especially with a small (1kW) electrolyzer where the demand was not satisfied.

In the last sub-figure of figure 4.13, the 1 kW surpasses 95% SOC for 2 or 3 days, and

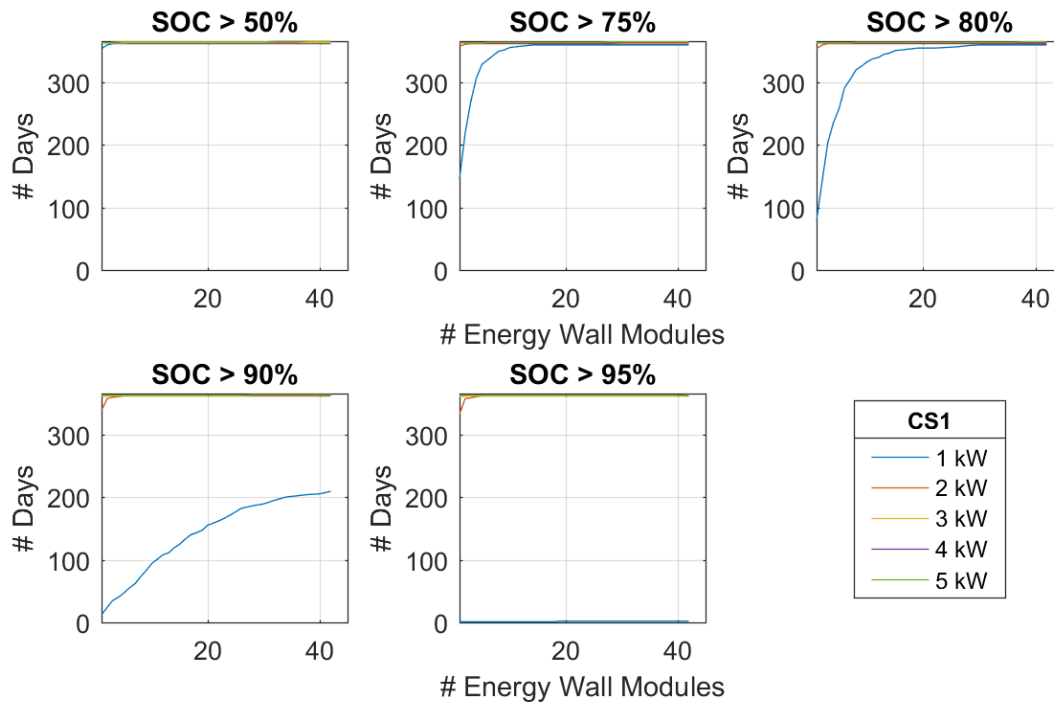


Figure 4.13: Daily State of Charge Levels for Different Electrolyzer Sizes

only at very large number of energy wall modules. This means that it never reaches 100%, and hence the annual demand for the 1 kW electrolyzer configuration is not completely met. The 1 kW struggled to meet 75% SOC for configurations with less than 10 Energy Wall modules.

For CS2, the number of days the SOC reached any level was constant (figure not shown but horizontal lines in the context of figure 4.13), since the electrolyzer was operated continuously until the daily demand was met. For the 1 kW electrolyzer, the daily SOC surpassed 75% for 359 days of year. The number of days it surpassed 95% was 6 days for the entire range of number of Energy Wall Modules.

4.7.5. AVOIDED EMISSIONS

Regulations around moped emissions have been developed by the EU. The class in which a vehicle is found depends on the year of manufacture. Recent models (>2017) are Euro4, while vehicles up to 2006 are Euro 2 and 2004 are Euro1. Moped emissions depend on the size of the vehicle (two-wheeled, incl. sidecar, tricycles, etc.) and their year of manufacture for Hybrid, Positive and Compression Ignition [65]. The gas scooter considered is Euro 4 (more specifically L1Be). The full regulations are available in [66].

The EU standard provides limits as to how much CO, NO_x and PM is emitted per km of operation. The limits of the L1Be are 1.0 g_{CO}, 0.17 g_{NO_x}, 0.63 g_{THC} (Total HydroCarbon) per kilometer. PM emissions were not allowed for new models from 2017 onwards. Thus any moped vehicle before this year had no restrictions on the Particulate Matter it emitted.

If one scooter travels 2.5 km per day, it covers 912.5 kilometers each year. Taking the

limits above, this would equate to 912.5 g_{CO}, 155.125 g_{NO_x}, and 574.5 g_{THC} per scooter per year avoided. For a fleet of 100 scooters as assumed in this project, this would be 91.25 kg_{CO}, 15.5 kg_{NO_x} and 57.5 kg_{THC}. These are not considered greenhouse gases themselves, but are harmful to human health.

5

COSTS: MODELING & FINDINGS

In order to assess the economic feasibility of the proposed Energy Wall system with hydrogen production system and how it compares to conventional fossil fuel powered scooters, the cost of the hydrogen delivered to the end users is assessed, i.e. the cost of hydrogen in the scooter canisters.

The cost calculation has been achieved by taking into consideration the cost of each individual component of the system for every conversion stage starting from energy production up to the delivered canisters, with the relevant assumptions stated in each subsection. The cost stages are shown in table 5.1. Each is explained in its dedicated section below.

This cost is then converted and compared with the equivalent cost of fossil fuel scooters on a per kilometer traveled basis. The main conversion stages considered are the renewable electricity production, the grid backup (these are contributors to the electricity delivered to the electrolyzer), the hydrogen production, buffer storage, and dispensing to the canisters. A summary of cost parameters used in the model is shown in table 5.1

Cost Component	Parameters	CAPEX	OPEX	Lifetime [years]	Ref.
$LCOE_{PV}$	PV	850 €/kW	2.5%	25	[67]
$LCOE_G$	Commercial Connection	G_{Sell}	0.174 €/kWh	-	[68]
		LCG_{H_2}	~ 400€/year	-	[16]
$LCOE_{H_2}$	PV Electricity	$LCOE_{PV}$		-	-
	Grid Electricity	$LCOE_G$		-	-
$LCOH_{PROD}$	Electrolyzer Electricity	1000 \$/kW	$2\%_{CAPEX}$	10	[69, 70]
		$LCOE_{H_2}$		-	-
$LCOH_{STOR}$	Buffer Tanks	700\$/kg	$1\%_{CAPEX}$	20	[69]

Table 5.1: Summary of Parameters Used in the Cost calculations

5.1. METHODOLOGY

In calculating the cost of hydrogen to the end user the costs accumulated throughout the process of converting irradiation to the dispensing of hydrogen are incorporated, providing the final cost to the users.

The levelized cost method was selected to analyze the economic value of the subsystem components shown in figure 4.1. This method concerns three main characteristic values for each subsystem of figure 4.1 namely the capital expenses (CAPEX), the operational expenses (OPEX) and the produced quantities, in this case being electricity (in kilowatt-hours) and hydrogen (in kilograms). The cost of each conversion stage is normalized per unit produced allowing for changes to the system configuration to be compared economically.

The levelized cost method provides an annualized values of the CAPEX and OPEX over the lifetime of the system. Capital expenses are significant since they concern the equipment and installation costs but are made once during the lifetime of the system. Operational & maintenance (O&M) expenses are usually much lower but are made more frequently.

An annuity factor is used to annualize the capital expenses over the lifetime of the project. The calculation of the annuity factor is shown in equation 5.1, where i is the real interest rate and t is the lifetime of the project [67]. The real interest rate is assumed to be 2%.

$$ANU = \frac{i \times (1 + i)^t}{(1 + i)^t - 1} \quad (5.1)$$

5.2. ELECTRICITY COST PARAMETERS

The levelized cost of electricity (LCOE) is a measure to express the value per unit of energy produced, hence expressed in €/kWh. It calculates the minimum price that system can produce electricity while repaying the value of its components and operation over its lifetime. Traditionally the LCOE takes into account the fuel and carbon emission costs, but renewable energies are favorable since these fuel costs are not applicable during the operation.

5.2.1. ENERGY WALL

The Energy Wall (EW) is essentially a PV system installed on a wall, hence its cost is modeled as such. A PV system consists of the modules, the balance of system (BOS) components. The latter are parts associated with the installation and operation; inverters, cabling, mounts, bypass diodes and charge controllers are included here.

The CAPEX is the hardware capital and installation costs. Transport equipment for the components, permits and taxes, and labour services make up the installation costs. While in operation the inspection and cleaning of panels, as well as any replacements required make up the OPEX of the system. These may be referred to as Operation and Maintenance (O&M).

In [67] the CAPEX of commercial size systems is given between 800 and 1000 €/W. The paper involves prices in Germany in 2018, therefore it was considered the most valid source for this type of system. The OPEX was stated as 2.5% of the CAPEX.

At the time of writing solar electricity is as cheap if not cheaper than other conventional forms of electricity [9]. The same source states that the average LCOE of photovoltaic installations globally has reached a value of 0.085 USD\$/kWh in 2018. A groundbreaking price of 0.26 €/W was reported in [71] for Europe, which was an average price of mainstream technology in April 2019.

The cost considerations here are taken without incentive or subsidy calculations, since these may expire, or be unavailable in the future. Thus the cost of the PV energy is assessed purely on the necessary components and their true costs.

5.2.2. GRID

With a grid connected configuration, the electrolyzer is able to produce hydrogen reliably and meet the demand of the scooters. There are two grid cost components which are eventually and partially borne by the hydrogen user. In summary they are as follow:

1. The cost of buying electricity commercially from the grid (grid sell price), G_{sell}
2. the cost of making the connection to the grid itself, LCG_{H_2}

GRID: COMMERCIAL PRICES

The grid sells electricity to the hydrogen production system at a price, G_{sell} and buys electricity from the Energy Wall at a different price G_{buy} .

The grid sell (G_{sell}) price differs between households, small/medium enterprises, and all size industries (small, medium or large). The larger the consumer, the cheaper the electricity. The Energy Wall exchange is classified as the smallest type of consumer. The price given by CBS for small scale users (more than 2.5 and less than 500 MWh/year) including taxes and VAT is 0.174 €/kWh in the last quarter of 2018. The VAT and taxes alone for that period were 0.059 €/kWh, roughly 40% of the total price [68]. Therefore G_{sell} is assumed to be 0.174 €/kWh.

G_{buy} is the price at which the grid buys energy from the Energy Wall. Ideally, this price should be equal to or greater than the cost to produce the electricity, i.e. $LCOE_{REN}$ if the system is to make a profit, but this is not considered in this set of calculations since it is not relevant to the cost of H₂ produced. It is in the interest of the grid to buy energy at lower prices than it sells it for, i.e. $G_{sell} > G_{buy}$.

GRID: CONNECTION COSTS

Naturally, the connection to the grid has an associated cost which determined by the grid operator. In the case of South Holland the operator is Stedin [16]; data on the connection cost is provided and reproduced in tables G.1 & G.2. The cost of connection consists of the one-off fee for the new connection point which includes 25m of cable, the cost per additional length of cable, and an annual fee for the operation and maintenance of the

grid. The magnitude of the connection cost depends on the capacity of power which must be exchanged between the system and the grid.

The *annualized* cost of the grid *connection*, C_{CON} , is expressed in equation 5.2, where $CAPEX_{Grid}$ represents the connection and associated cable costs and $OPEX_{Grid}$ is the operation and maintenance costs paid to the grid operator.

$$C_{CON} = ANU \cdot CAPEX_{Grid} + OPEX_{Grid} \left[\frac{\text{€}}{\text{year}} \right] \quad (5.2)$$

The 2 users of the grid connection are the Energy Wall and the electrolyzer system, denoted by the subscripts REN and H_2 respectively. The proportion of electricity sent to- or received from- the grid by users are not equal, therefore the connection cost is split between its users. The cost is split and allocated depending on how much electricity is handled by the transformer for each user. A detailed explanation of how the cost was divided between the users is shown in appendix G.

The levelized cost of connection, LCG , is defined as the cost of connection divided by the amount of electricity sent to and received from the grid (eq. G.3). It is split into LCG_{H_2} which is allocated to the hydrogen produced, and LCG_{REN} borne by the energy wall. Equation 5.3 gives the connection cost allocated to the hydrogen production, where E_G is the gross energy handled by the grid, E_{G2H_2} is the energy sent to the electrolyzer from the grid, and LCG is the total connection cost.

$$LCG_{H_2} = LCG \times \frac{E_{G2H_2}}{E_G} \left[\frac{\text{€}}{kWh} \right] \quad (5.3)$$

The **final cost** of electricity that the electrolyzer pays for is defined as $LCOE_G$, expressed in equation 5.4. From the grid connection cost, only the cost associated with the electricity that is sent to the electrolyzer is considered, LCG_{H_2} . This is the only cost which trickles down to the cost for the user.

$$LCOE_G = LCG_{H_2} + G_{sell} \left[\frac{\text{€}}{kWh} \right] \quad (5.4)$$

5.2.3. COST OF ELECTRICITY TO ELECTROLYZER

The cost of electricity is proportionally between the Energy Wall and the grid, according to how much it uses from each source. Therefore, the respective costs are transferred to the cost of hydrogen and eventually to the scooter user as the price of a canister. The element $LCOE_{H_2}$ is an all-encompassing factor used to express the price of the electricity sent to the hydrogen production system. During electrolysis, one of the essential requirements is the electricity, and therefore the cost of it is important.

The system was envisioned to contain passive auxilliary components rather than active ones in order to keep the system simple and to minimize the auxilliary component energy demand. The auxiliary components electricity is negligible compared to the electrolyzer consumption. An energy controller primarily regulates the power input to the electrolyzer,

and secondly redirects the surplus renewable energy to the grid. The electricity consumption of this component is also considered negligible compared to the consumption of the electrolyzer.

The levelized cost of electricity sent to the electrolyzer, defined as $LCOE_{H_2}$ is therefore made up of the following cost components:

- Cost of electricity from the Energy Wall
- Cost of electricity purchased from the grid

These cost elements are expressed in equation 5.5 in the respective order. The denominator, E_{H_2} of the equation is the annual electricity received by the electrolyzer.

$$LCOE_{H_2} = \frac{(LCOE_{PV} \cdot PV2E) + (LCOE_G \cdot PG2E)}{E_{H_2}} \left[\frac{\text{€}}{kWh} \right] \quad (5.5)$$

5.3. HYDROGEN COST PARAMETERS

The total levelized cost of hydrogen is determined by the cumulative cost of producing and storing the hydrogen. The production costs include the electricity, electrolyzer, and water; the (buffer) storage costs are mainly the compressed gas tanks.

The following sections provide values and reasoning associated with the levelized cost of hydrogen (LCOH) of -production and -storage. W is the quantity of hydrogen processed annually in kilograms. Production in section 5.3.1, Storage in section 5.3.3. The final price that is sought is the price of hydrogen to the end user, $LCOH_{User}$, which includes the production and storage costs discussed below. Dispensing costs are attributed to the user since they are the owners of the canisters and hence not included in the final $LCOH_{user}$.

It is important to state that there are losses along the way, such as heat losses in the process of refilling the canisters. This is viewed as an additional requirement for electricity (i.e. to cool the canisters while they refill, since heat is generated in the process), however these are not considered as losses of the mass of hydrogen. Therefore the mass of H₂ produced is assumed to be the same mass that is dispensed to the canisters. Better conversion efficiencies will decrease the costs.

The costs accumulated in the process of production and buffer storage of hydrogen both contribute to the cost of the hydrogen in the canister. Therefore, the cost per kg of each of these is added to find the final LCOH, as shown in equation 5.6.

$$LCOH = LCOH_{prod} + LCOH_{stor} \left[\frac{\text{€}}{kg_{H_2}} \right] \quad (5.6)$$

The cost of production is shown in equation 5.7. It consists of the levelized cost of the electrolyzer ($LCOH_{Elec}$), the electricity input into the electrolyzer, and the water costs. The first two are discussed below, while the water costs are quite low and therefore only described in appendix C for reference.

$$LCOH_{Prod} = LCOH_{Elec} + LCOH_{Electricity} + LCOH_{Water} \left[\frac{\text{€}}{kg_{H_2}} \right] \quad (5.7)$$

5.3.1. PRODUCTION: ELECTROLYZER COSTS

A PEM electrolyzer was chosen for the hydrogen production due to its high efficiency, load following capabilities and compact design. In section 2.2.2 it was ascertained that PEM technology is more expensive than alkaline due to its novelty and materials. This is changing as research and implementations of PEM systems progress, and it is becoming a more viable electrolysis technology, especially for intermittent renewable energy generation applications. Cost aside, PEM was deemed more suitable for such an application due to its dynamic load following capabilities and high efficiency.

The cost of State-of-the-Art PEM systems used for energy storage from renewables with grid balancing was laid out by [14], for the years 2012 and 2017. Predictions were also made for 2020, 2024, and 2030. The capital expenses depended on the conversion efficiency of the electrolysis systems. The data is summarized in table 5.2. The operating cost of an electrolyzer is assumed to be 2.0% of the capital cost [14, 72]. The 2020 column in table 5.2 is used as the assumption guide, however a conservative value of 1000€/kW is assumed since the figures stated are predictions rather than real data. The electrolyzer modeled in this study has achieved the 55 kWh/kg conversion efficiency.

$$LCOH_{Elec} = \frac{(ANU \cdot CAPEX_{elec}) + OPEX_{Elec}}{W_{Annual}} \left[\frac{\text{€}}{\text{kg}_{H_2}} \right] \quad (5.8)$$

	2012	2017	2020	2024	2030
Efficiency [kWh/kg]	60	58	55	52	50
CAPEX [\$/kW]	3200	1200	900	700	500
O&M [\$/kW/year]	2% _{CAPEX}				

Table 5.2: Operational and Capital Costs of PEM Hydrogen Production from Renewables [14]

5.3.2. PRODUCTION: ELECTRICITY

The cost of the electricity received by the electrolyzer is shown in equation 5.5. Equation 5.9 represents the electricity cost in terms of the hydrogen produced. It depends on the electricity input from the grid and the Energy Wall. E_{H_2} is the electricity input to the electrolyzer. Therefore the annual gross cost of electricity is found and divided by the annual quantity of hydrogen produced. The same could be achieved by multiplying $LCOE_{H_2}$ and η_{Elec} .

$$LCOH_{Electricity} = \frac{LCOE_{H_2} \cdot E_{H_2}}{W_{Annual}} \left[\frac{\text{€}}{\text{kg}_{H_2}} \right] \quad (5.9)$$

$$LCOH_{Electricity} = LCOE_{H_2} \cdot \eta_{Elec} \left[\frac{\text{€}}{\text{kg}_{H_2}} \right]$$

The cost per electricity unit is converted to the equivalent cost per kilogram hydrogen. In the production modelling section (4.5), the conversion efficiency, η_{Elec} , was taken as 55 kWh/kg_{H₂}. The mass value was used instead of the volume of hydrogen since the energy

content of a volume of hydrogen may change with pressure or temperature. Since there are various points of pressure changes (fig 4.6) the gravimetric energy density was preferred.

Cost reductions are expected in the levelized cost of hydrogen in two areas. First, the conversion efficiency of electrolyzers is expected to increase, meaning less electricity will be required to produce a kilogram of hydrogen. This will decrease the overall electricity requirement, and hence the cost of electricity into the electrolyzer. The CAPEX and OPEX of electrolyzers is also expected to decrease in the future [14] thus, lowering the overall levelized cost of hydrogen production.

5.3.3. BUFFER STORAGE COSTS

The cost of storing the hydrogen is defined as $LCOH_{Stor}$. An estimation of an 8000 L tank is given in [69] at a value of 9,000\$ which operates at 20 bar. Therefore, the cost per kg H_2 stored is 700 \$/kg.

$$LCOH_{Stor} = \frac{ANU \cdot CAPEX_{Stor} + OPEX_{Stor}}{W_{Annual}} \left[\frac{\text{€}}{kg_{H_2}} \right] \quad (5.10)$$

5.3.4. LEVELIZED COST OF HYDROGEN TO USER

The conversion of the cost per kilogram to the cost per canister is achieved by multiplying the LCOH by $0.045 kg_{H_2}$ ($45 g_{H_2}$), the value contained in each canister. The overall cost of hydrogen is multiplied by this value to find the cost per canister, expressed in equation 5.11. This is the lowest price possible to repay the capital costs, therefore it is assumed that eventually this value will be higher to cover the supplier margins or other commercial costs.

$$LCOH_{User} = LCOH \times 0.045 \left[\frac{\text{€}}{canister} \right] \quad (5.11)$$

5.4. COST MODEL FINDINGS

In the first investigation, we look at how the cost of electricity is impacted by the size of share provided by the Energy Wall and the Grid. This will ultimately affect the price of hydrogen to the user. In this second aspect, the price will also be affected by the size of the electrolyzer. To conclude, the price per kilometer driven is found and compared to other forms of scooters.

5.4.1. LEVELIZED COST OF ELECTRICITY OF FOUR LOCATIONS

Each location had a different cost of electricity, which remained unchanged regardless of the control strategy used or the coupling with the hydrogen production system. This cost has to do with how much electricity the system produces, based on its location characteristics. More electricity production throughout the year means a lower levelized cost due to maximized output of the PV panels. When the panels are not placed in desirable locations or positions, the output decreases, increasing the $LCOE_{PV}$. The levelized cost values presented below are directly related to the capacity factors of the locations in table 4.3.

Location	Orientation	Tilt	LCOE _{PV} [€cents/kWh]
Amsterdam West	270°	10°	10.31
Amsterdam South East	150°	10°	8.44
Rotterdam	170°	10°	7.98
Delft	170°	10°	8.04

Table 5.3: Base Case LCOE_{PV} of each Case Study Location

TILT SENSITIVITY

For all of the cases when the tilt of the barrier was perpendicular (i.e. NB tilt of 0°) the price of the PV electricity was 13-14% higher than when it was tilted at 10°. In addition, when the tilt of the barrier was increased by a further 10° (to 20°) the LCOE_{PV} decreased by 9% for all the cases.

In conclusion, it is more favourable to have a larger tilt in the barrier. This comes down to the fact that the higher the tilt of the barrier, the closer the slope of the panels is to the optimal slope for the Netherlands (~ 38° panel slope, equivalent to 52° NB tilt). The solar panels are also able to produce more electricity in the same period, therefore decreasing the unit energy cost.

5.4.2. CONTRIBUTIONS TO LCOH

The cost of hydrogen, including auxiliary costs was made up of the following components:

- Storage Tanks
- Electrolyzer
- Grid Electricity
- Energy Wall (PV) Electricity

The contributions to the LCOH for each configuration are shown in figure 5.1. Water is a negligible part of the cost of production and is therefore not included in the figure.

BUFFER STORAGE TANK CONTRIBUTION

The tanks were sized according to the daily demand. The assumption of the cost per kg stored is provided in section 5.3.3. The quantity of hydrogen produced and stored was ~ $0.5 \frac{\text{kgH}_2}{\text{day}}$. The tanks were therefore sized to accommodate this production. The contribution to the LCOH by the storage tanks remained constant regardless of the configuration, since the demand was kept constant.

Commercial tanks (such as the one mentioned in section 2.2.4) are able to hold 4.2 kg. This is significantly higher than the amount required in this study. However the modeling of a small scale of the system allows for localization and decentralization of the hydrogen refueling station.

One of the future work points would be to oversize the tanks and observe the reliability of the system (from the user perspective), where configurations are allowed to produce

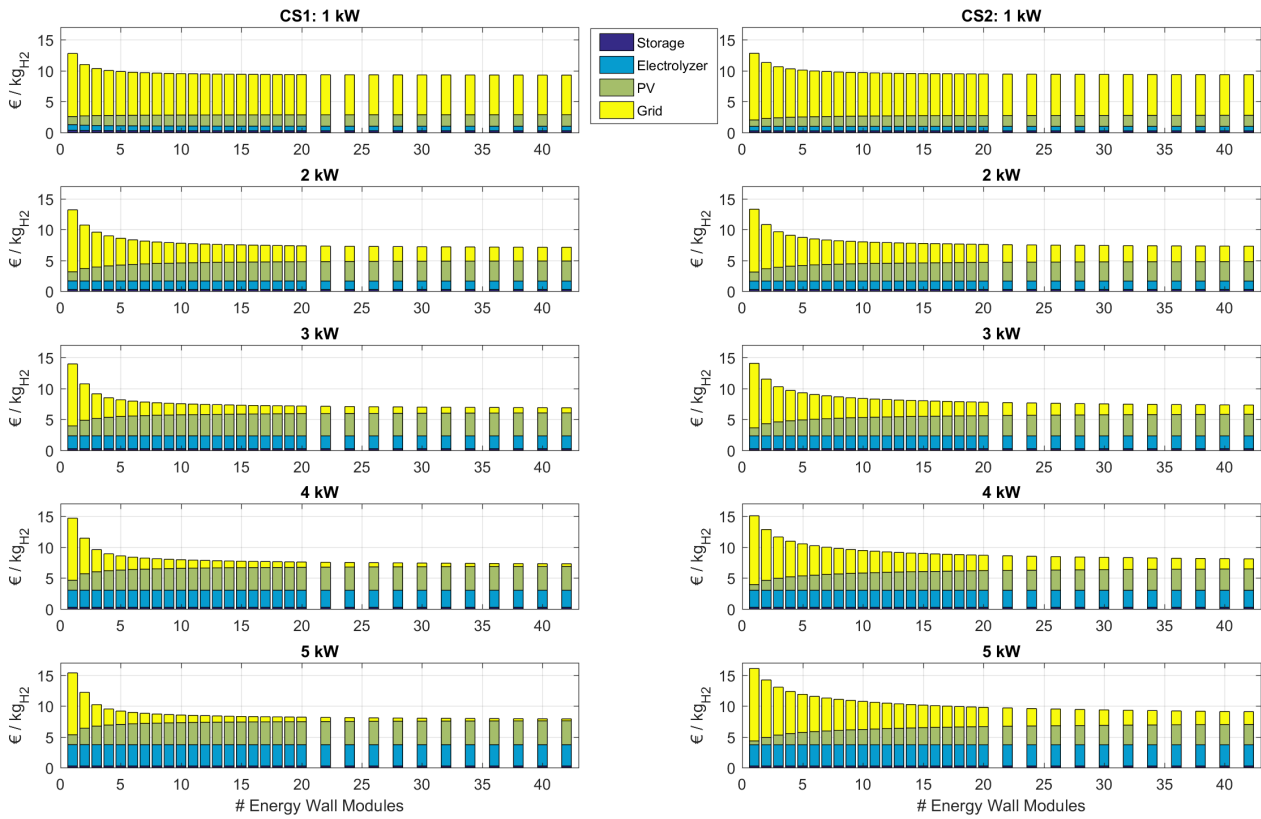


Figure 5.1: Breakdown of LCOH Contributions

more hydrogen than the daily requirement, for use on a low-PV day. The possibility of the buffer storage tank capacity being higher is not excluded as a suggestion for future system designs since the contribution to the LCOH is already quite low.

ELECTROLYZER COST CONTRIBUTION

The levelized cost of the electrolyzer ($LCOH_{Elec}$) is shown in figure 5.2. The cost is not influenced by the control strategies, except using CS1 with a 1 kW electrolyzer. $LCOH_{Elec}$ decreases between 1 and 15 energy Wall modules. The electrolyzer capacity factor, CF_{Elec} increases along the same range.

A correlation between $LCOH_{Elec}$ and CF_{Elec} for the range of electrolyzer capacities is observed. The relation of $LCOH_{Elec}$ is shown in figure 5.2, while the CF_{Elec} trend is given in figure 4.12; the two aforementioned figures are combined and shown in figure 6.1.

In figure 4.12 one can see that for each upward step in electrolyzer capacity size, the annual capacity factor decreases; as a result the levelized cost of the electrolyzer increases. Therefore, an unnecessarily large electrolyzer, such as the 5 kW configuration in this case, mainly adds to the overall LCOH, without providing significant reliability benefits as compared to smaller electrolyzer sizes.

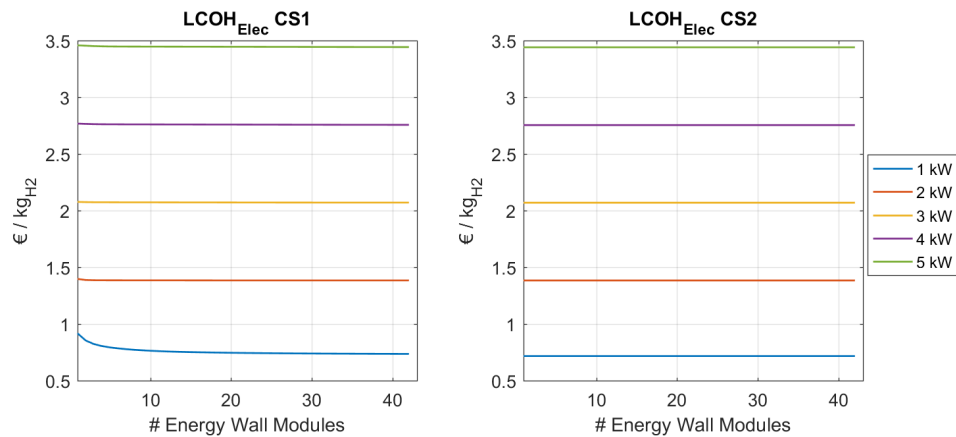


Figure 5.2: Levelized Cost of Electrolyzer

In summary, the findings of the electrolyzer cost influences are as follow:

- For electrolyzer capacities of 2 kW or more, the capacity factor of the electrolyzer was $\leq 52\%$
- The levelized cost of the electrolyzer increased with increasing electrolyzer capacities, since the CAPEX and OPEX of the component increased but the quantity of hydrogen demanded (and hence produced) remains constant.
- For small electrolyzer capacities (i.e. 1 kW), where the capacity factor of the configuration increases with increasing Energy Wall modules, the electrolyzer levelized cost decreases accordingly; it reaches a steady state value when the production level matches the demand requirement.
- In CS2, the $LCOH_{Elec}$ remains truly constant as the quantity of hydrogen produced is constant throughout the range of Energy Wall modules

In conclusion the number of Energy Wall modules does not affect the usage, and consequently the $LCOH_{Elec}$, of the electrolyzers when the electrolyzer is over 2 kW. Maximization of capacity factor tends to decrease the levelized cost of the electrolyzer, however the electrolyzer should also have a high enough capacity to be able to meet the daily demand, and hence have a high daily SOC. As electrolyzer capacity is added, the levelized cost increases if the hydrogen production quantity remains unchanged since the capital and operational expenses increase while the denominator quantity of hydrogen stays constant.

ELECTRICITY CONTRIBUTION

The parameters which influence the electricity cost are the choice of control strategy (CS1 or CS2), the size of the Energy Wall, and the size of the electrolyzer. The cost of PV electricity tends to be lower than the commercial grid prices, with reference to table 5.3 and section 5.2.2 respectively. The PV price for the Rotterdam case was around 8 €/kWh, whereas grid prices are at least 17.4 €/kWh. The price of electricity into the electrolyzer was thus governed by the contribution of each of these two sources, expressed in equation 5.9. The

more electricity taken from the Energy Wall, the lower the final cost of electricity used for electrolysis. Therefore, it becomes desirable to utilize more PV energy rather than grid, without compromising the ability of the system to meet the daily demand of hydrogen.

The contribution and utilization of the Energy Wall modules is shown in section 4.7.2. The contribution to the hydrogen production is important since it shows how much electricity is sourced from the Energy Wall. Preferably this value should be high for two reasons:

- the PV system has the purpose of serving the hydrogen production, therefore if the contribution is low (high grid input) the system becomes redundant
- a higher Energy Wall contribution means a lower $LCOE_{H_2}$ as compared to configurations with low contribution values

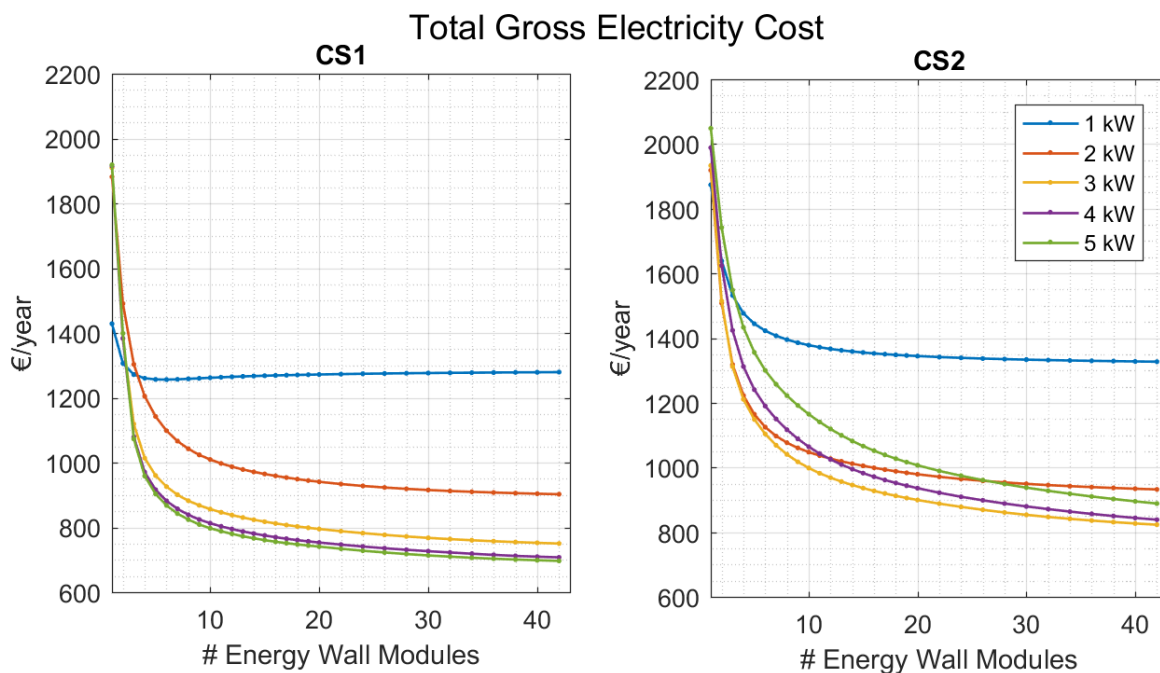


Figure 5.3: Total Gross Cost of Electricity for CS1 & CS2

Overall, for each configuration combination, CS1 yielded lower costs of electricity as compared to CS2. The effect of CS1 in when comparing the gross electricity cost is shown in figure 5.3, while the cost contributed by each source can be seen in figure 5.4. CS1 uses more electricity from the Energy Wall, decreasing $LCOE_{H_2}$ and eventually $LCOH_{Prod}$ and $LCOH_{User}$.

As the number of Energy Wall modules increases, the levelized cost of electricity always decreases, however the rate of decrease becomes smaller at large Energy Wall module configurations. Therefore more Energy Wall modules lead to a lower final levelized cost of hydrogen. One aspect not illustrated is the total capital cost and its increase with increasing Energy Wall modules. However the cost of the PV electricity reflects the minimum price of the electricity in order to repay the capital costs; therefore a larger number of Energy Wall

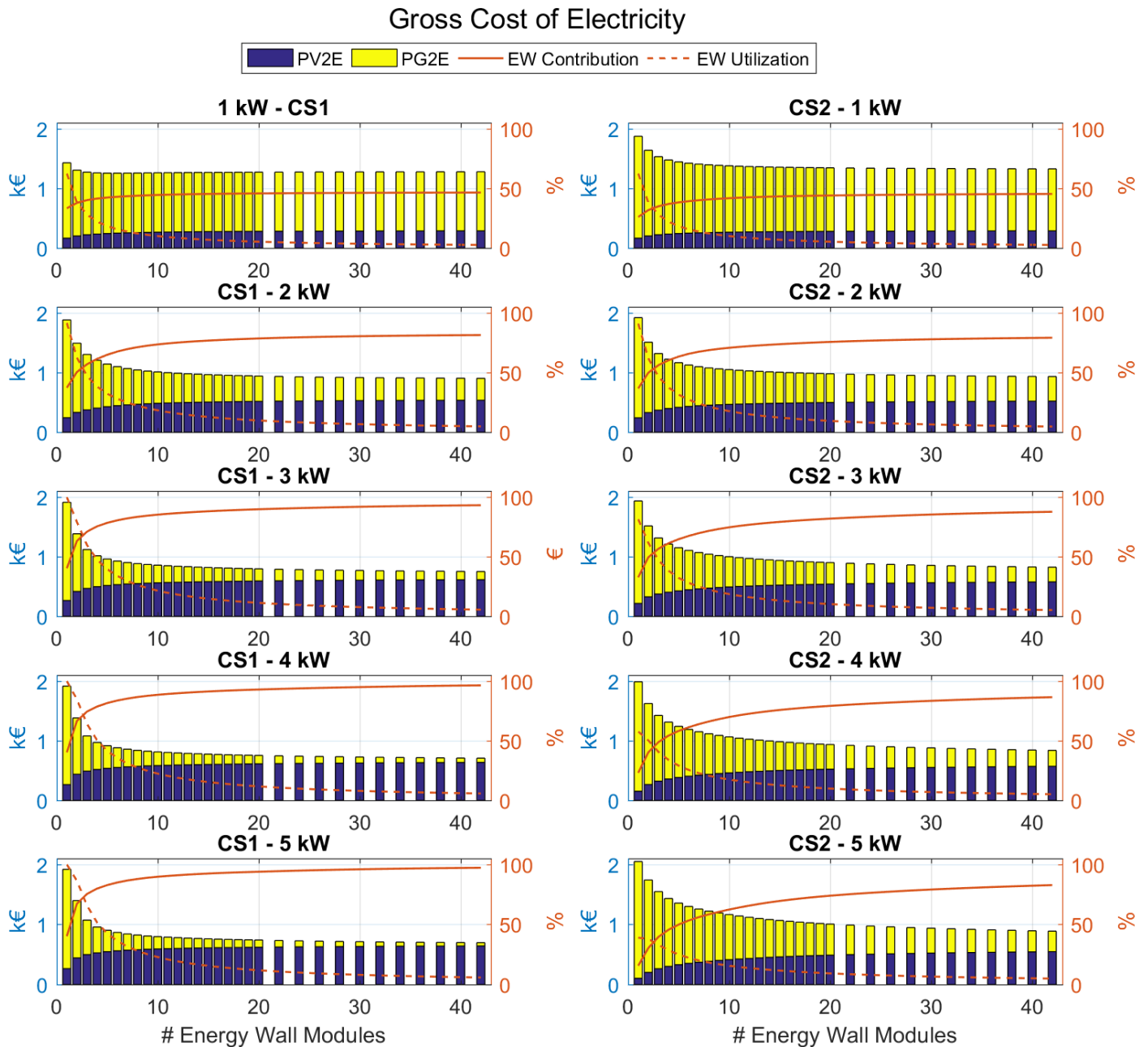


Figure 5.4: Gross Cost of Electricity by Source for CS1 & CS2

modules will decrease the cost associated with the hydrogen. The capital cost is limited by the utilization and contribution constraint placed in section 4.7.2.

The gross cost of electricity differs among the different electrolyzer sizes. For CS1, where the PV electricity use is maximized, the cost of electricity decreases with increasing electrolyzer capacity. Thus with a 1 kW electrolyzer configuration more is being paid annually for electricity than 2 kW and so forth. The cost difference between 1 kW and 2 kW is substantial, however, between 2 kW and 3 kW the difference is reduced. Finally for 3 kW or higher the cost differences are minor, however it is in the interest of the overall LCOH to keep the electrolyzer capacity small rather than oversized to minimize the electrolyzer

capital costs and keep the capacity factor reasonable.

Therefore the 3 kW is considered sufficient to supply the demand, keep the electricity cost low and the electrolyzer cost considerably low as well. The capacity factor of a 3 kW electrolyzer is 35%, while that of a 2 kW unit is around 52%. A benefit of a low capacity factor is that the electrolyzer will have a longer operational life before it needs to be replaced. Lifetime of components is measured either in years or operational hours, therefore with fewer operational hours the electrolyzer may take longer (than the manufacturer lifetime) before it needs to be replaced.

A different pattern is observed for CS2, where the total gross cost of electricity decreases between 1 kW and 3 kW, but then starts to increase when the electrolyzer is larger than 3 kW. Hence, the lowest gross electricity cost is achieved with a 3 kW electrolyzer for the given demand. The difference between 2 kW and 3 kW for CS2 is not great, therefore either could be considered depending on the overall *LCOH*.

The 3 kW CS2 configuration yields gross electricity costs similar to the 2 kW CS1 configuration. Therefore CS1 was considered the best strategy in terms of keeping the gross cost of electricity low, and the electrolyzer capacity (and hence capital cost of electrolysis) low.

OVERALL LCOH OF CONFIGURATIONS & COST PER KILOMETER

The overall LCOH for every configuration is shown in figure 5.5. Increasing the capacity of PV lowers the price regardless of the size of the electrolyzer and control strategy. In summary, the observations made above are as follow:

- CS1 yields a lower overall LCOH when configurations are compared to the CS2 counterpart. This was due to higher CC_{PV} values, which decrease $LCOE_{H_2}$
- The buffer storage tank levelized cost did not change with any configurations since the demand was kept constant
- $LCOH_{Elec}$ increased with increasing electrolyzer capacities, while the capacity factor decreased accordingly.
- The effect of number of Energy Wall segments did not impact $LCOH_{Elec}$ for electrolyzers larger than 1 kW with CS1. CS2 had constant $LCOH_{Elec}$ values.
- Using CS1, the value paid for electricity decreased as the electrolyzer increased.
- Using CS2, the lowest electricity gross cost was achieved with a 3 kW electrolyzer however using a 2 kW electrolyzer the gross cost of electricity was also considerably low.

For CS1 the lowest LCOH was achieved with a 3 kW electrolyzer for 2 or more Energy Wall modules. This was due to its ability to utilize high input from the Energy Wall. For larger electrolyzers, although the gross cost of electricity is slightly lower (figure 5.3), the overall LCOH is higher due to an increased electrolyzer capital cost, and hence $LCOH_{Elec}$. Every step increase in electrolyzer size adds between 48 and 70 cents per kg_{H_2} .

For both control strategies, the LCOH is high for a 1 kW electrolyzer, mainly due to the high cost of electricity. This happens because the electrolyzer is not able to use large

amounts of the PV electricity, therefore resorting to high grid dependency, bringing up the value of $LCOE_{2H_2}$.

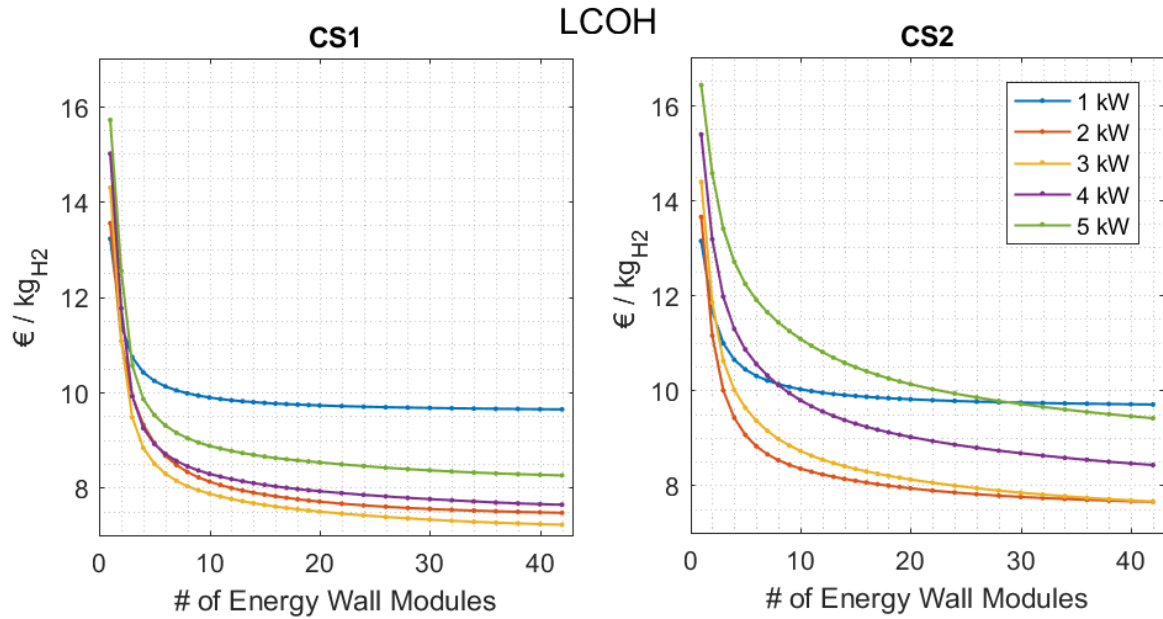


Figure 5.5: Overall LCOH of Configurations

When using CS2 the costs decrease along with the capacity installed, but at different rates for different sized electrolyzers. The smallest electrolyzer is the cheapest option at small capacities, but becomes the most expensive as the capacity reaches the maximum installable. Table 5.4 gives the cost of hydrogen for a range of Energy Wall modules for the most economically feasible configuration using a 3 kW electrolyzer and CS1.

# EWM	PV capacity [kWp]	LCOH [€/kg _{H2}]	LCOH _{User} [€/canister]	Cost/km* [€/km]
1	4.08	14.29	0.643	2.572
2	8.16	11.07	0.498	1.992
3	12.24	9.47	0.426	1.704
4	16.32	8.83	0.397	1.588
5	20.4	8.50	0.383	1.532
6	24.48	8.29	0.373	1.492
7	28.56	8.14	0.366	1.464
8	32.64	8.03	0.361	1.444
9	36.72	7.94	0.357	1.428
10	40.8	7.87	0.354	1.416
11	44.88	7.81	0.352	1.408
12	48.96	7.76	0.349	1.396

Table 5.4: LCOH for 3 kW-CS1 Configuration for a Range of EWM, *50km range assumed

5.4.3. COMPARISON OF COST PER KILOMETER BETWEEN DIFFERENT TYPES OF SCOOTERS

In the process of comparing the feasibility of a hydrogen refueling station for scooters, the price per kilometer driven was calculated, and compared with the equivalent metric for battery powered vehicles and gas scooters. The mileage of a vehicle is defined as the distance it is able to travel with the fuel available to it. The cost of producing the hydrogen eventually is borne to the scooter user. Three scooter models are provided in section 2.4.3, and reproduced in table 5.5. Equation 5.11 was used to find the cost of hydrogen to the user.

	APFCT	Niu:NQi Sport+	AGM iCON50
Type	Fuel Cell	Battery	Gas
Capacity	90 g_{H_2}	1.74 kWh	5 L
Cost of 1 Refill	1.29 - 0.70 €	0.3 €	7.5 €
Range	50* - 80 km	50 - 80 km	150 - 250 km
Cost / km ¢/km	2.6 - 1.4	0.6 - 0.3	5 - 3

Table 5.5: Summary of Scooter Operating Costs, *50 km range assumed for FC Scooter

CONVENTIONAL FOSSIL FUEL SCOOTERS

The price of gasoline changes according to a plethora of variables, including the origin, geopolitical situations, and government price measures. At the time of writing a liter of gasoline was about 1.5€/L.[73] This price includes taxes paid to the government, which is not the case for the Energy Wall electricity (since it can be considered a private solar producer).

The mileage of scooters can vary depending on the model, the year of construction, and most importantly the driving style of the user. The fuel efficiency of the iCON model described in section 2.4.3 is given as 50 km per liter of gas, resulting in 250 km per tank of gas. The range may be reduced depending on the driving habits of the user, therefore a lower more conservative value of 40 km/L is assumed.

$$1.5 \frac{\text{€}}{\text{L}} \times \frac{5\text{L}}{200\text{km}} = 0.03750 \frac{\text{€}}{\text{km}} = 3.75 \frac{\text{¢}}{\text{km}} \quad (5.12)$$

BATTERY POWERED ELECTRIC SCOOTERS

The cost of an electric scooter could vary depending on the price of electricity, the country, or the technology. It is assumed that the electricity is from the grid, therefore taking the grid prices mentioned in section 5.2.2.

Various manufacturers quote prices for charging, such as in [74] where the price was 50 cents/100km. In [75] the prices of electricity for public EV car chargers are given. The standard rate (e.g. Amsterdam) is given as 0.3388 € per kWh, but the prices can range between 0.23 and 0.484 €/kWh depending on the provider and the location. The electricity

price increases above that range for fast charging stations, ranging between 0.55 and 0.7139 € per kWh.

The model described in section 2.4.3 has a battery capacity of 1.74 kWh. Using commercial grid prices, this would cost a user 30.28 cents to recharge. This equates to a cost per km of between 0.61 and 0.4 cents/km (depending on the range considered).

HYDROGEN (FUEL CELL) ELECTRIC SCOOTERS

This is the determining factor to whether an Energy Wall with a hydrogen system for scooters is feasible for the chosen location in Rotterdam. The cost does not include taxes such as VAT. The lowest LCOH configurations were used to determine the cost per km, while attempting to fulfill the hydrogen demand each day. The range of costs is shown in table 5.4

The cost per kilometer driven of the fuel cell mopeds was found to be between 1.4 and 2.6 cents per km. This is still lower than the gas scooter cost per km, even when compared to the 250 km range that the gas scooter is able to achieve. The FC scooter figures are based on a range of 50 km. This value decreases if a larger range is achieved, such as the 80 km "highway mode".

6

RESULTS AND CONCLUSIONS

This section provides the findings of the undertaken work. The main and sub-research questions are reiterated here for completeness. A discussion around the proposed system is provided, followed by future work directions and propositions.

What is the feasibility of a hydrogen fueling station for scooters, powered by solar energy at a noise barrier?

SUB-RESEARCH QUESTIONS

1. In terms of usable noise barriers, how many are feasible to be coupled with a hydrogen supply and canister refueling station in the Netherlands?
2. In technical design terms, what would the Energy Wall with hydrogen production look like?
3. How economically feasible is it to supply hydrogen canisters to scooter users?
4. What are the technical barriers or benefits of this type of system in the Netherlands?

Noise barriers are stationary structures. They are normally found near inhabited areas rather than remote locations. Therefore it is reasonable to use these structures as the base for an electricity generation system for commercial mobility applications.

Through this study it was found that fuel cell scooters can cost less to operate than gas scooters (7.5 €/refuel, ≥ 3 ¢/km), but more than battery electric (30 ¢/refuel, ≥ 0.38 ¢/km) vehicles when using the proposed Energy Wall with H₂ production & storage system. The cost of hydrogen using a 3 kW electrolyzer produced hydrogen between 14.3 and 7.2 €/kg_{H₂}, depending on the number of Energy Wall Modules. The cost to refuel is thus between 2.57 - 1.29 €/refuel for a pair of canisters. With the most conservative distance range (50 km), and the highest cost hydrogen (1 Energy Wall Module, 14.3€/kg), the cost per km of a fuel cell scooter is 2.58¢/km, still lower than that of an optimistically ranged (250 km) gas scooter, which operates at 3 ¢/km.

6.1. GEOGRAPHICAL FEASIBILITY OF NOISE BARRIERS AS ENERGY WALLS WITH HYDROGEN PRODUCTION FOR SCOOTERS IN THE NETHERLANDS

This question was approached in three parts: the scooter distribution in various geographical entities, noise barrier suitability in the Netherlands, and the coupling potential between theoretical fuel cell scooter demand and noise barrier electricity generation capability (extensively discussed in chapter 3).

There are currently a little more than 1 million scooters registered in The Netherlands, ranking it 6th amongst European countries. Due to the high number of scooters and population density that The Netherlands demonstrated compared to other European countries, the possibility of a successful system is likely. The scooter population of the Netherlands was examined using Geographic Information Systems (GIS). For the scooter analysis, a dataset provided by the central bureau of statistics (CBS [52]) was used which provided the distribution of light scooters (snorfiets). Snorfiets represent 61% of the total scooters in the Netherlands.

Three levels of land classification were examined: national, provincial and municipal (for those which had over 4,000 scooters). It was found that around a quarter (24.6%) of the total number of light scooters (snorfiets) were registered in the 25 municipalities which had the highest number of scooters.

The noise barrier analysis focused on filtering out unsuitable barriers in terms of their material and tilt direction properties. It was found that 34.53% of existing noise barriers *were* suitable to be converted into Energy Wall units; 65.47% of noise barriers were unsuitable. A table summarizing the filtering criteria, and what length was removed/kept due to which filter is presented in table 6.1. The materials that were suitable also provide structural integrity for the installation of a micro wind turbine if desired.

The coupling feasibility part of this research examined the PV electricity generation potential of the barriers both at the nationwide and at the municipal level (for the highest ranked municipalities). The nationwide potential (i.e. the entire length of suitable barriers) was estimated to be 60.1 *GWh/year* for a length of 370 km of noise barriers. The population of scooters consists of 655,965 light scooter (snorfiets) units, which would theoretically require 59.26 *GWh/year* of electricity to produce enough hydrogen to satisfy the annual distance covered by these scooters. Therefore, in theory the entire population of snorfiets could be satisfied purely on noise barrier electricity generation since the nationwide noise barrier potential was slightly greater than the total scooter electricity demand.

The conclusion that all the scooters could be satisfied by the noise barriers is made on an annual electricity generation basis, which excludes the complications of seasonal and daily energy production profiles from PV systems, however these could be aided by storage methods. Here hydrogen would be recommended since it is advantageous long term and the possibility to expand the infrastructure is there.

Next the electricity potential of the barriers only found within the top 25 municipalities was estimated, as well as the corresponding demand of electricity for hydrogen production

Filtering Criterion	Length [km]	Share of Total NBs
Unfiltered (Total) Barriers	1071.4	100%
Material Kept	494	46.12%
Concrete	226.3	21.12%
Glass/Plastic Transparent	10.6	0.98%
Glass/Plastic Non-Transparent	186.2	17.38%
Metal	71.2	6.65%
Material Filtered Out	-577	-53.88%
Earth	-399.6	-37.31%
Wood Fiber Concrete	-99.7	-9.30%
Wood	-50.7	-4.73%
Growth Screen	-11.3	-1.05%
Stone	-7.0	-0.65%
Gabion	-4.8	-0.45%
Others	-4.1	-0.38%
Tilt Filtered Out	-124.4	-11.61%
Forward Tilt - North of Road	-5.2	-0.48%
Backward Tilt - South of Road	-119.2	-11.13%
Remaining Suitable Barriers	370	34.53%

Table 6.1: Noise Barrier Filtering Characteristics and Lengths

that would hypothetically be required by the scooters in close proximity to said barriers. The results are reproduced in table 6.2 where the last column shows the ratio between the noise barrier potential and the theoretical scooter demand.

Detailed maps of the municipalities with the most scooters can be seen in appendix D. In summary, the following conclusions were found:

- The Netherlands is ranked 6th in the number of scooters in Europe
- In 2018, there were 1,107,700 registered scooters in the Netherlands (678,363 snorfietts & 429,337 bromfietts) [7]
- Amsterdam had the highest number of scooters (>18,000). Rotterdam and Den Haag also had very high numbers, with >10,000 each.
- The group of municipalities around Amsterdam (i.e. Amsterdam, Haarlem, and Zaanstad) contained >30,000 scooters together. People who live in these areas commonly work in or around Amsterdam, therefore a refueling station there could serve commuters in these neighborhoods for example
- The 25 most scooter-rich municipalities accounted for 24.6% of the nationwide snorfietts population
- Estimated nationwide Energy Wall electricity generation potential: 60.1 GWh/year
- Nationwide snorfietts electricity demand (100% FC scooters): 59.26 GWh/year

Municipality Names	No. Scooters	Demand [GWh/year]	NB length [km]	NB Potential [GWh/year]
Amsterdam, Haarlem & Zaanstad	30,015	2.71	48.82	8.33
Rotterdam	20,280	1.83	41.92	6.82
The Hague & Zoetermeer	11,865	1.07	16.93	2.24
Utrecht	10,775	0.97	17.23	2.48
Eindhoven	8,520	0.77	18.22	2.90
Amersfoort	6,805	0.61	4.22	0.79
s-Hertogenbosch	5,930	0.54	20.20	3.55
Breda	5,130	0.46	8.21	1.50
Apeldoorn	4,465	0.40	3.24	0.44
Ede	4,465	0.40	2.77	0.40
Zwolle	4,200	0.38	4.66	0.99
Groningen	4,165	0.38	1.07	0.13
Tilburg	3,940	0.36	1.41	0.22
Enschede	2,980	0.27	0.46	0.06
Arnhem	2,855	0.26	4.67	0.65
Haarlemmermeer	2,450	0.22	4.56	0.86
Alkmaar	2,435	0.22	1.07	0.13
Emmen	2,150	0.19	0.70	0.12
Alphen aan den Rijn	1,945	0.18	5.32	1.04

Table 6.2: Selected municipality data about scooters, electricity demand, noise barrier length & potential electricity generation

- The length of suitable barriers is sufficient to supply the demand of electricity for hydrogen production for the entire population of snorfiets on an annual basis
- Municipal: 19 of the 25 scooter-rich municipalities had sufficient noise barrier length (at appropriate orientation and tilt) to meet the annual electricity demand of scooters. The comparison of scooter demand to noise barrier potential is shown in figure 3.10; the details of the number of scooters, length of barriers, electricity potential, and scooter demand for (grouped) municipalities is shown in table 6.2.

6.2. DESIGN & SIMULATION OF ENERGY WALL COUPLED WITH HYDROGEN PRODUCTION AND STORAGE UNITS

Various aspects were explored in the simulation of the Energy Wall with hydrogen production. The patterns of energy exchange influenced parameters such as the state of charge (SOC) of the tanks, the number of days that the SOC was sufficient, the capacity factor of

the electrolyzer and the Energy Wall and how much the Energy Wall contributed to the production of hydrogen for each configuration. Reiterating a part of section 5.4, the three energy exchange flows were defined as follow:

- PV2E: Energy Wall to Electrolyzer
- PV2G: Energy Wall to Grid
- PG2E: Grid to Electrolyzer

The demand of the hydrogen production system was sized based on the scooter mileage and hence "fuel" consumption demand. The total distance travelled by all bromfiets in 2017 was 939 million kilometers, over a third of which were to and from work. [7] A value of 2.5 km/day/scooter was assumed (method and reasoning was explained in section 4.1), however this value could change according to the intensity of use of the user. For occasional scooter users this value is lower, however for more intensive users such as delivery scooters the assumed value is probably underestimated. The fleet of scooters assumed was 100 units, as this would be a decent fleet in the larger cities, and would enable a gradual roll-out of stations.

The system simulated explored sizes of Energy Wall modules, which consisted of 12 panels, or 4.08 kWp each. Therefore 2 Energy Wall modules are 24 panels, 8.16 kWp and so forth. The range of electrolyzers explored was in 1 kW steps between 1 and 5 kW input.

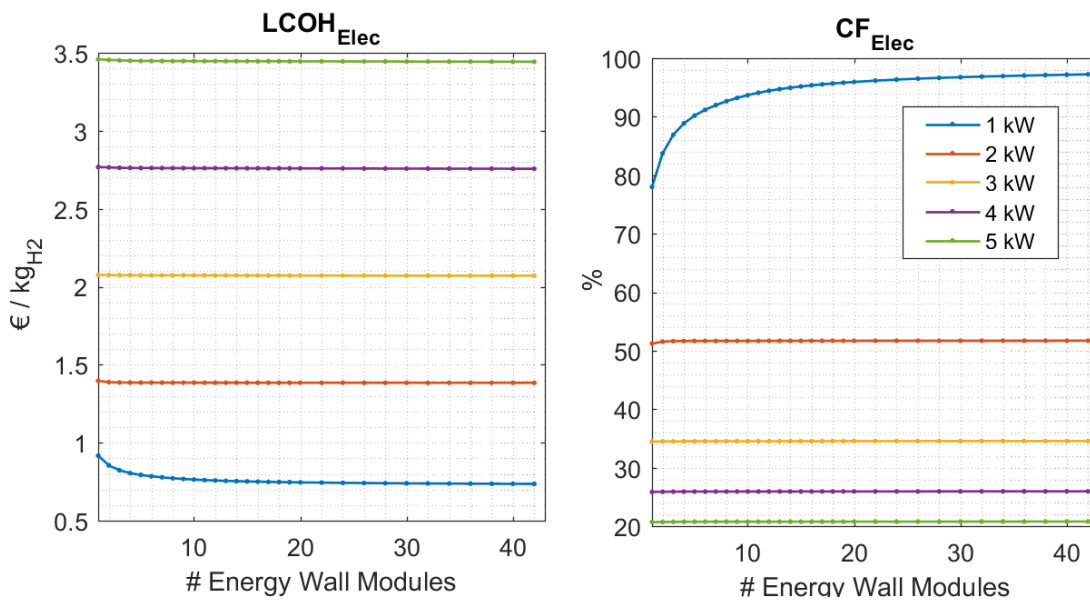


Figure 6.1: Trend of $LCOH_{Elec}$ and CF_{Elec} with increasing Electrolyzer Capacity

DAILY STATE OF CHARGE

The daily state of charge (SOC) is the buffer tank level at the end of the day, and the values for small electrolyzers are shown in figure 6.2; larger electrolyzers achieved >95% for the majority of configurations and hence their figures were not included here (values can be seen in figure 4.13). In summary it was found that the number of days which the daily SOC surpassed 90% using a 1 kW electrolyzer increased with increasing number of Energy Wall modules, however even with the largest Energy Wall setup, the SOC was >90% for 210 out

of 365 days a year. At this size Energy Wall, the 1 kW electrolyzer still struggled to surpass 95%. With a 2 kW electrolyzer the days which the SOC reached sufficient levels was much higher, and for 5 or more Energy Wall modules a >95% was achieved more than 360 days of the year.

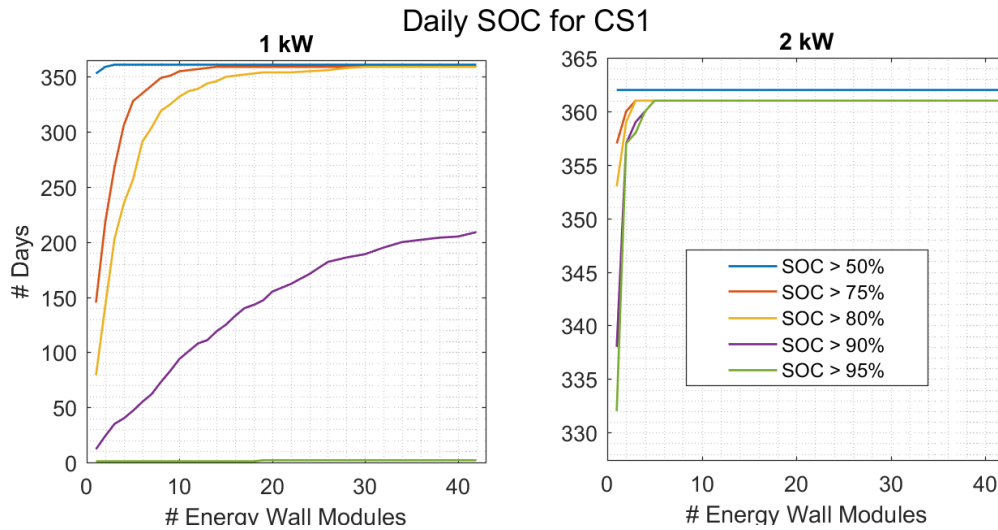


Figure 6.2: State of Charge of 1kW and 2 kW Electrolyzers using CS1

ELECTROLYZER CAPACITY FACTOR

The electrolyzer capacity factor (CF_{Elec}) varied with different sized electrolyzers. The larger the electrolyzer, the smaller the CF_{Elec} . The highest CF_{Elec} achieved was with a 1 kW electrolyzer (for >20 Energy Wall module configurations). The variation of CF_{Elec} with electrolyzer size for CS1 is shown in figure 6.1 alongside the overall levelized cost of hydrogen.

CONTRIBUTION OF ENERGY WALL

The contribution of the Energy Wall was directly correlated to the LCOH of the configurations. More electricity from the Energy Wall meant a lower weighted cost for electrolysis.

The relationship was almost the same, however because the contribution is a percentage value and the grid cost changes according to the quantity of electricity it must process, the proportions are not exactly the same. In conclusion, the lower the contribution by PV, the higher the grid input, and hence the higher the cost of electricity sent to the electrolyzer, which was one of the most influential factors of the LCOH.

CONTROL STRATEGY EVALUATION

Two control strategies were simulated. The first, CS1, maximized the use of Energy Wall electricity where possible. The second, CS2, focused on operating the electrolyzer at full capacity when the tank level wasn't full, using both Energy Wall and grid electricity.

The cost of electricity was lower when CS1 was used since a larger portion of the electricity input for electrolysis came from the lower-cost PV system as compared to CS2. The capacity factor and levelized cost of the electrolyzer varied with the number of energy wall

units when the electrolyzer was 1 kW. The increasing capacity factor indicates that the electrolyzer is operates more efficiently at large Energy Wall modules, thereby reducing its levelized cost in these ranges.

CS2 was beneficial in terms of minimizing the levelized cost of the electrolyzer regardless of the number of Energy Wall modules. The rate of hydrogen production was maximized in the hours that the electrolyzer was operating; the number of operating hours were limited by the demand, since after the point where the demand is certainly supplied (>2 kW for this setup) CF_{Elec} decreases as installed electrolyzer capacity increases. This applies for both control strategies: in figure 6.1, the larger the electrolyzer capacity, the lower the annual capacity factor since the demand is satisfied quicker.

In conclusion, CS1 was more beneficial to the cost of hydrogen when the electrolyzer capacity was sufficient. Each 1 kW step increase in electrolyzer capacity increased the LCOH by 48-68 ¢/kg_{H₂}. CS1 was able to deliver lower cost hydrogen reliably with a 2 kW electrolyzer, but the overall LCOH was lower using a 3 kW electrolysis unit. CS2 was able to reliably supply hydrogen with a 2 kW electrolyzer, however the cost achieved by the 3 kW electrolyzer configuration was more competitive with the 2 kW-CS1 configuration. The 3kW-CS2 had a lower cost due to the capability of the electrolyzer to use more Energy Wall electricity at any given hour, increasing the contribution.

6.3. ECONOMIC FEASIBILITY OF AN ENERGY WALL H₂ REFUELING SYSTEM

The method, assumptions, and findings of the cost modelling of the components of a hydrogen refueling station are detailed in Chapter 5. The cost findings present the electricity, electrolyzer, final cost of delivered hydrogen, and include a cost comparison between different types of scooters.

LCOH OF ENERGY WALL CONFIGURATIONS

From all the configurations considered, the lowest levelized cost of hydrogen was achieved with a 3 kW electrolyzer using CS1, by using PV electricity primarily and topping up from the grid during the night. Figure 6.3 shows the levelized cost of all configurations simulated; the 3 kW-CS1 electrolyzer ranged between 14.3 and 7.2 €/kg_{H₂}.

This leads to a canister (45g_{H₂}) cost between 64.3 and 32.4 ¢/canister. The cost per kilometer of the hydrogen scooter, assuming a 50 km range, was thus found to be between 2.57 and 1.29 ¢/km. The choice of price depends on the number of Energy Wall modules. Fewer modules meant a higher LCOH, canister cost and cost/km, but lower capital expenses.

The lower cost of CS1 was attributed to the lower electricity costs. CS2 made better use of the electrolyzer however the savings on electrolysis were less than those incurred by higher electricity prices. Given the constant demand, CF_{Elec} decreases with increasing electrolyzer sizes, while $LCOH_{Elec}$ increases accordingly, shown in figure 6.1.

It should be noted that the daily demand of the simulation was kept constant for each day of the year, and the buffer storage tanks were sized to accommodate this quantity. It would be interesting to see how the system might behave in the case where the tanks were

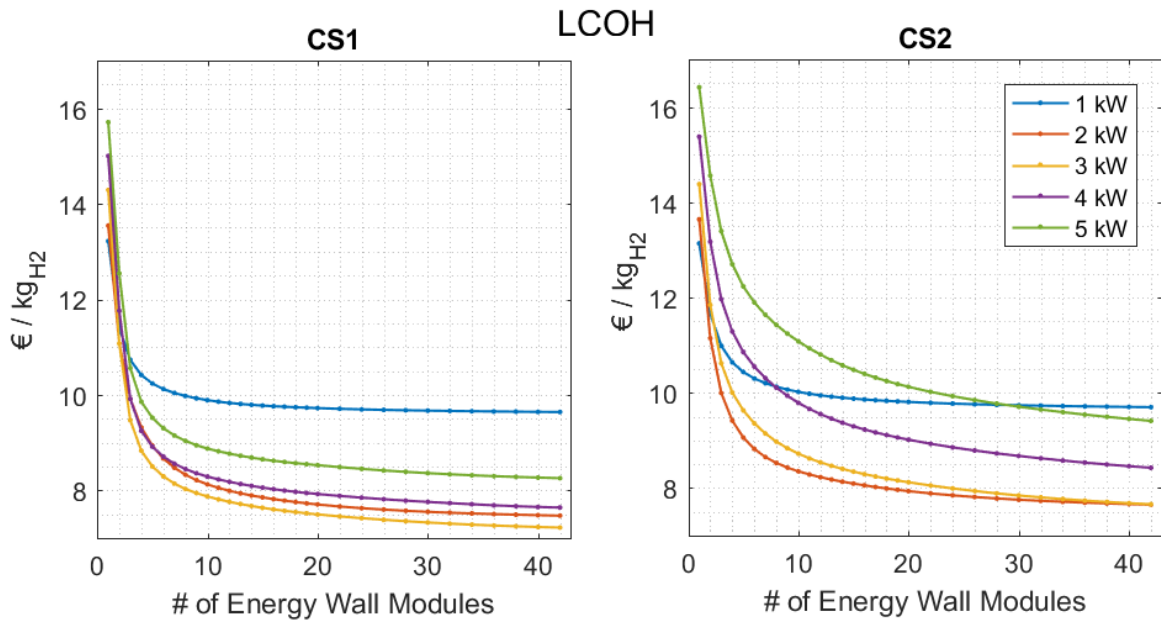


Figure 6.3: Overall LCOH of Configurations

larger than the daily demand, and were used to top up in periods of low PV electricity production, such as the winter when there are fewer sun hours.

SCOOTER FUEL COST PER KM COMPARISON

The question is whether the price of hydrogen as a fuel is competitive with conventional fuel or battery electric scooters. The scooter acquisition cost will be higher on average, as fuel cell mopeds are a novel technology, still mostly in the demonstration and development phase, disadvantaged at the maturity and availability of gas scooters (and the option to buy second or third hand). The availability of refueling stations is also limited in the case of FCEVs, but there are hopes that this will not be the case for long.

The cost of hydrogen as fuel per kilometer driven was estimated for three scooter technologies: gas, battery electric, and fuel cell electric. Details of the scooters sampled and their per km costs are reproduced in table 6.3. The low and high end of ranges achievable were explored for completeness, since this varies amongst driving styles and situations.

	APFCT	Niu:NQi Sport	AGM iCON50
Type	Fuel Cell	Battery	Gas
Capacity	90 g _{H₂}	1.74 kWh	5 L
Cost of 1 Refill	1.29 - 0.70 €	0.3 €	7.5 €
Range	50* - 80 km	50 - 80 km	150 - 250 km
Cost / km <i>€/km</i>	2.57 - 1.29	0.6 - 0.38	5 - 3

Table 6.3: Summary of Scooter Operating Costs, *50 km range assumed for FC Scooter

A gas scooter, such as the AGM iCON50, holds 5 L of fuel, and at an average price of

1.5€/L in the Netherlands [73] the cost per refill is 7.5€. An optimistic range of 250 km (50km:L) or a conservative range of 150 km (30km:L) means operational costs of 3 ¢/km to 5 ¢/km respectively.

The battery electric model chosen had a battery capacity of 1.74 kWh, therefore at a grid price of 17.4 ¢/kWh, one recharge costs 30 ¢. The driving range is between 50 and 80 km. The optimistic 80 km range costs 0.3 ¢/km, while in city-mode (50km range) its 0.6 ¢/km. This is the target price at which fuel cell scooters could be competitive with battery electric vehicles.

Fuel cell scooters depend on the price of hydrogen. In the simulated electricity production and hydrogen system, the cost of h2 was as low as 7.2 €/kg, but could be as low as 5.89€/kg, the lower end of solar electrolysis in [15]. The cost depending on the price of H₂ and range is shown in table 6.4.

	Energy Wall			Low-cost solar electrolysis [15]	Competitive with BEV scenario
Price of H ₂	14.2€/kg _{H₂}	7.9€/kg _{H₂}	7.2€/kg _{H₂}	5.89 €/kg _{H₂}	3.33€/kg _{H₂}
Energy Wall Modules	1	10	40	N/A	N/A
PV Capacity	4.08 kWp	40.8 kWp	163.2 kWp		
Cost of Refuel	1.29 €	71.1 ¢	64.8¢	52¢	30¢
50 km Range Cost	2.58¢/km	1.42¢/km	1.30¢/km	0.95¢/km	0.6¢/km
80 km Range Cost	1.61¢/km	0.89¢/km	0.81¢/km	0.65¢/km	0.38¢/km

Table 6.4: Fuel Cell Scooter Cost Scenarios

6.4. EVALUATION OF H2 REFUELING STATION FOR SCOOTERS SYSTEM IN THE NETHERLANDS

The Dutch lifestyle allows for scooter use in daily life. Even during pandemic times, scooters seem to be a good option to get around.

In the choice of Fuel Cell or Battery electric vehicles, it should not be argued but rather discussed as to which one is more suitable. Different things suit different people, more importantly the point is to build infrastructure to cater for those able and willing to transition. A detailed comparison is provided in section 2.4.

In cases where a shortage of hydrogen occurs, the option of importing it from elsewhere is available. For battery powered vehicles this would be the equivalent of the grid, but electricity is less easily quantified as compared to hydrogen which is a "tangible" fuel.

The cost of battery powered electric mopeds remains the lowest to date, followed by fuel cell electric and finally gas powered scooters. The cost comparison is shown in table 6.3

IMPORTING HYDROGEN

An alternative set up to this system would be to import hydrogen from industrial production facilities. Although the majority of industrial hydrogen is grey, given the ambitions of various organizations to move towards sustainable economies, blue and green facilities are being implemented.

For fuel cell scooters to be competitive with battery electric, the price of hydrogen needs to be lower, which is possible when using industrially produced hydrogen (however currently the majority of this is not *green*, but rather grey or blue hydrogen). Electric scooters are able to achieve a per km cost of 0.6 ¢/km (assuming a 50 km range). The price per refill is 30 ¢. For one canister (45g_{H₂}) to cost 15¢ (30¢ per pair to refill), the price of hydrogen needs to be 3.33€/kg.

Process	Energy source	Feedstock	Capital cost (M\$)	Hydrogen cost (\$/kg)
SMR with CCS	Standard fossil fuels	Natural gas	226.4	2.27
SMR without CCS	Standard fossil fuels	Natural gas	180.7	2.08
CC with CCS	Standard fossil fuels	Coal	545.6	1.63
CG without CCS	Standard fossil fuels	Coal	435.9	1.34
ATR of methane with CCS	Standard fossil fuels	Natural gas	183.8	1.48
Methane pyrolysis	Internally generated steam	Natural gas	–	1.59–1.70
Biomass pyrolysis	Internally generated steam	Woody biomass	53.4–3.1	1.25–2.20
Biomass gasification	Internally generated steam	Woody biomass	149.3–6.4	1.77–2.05
Direct bio-photolysis	Solar	Water + algae	50 \$/m ²	2.13
Indirect bio-photolysis	Solar	Water + algae	135 \$/m ²	1.42
Dark fermentation	–	Organic biomass	–	2.57
Photo-fermentation	Solar	Organic biomass	–	2.83
Solar PV electrolysis	Solar	Water	12–54.5	5.78–23.27
Solar thermal electrolysis	Solar	Water	421–22.1	5.10–10.49
Wind electrolysis	Wind	Water	504.8–499.6	5.89–6.03
Nuclear electrolysis	Nuclear	Water	–	4.15–7.00
Nuclear thermolysis	Nuclear	Water	39.6–2107.6	2.17–2.63
Solar thermolysis	Solar	Water	5.7–16	7.98–8.40
Photo-electrolysis	Solar	Water	–	10.36

Table 6.5: Comparison of different hydrogen production methods, reproduced from [15]

The price of commercially produced is provided in [15] for various forms of production, reproduced in table 6.5. It is shown below for reference. This system was able to achieve a

cost of 7.2 €/kg, which is within the range provided for solar electrolysis.

REFUELING POINT

The logistics of a refueling station would work as a conventional refueling station, where a consumer arrives, pays for a refill of their canister, and exchanges their (almost) empty canister for a full one. With a proper IT system to manage safe transactions and mechanisms prohibiting theft or damage, the station could, to a large extent, function independently.

The refueling time is very short, but it requires the user to travel to a refueling point. One possibility could be the distribution of canisters to other common points such as convenience stores or stations. Battery electric scooters generally need to stay at the charging point for a longer time, although this could be at the place of work or home of the user, or at a public charging station. One issue here is the length of time one can leave their vehicle at a charging station, as it may be used by multiple users and the availability of the charging point is a consideration to whether one can charge their vehicle or not.

SEASONALITY

One system configuration which could be explored could be the production of hydrogen with a standalone PV system (rather than grid connected). This would require larger buffer storage tanks since they would be filling up to provide through seasons with less PV production (i.e. winter). This also provides a competitive advantage to an isolated system (where grid connection may not be present) as it provides independence and self-sufficiency.

AVOIDED EMISSIONS

The avoided emissions that this case study would achieve are shown in table 6.6. These emissions are quite harmful to the health of people, therefore when avoided provide a better quality of life. The emissions in major cities are quite high, often above the limits set by health organizations.

Pollutant	CO	NO _x	THC
Quantity [kg]	91.25	15.5	57.5

Table 6.6: Estimated Avoided Annual Emissions of 100 FC Scooters

6.5. FUTURE WORK

This field is quite novel, hence the scope of work had to be limited. There are many aspects that could be explored further, some of which are mentioned below.

- Further analysis of PV and wind potential of noise barriers in the Netherlands.
- More indepth filtering of noise barriers could include assessing the horizon of the NBs. Some may have high buildings in front, or taller noise barriers, or low PV potential.
- Vary the size of the storage tanks and observe effects on PV utilization, cost of hydrogen, and other parameters.

- Explore the addition of other applications to one refueling station, such as large trucks or busses (producing hydrogen for "their" empty tanks, in a decentralized manner)
- Using buffer batteries rather than a grid connection and exploring the cost of this configuration set up
- Set this system up for a scooter-sharing business model (such as felyx scooters in the Netherlands [76])

BIBLIOGRAPHY

- [1] O. Isabella, A. Smets, K. Jäger, M. Zeman, and R. van Swaaij, *Solar energy: The physics and engineering of photovoltaic conversion, technologies and systems*, UIT Cambridge Limited (2016).
- [2] J. Toothman and S. Alodous, <https://science.howstuffworks.com/environmental/energy/solar-cell.htm> (2000).
- [3] *7 different types of solar panels explained*, <https://www.greenmatch.co.uk/blog/2015/09/types-of-solar-panels> (2018).
- [4] A. M. Bagher, M. M. A. Vahid, and M. Mohsen, *Types of solar cells and application*, American Journal of optics and Photonics **3**, 94 (2015).
- [5] IEA, *Iea countries: The netherlands*, <https://www.iea.org/countries/the-netherlands> (2019).
- [6] *Hydrogen storage*, <https://www.energy.gov/eere/fuelcells/hydrogen-storage>.
- [7] *Mobiliteit in cijfers: Tweewielers 2018-2019*, (2018).
- [8] M. A. Nash, *Multi-criteria analysis of the Energy wall*, Master's thesis, Delft University of Technology (2018).
- [9] IRENA, *Renewable Power Generation Costs in 2018*, Tech. Rep. (International Renewable Energy Agency, 2019).
- [10] R. Fu, D. Feldman, R. Margolis, M. Woodhouse, and K. Ardani, *US solar photovoltaic system cost benchmark: Q1 2017*, Tech. Rep. (EERE Publication and Product Library, 2017).
- [11] eurostat, *Shares: Short assessment of renewable energy sources*, <https://ec.europa.eu/eurostat/web/energy/data/shares>.
- [12] M. M. Rashid, M. K. Al Mesfer, H. Naseem, and M. Danish, *Hydrogen production by water electrolysis: A review of alkaline water electrolysis, pem water electrolysis and high temperature water electrolysis*, International Journal of Engineering and Advanced Technology (IJEAT) **4** (2015).
- [13] J. J. Hwang, *Review on development and demonstration of hydrogen fuel cell scooters*, Renewable and Sustainable Energy Reviews **16**, 3803 (2012).

- [14] *Addendum to the multi-annual work plan 2014-2020*, https://www.fch.europa.eu/sites/default/files/MAWP%20final%20version_endorsed%20GB%2015062018%20%28ID%203712421%29.pdf.
- [15] M. Kayfeci, A. Keçebaş, and M. Bayat, *Chapter 3 - hydrogen production*, in *Solar Hydrogen Production*, edited by F. Calise, M. D. D'Accadia, M. Santarelli, A. Lanzini, and D. Ferrero (Academic Press, 2019) pp. 45 – 83.
- [16] *Elektriciteit tarieven 2019*, <https://www.stedin.net/zakelijk/~media/files/stedin/tarieven/gv/stedin-2019-tarieven-gv-elektriciteit.pdf> (2018).
- [17] IRENA, *Trends in renewable energy*, <https://www.irena.org/Statistics/View-Data-by-Topic/Capacity-and-Generation/Statistics-Time-Series> (2019).
- [18] eurostat, *Energy balance flow of european countries*, https://ec.europa.eu/eurostat/cache/sankey/energy/sankey.html?geos=NL&year=2018&unit=KTOE&fuels=TOTAL&highlight=_&nodeDisagg=11111111111111&flowDisagg=true&translateX=-2908.015530368638&translateY=-278.50490975804723&scale=2.487391833915301&language=EN (2019).
- [19] International Energy Agency, *Co2 emissions from fuel combustion*, <https://iea.blob.core.windows.net/assets/38460ae3-b53d-4d47-af2a-d6180377e2e0/CO2Highlights2019-Excelfile.XLS> (2019).
- [20] *Intended nationally determined contribution of the eu and its member states*, <https://www4.unfccc.int/sites/ndcstaging/PublishedDocuments/Netherlands%20First/LV-03-06-EU%20INDC.pdf> (2015).
- [21] <https://ec.europa.eu/eurostat/documents/2995521/10335438/8-23012020-AP-EN.pdf/292cf2e5-8870-4525-7ad7-188864ba0c29> (2020).
- [22] A. van Wijk, *The Green Hydrogen Economy in the Northern Netherlands*, (2017).
- [23] R. Dixon, J. Li, and M. Wang, *13 - progress in hydrogen energy infrastructure development—addressing technical and institutional barriers*, in *Compendium of Hydrogen Energy*, Woodhead Publishing Series in Energy, edited by R. B. Gupta, A. Basile, and T. N. Veziroğlu (Woodhead Publishing, 2016) pp. 323 – 343.
- [24] A. Körner, C. Tam, S. Bennett, and J. Gagné, *Technology roadmap-hydrogen and fuel cells*, International Energy Agency (IEA): Paris, France (2015).
- [25] K. E. Ayers, E. B. Anderson, C. Capuano, B. Carter, L. Dalton, G. Hanlon, J. Manco, and M. Niedzwiecki, *Research advances towards low cost, high efficiency pem electrolysis*, *Ecs Transactions* **33**, 3 (2010).

- [26] A. Vilarasau-Amoros, *Turning noise barriers into sustainable energy systems*, Master's thesis, Delft University of Technology (2018).
- [27] Provincie Zuid Holland, *N470 geeft energie: Innoveren*, <https://www.zuid-holland.nl/onderwerpen/energie/energiewegen-0/n470-geeft-energie/innoveren/>.
- [28] N. Chrysochoidis-Antsos, V. Oldenbroek, F. Bisschop, and A. Wijk, *The wind energy potential along highways to fuel a sustainable transportation sector*, (2015).
- [29] *Fijn stof (pm2,5/pm10)*, <https://www.samenmetenaanluchtkwaliteit.nl/fijn-stof-pm25pm10>.
- [30] M. Gelofs-Nijland, E. Mathijssen, W. Jongeneel, and F. Cassee, *Gezondheidseffecten van brommeremissies*, <https://www.rivm.nl/bibliotheek/rapporten/630315001.pdf> (2011).
- [31] S. M. Platt, I. E. Haddad, S. M. Pieber, R.-J. Huang, A. A. Zardini, M. Clairotte, R. Suarez-Bertoa, P. Barnet, L. Pfaffenberger, and R. Wolf, *Two-stroke scooters are a dominant source of air pollution in many cities*, *Nature communications* **5**, 3749 (2014).
- [32] R. Maas, P. Fischer, J. Wesseling, D. Houthuijs, and F. Cassee, *Luchtkwaliteit en gezondheidswinst*, https://www.rivm.nl/sites/default/files/2018-11/RIVM%20nota%20Luchtkwaliteit%20en%20gezondheidswinst_REV20170317.pdf (2015).
- [33] D. W. E. Association, *What is distributed wind?* <https://distributedwind.org/home/learn-about-distributed-wind/what-is-distributed-wind/> (2019).
- [34] M. Carmo, D. L. Fritz, J. Mergel, and D. Stolten, *A comprehensive review on pem water electrolysis*, *International Journal of Hydrogen Energy* **38**, 4901 (2013).
- [35] R. L. Busby, *Hydrogen and fuel cells: a comprehensive guide* (Pennwell Books, 2005).
- [36] J. Ivy, *Summary of electrolytic hydrogen production: milestone completion report*, Tech. Rep. (National Renewable Energy Lab., Golden, CO (US), 2004).
- [37] A. Awasthi, K. Scott, and S. Basu, *Dynamic modeling and simulation of a proton exchange membrane electrolyzer for hydrogen production*, *International journal of hydrogen energy* **36**, 14779 (2011).
- [38] R. Carriveau and D. S.-K. Ting, *Hydrogen storage and compression*, in *Methane and Hydrogen for Energy Storage* (Institution of Engineering and Technology, 2016) Chap. 1.
- [39] *Mahytec: Products*, <http://www.mahytec.com/en/products/>.
- [40] Mahytec, *Datasheet mht-60bar 850l: Type iv buffer tank at 60 bar*, <http://www.mahytec.com/wp-content/uploads/2018/07/CL-DS10-Datasheet-60bar-201801.pdf>.

- [41] *Asia pacific fuel cell technologies: Products*, <http://www.apfct.com/en>.
- [42] D. Ewalds, G. Moritz, and M. Sijstermans, *Bromfietsen in nederland*, <https://www.cbs.nl/-/media/imported/documents/2013/22/2013-bromfietsen-in-nederland-pub.pdf> (2013).
- [43] K. Ash, *Suzuki fuel cell burgman*, <http://www.ashonbikes.com/content/suzuki-fuel-cell-burgman> (2013).
- [44] *Mobiliteit in cijfers: Tweewielers 2016-2017*, (2016).
- [45] E. Ibrahim, *Are batteries sustainable?* <https://www.energycentral.com/c/pip/are-batteries-sustainable>.
- [46] S. Curtin and J. Gangi, *Fuel cell technologies market report 2013*, Fuel cell and Hydrogen Energy Association, Washington (2014).
- [47] *Hydrogen scaling up: A sustainable pathway for the global energy transition*, (2017).
- [48] G. Guizzi, M. Manno, and M. D. Falco], *Hybrid fuel cell-based energy system with metal hydride hydrogen storage for small mobile applications*, *International Journal of Hydrogen Energy* **34**, 3112 (2009).
- [49] *AGM iCON 50 EURO4*, <https://www.fastfuriousscooters.nl/agm/icon-50#lees-product-info>.
- [50] Niu, *NQi Series*, <https://www.niu.com/en/n-series/>.
- [51] AGM, *iCON50*, <https://agm.nl/modellen/benzine-scooters/agm/icon50/>.
- [52] *Wijk- en buurtkaart 2018*, <https://www.cbs.nl/nl-nl/dossier/nederland-regionaal/geografische%20data/wijk-en-buurtkaart-2018> (2018).
- [53] Office of Natural Environment, *Highway renewable energy: Photovoltaic noise barrier*, (2017).
- [54] D. Lenardic, *Photovoltaic noise barriers*, <http://sunenergysite.eu/en/pvpowerplants/noisebarriers.php> (2015).
- [55] *Unique noise barrier generates energy on both sides*, <https://www.tno.nl/en/tno-insights/articles/unique-noise-barrier-generates-energy-on-both-sides/> (2019).
- [56] Rijkswaterstaat, *Solar highways*, <https://solarhighways.eu/en/about-solar-highways/project> (2018).

- [57] N. Chrysochoidis-Antsos, *Micro wind turbines integrated on noise barriers*, <https://www.researchgate.net/project/Micro-wind-turbines-integrated-on-noise-barriers/figures> (2017).
- [58] *Photovoltaic geographical information system*, https://re.jrc.ec.europa.eu/pvg_tools/en/tools.html (2017).
- [59] A. D. L. Barbara Vanhooreweder, Sebastien Maroccoi, *Technical Report 2017-02 - State of the art in managing road traffic noise: noise barriers*, Tech. Rep. (2017).
- [60] T. Nordmann and L. Clavadetscher, *Pv on noise barriers*, (2004).
- [61] *Green hydrogen - from renewable energy*, <http://greenhydrogen.dk/>.
- [62] R. A. Blackman, *The increased popularity of mopeds and motor scooters: Exploring usage patterns and safety outcomes*, <https://eprints.qut.edu.au/52685/> (2012).
- [63] M. Solanki, *It's started: Fines for scooters on amsterdam cycle paths*, <https://www.iamexpat.nl/expat-info/dutch-expat-news/its-started-fines-scooters-amsterdam-cycle-paths> (2019).
- [64] *Electricity output explained*, <https://news.energysage.com/what-is-the-power-output-of-a-solar-panel/>.
- [65] *EU: Motorcycles: Emissions*, <https://www.transportpolicy.net/standard/eu-motorcycles-emissions/> (2018).
- [66] *Eur-lex - 32013r0168 - en*, <https://eur-lex.europa.eu/legal-content/EN/ALL/?uri=CELEX:32013R0168> (2013).
- [67] C. Kost, S. Shammugam, V. Jülch, N. Huyen-Tran, and T. Schlegl, *Levelized cost of electricity renewable energy technologies*, Fraunhofer Institute for Solar Energy Systems ISE (2018).
- [68] CBS, *Aardgas en elektriciteit, gemiddelde prijzen van eindverbruikers*, <https://statline.cbs.nl/StatWeb/publication/?VW=T&DM=SLNL&PA=81309NED&D1=0-1,3,5,7-8,11,15&D2=0&D3=a&D4=a&HD=121114-1344&HDR=G1,G2,T&STB=G3> (2019).
- [69] S. M. Ali and J. Andrews, *Low-cost storage options for solar hydrogen systems for remote area power supply*, <https://www.cder.dz/A2H2/Medias/Download/Proc%20PDF/PARALLEL%20SESSIONS/%5BS12%5D%20Storage%20-%20Gaseous%20Hydrogen/15-06-06/282.pdf> (2006).
- [70] V. Barsukov and F. Beck, *New promising electrochemical systems for rechargeable batteries*, Vol. 6 (Springer Science & Business Media, 2013).

- [71] *Module price index*, <https://www.pv-magazine.com/features/investors/module-price-index/> (2019).
- [72] J. Mason and K. Zweibel, *Centralized production of hydrogen using a coupled water electrolyzer-solar photovoltaic system*, in *Solar hydrogen generation* (Springer, 2008) pp. 273–313.
- [73] *Netherlands gasoline prices*, https://www.globalpetrolprices.com/Netherlands/Amsterdam/gasoline_prices/ (2020).
- [74] *Elektrische scooters*, <https://www.fastfuriousscooters.nl/elektrische-scooter/>.
- [75] *Een laadpas voor je elektrische auto - de laadtarieven met een vattenfall in-charge laadpas*, <https://www.vattenfall.nl/producten/elektrisch-rijden/laadpas-en-tarieven/>.
- [76] Felyx, *felyx: Travel fast & affordable by felyx scooter through the city*, <https://felyx.com/nl/en>.
- [77] M. Blackwood, *Maximum efficiency of a wind turbine*, <https://scholarcommons.usf.edu/ujmm/vol6/iss2/2> (2016).
- [78] DataGenetics, *Wind turbine efficiency*, <http://datagenetics.com/blog/june12017/index.html> (2017).
- [79] *Electric power monthly*, https://www.eia.gov/electricity/monthly/epm_table_grapher.php?t=epmt_6_07_b (2019).
- [80] W. Europe, *Wind energy in europe in 2018: Trends and statistics*, <https://windeurope.org/wp-content/uploads/files/about-wind/statistics/WindEurope-Annual-Statistics-2018.pdf> (2018).
- [81] <https://windchallenge.com/the-windleaf/#buy> (2019).
- [82] *Unit conversion data for hydrogen*, http://www.uigi.com/h2_conv.html (2017).
- [83] *PEM electrolyzers*, http://www.arevah2gen.com/wp-content/uploads/2015/12/AREVA_H2GEN_FICHE_PRODUIIT.pdf (2015).
- [84] *Brochure: Nel hydrogen electrolyzers*, <https://nelhydrogen.com/assets/uploads/2016/05/Nel-Electrolysers-Brochure-2018-PD-0600-0125-Web.pdf> (2018).
- [85] *Hogen ® s series technical specifications*, https://www.gastech.co.il/images/generators/S-Series%20265-105Nmh_Proton%20Tech%20Specs_RevC.pdf.
- [86] *Hogen ® h series technical specifications*, <https://diamondlite.com/wp-content/uploads/2017/05/H-Serie-Englisch-1.pdf> (2017).

- [87] HydroGenics, *Onsite hydrogen generation:hylyzer pem electrolysis technology*, <http://www.hydrogenics.com/wp-content/uploads/2-1-1-1-hylyzer-1-223F620871645.pdf>.
- [88] *Itm power: Product guide*, <https://www.itm-power.com/wp-content/uploads/2013/04/ITM-ProductGuide-08-2013.pdf>.
- [89] *Water, astm type ii, deionized*, <https://us.vwr.com/store/product/4544438/water-astm-type-ii-deionized> ().
- [90] *An introduction to industrial water demineralization systems*, <https://cdn2.hubspot.net/hubfs/2531874/Demineralization%20E-Book/An%20Introduction%20to%20Industrial%20Demineralization%20Systems.pdf> ().
- [91] *Type 2 (pure) water*, <https://www.evoqua.com/en/brands/lab/Pages/type-2-water-pure.aspx>.
- [92] *Reverse osmosis basics*, https://www.toraywater.com/knowledge/kno_001_01.html.
- [93] *Canadian solar poly 275wp zonnepaneel*, <https://stralendgroen.nl/categorie/zonnepanelen/> ().
- [94] *Solar price per watt*, <https://kenbrooksolar.com/price-list> ().
- [95] *zonnepaneel (pv) los*, <https://www.janseninstalshop.nl/zonnepaneel-pv-los> ().
- [96] M. Woodhouse, R. Jones-Albertus, D. Feldman, R. Fu, K. Horowitz, D. Chung, D. Jordan, and S. Kurtz, *The role of advancements in solar photovoltaic efficiency, reliability, and costs*, Tech. Rep. (Tech. Rep.(NREL/TP-6A20-65872), National Renewable Energy Laboratory (NREL), 2016).
- [97] *Solar cost terminology: Cost per watt, \$/w and lcoe*, <https://news.energysage.com/measuring-the-cost-of-solar-power-dollars-per-watt-w-and-levelized-cost-of-energy-> ().
- [98] *The price of residential solar power*, <https://www.sunrun.com/solar-lease/cost-of-solar>.



WINDLEAF SPECIFICATIONS AND WORKING PRINCIPLE

This section outlines the working principles of wind turbines and briefly goes over the physics associated with wind energy extraction as well as the auxiliary components that a wind turbine system consists of. The energy in wind can be extracted by placing an actuator disk, effectively a wind turbine rotor with blades, in the path of the wind flow. The turbine extracts the kinetic energy of the moving air by transferring it into motion of the blades, converting it into electricity.

WORKING PRINCIPLE

Wind energy is extracted from the kinetic energy in the wind as it passes the blades of the rotor which generate lift forces causing the rotor to turn. The rotor is connected to a shaft and gearing mechanism, unless it is a direct drive generator, which transmits the rotation from the rotor to the generator. The purpose of the generator is to convert the rotational kinetic energy to electrical energy and this is the final stage before transmission of electricity to the load.

The available power is expressed in equation A.1 below, where P_W is the maximum available power that can be extracted, A is the rotor swept area, ρ and U are the density and flow speed of the flowing medium respectively. The medium in this case is air. The variable η_W is the efficiency and is limited by the Betz limit which is the theoretical limit on the maximum amount of energy which can be extracted; the maximum value of η_W is 59.3%.

$$P_W = \frac{1}{2} \rho A U^3 \eta_W \quad (\text{A.1})$$

This equation is based on the kinetic energy of a flowing volume. The detailed derivation is out of the scope of this project, however it should be noted that in higher velocity flows there is much more energy contained in the flow. Therefore the rate of energy (or power) through a point is higher. The power is proportional to the cube of the velocity, thus

a slight increase in wind speed results in a higher increase in power. The power is also proportional to the rotor area, expressed as $A = \pi r^2$, where r is the radius of the rotor. Thus an increase in rotor swept area can lead to more power being extracted. This is part of the reason why large scale wind turbines and wind farms have been striving for rotors which are as large as possible.

POWER CURVE

In general the performance of commercial turbines is characterized by a power curve which defines the power the turbine is able to generate throughout a range of wind speeds. If the wind speed is too low (\leq cut in), the blades aren't moved by the air; if it is too high the blades and other components of the turbine might fail or become unsafe. An example power curve is shown in figure A.1.

The cut-in speed indicates the wind speed at which power starts to be generated; the cut-out speed is where the turbine stops generating power; the rated wind speed is the point at which the turbine generates its rated power. Between the cut-in speed and rated speed, the power coefficient, c_p , of the turbine increases. When it reaches rated power, control mechanisms such as blade pitching are activated to keep the rotational speed of the rotor constant, even if the wind speeds increase higher than the rated wind speed, effectively making the turbine less efficient at higher speeds in order to keep the power output constant. This is indicated by the plateau in figure A.1.

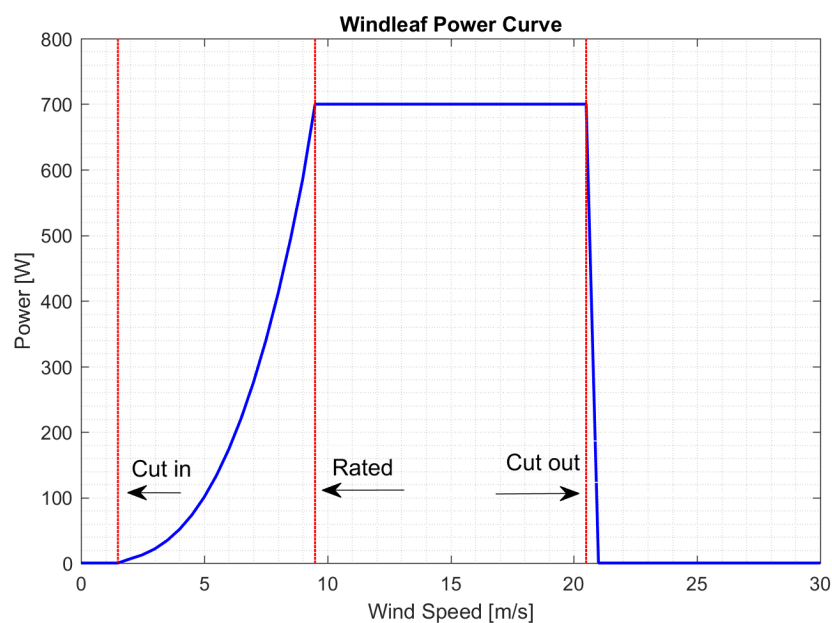


Figure A.1: Example of a Power Curve

COMPONENTS OF WIND TURBINE SYSTEMS

A wind turbine system consists mainly of the wind turbine itself and additional components which will be described in this section. The turbine itself is made up of a rotor, a

nacelle, and a generator. The generator type is a permanent magnet, brushless direct drive. Direct drive generators do not include additional gearing systems, making them lighter and more compact than geared generators. They are also more reliable since they have one less component which might need to be replaced since gears are subjected to very large forces and could become worn or break under cyclic operation. Brushless generators are beneficial since they reduce the friction and associated losses of generation.

The generated electricity is typically 3 phase, therefore depending on the load, a converter is placed between the output of the turbine and the load. It serves to convert the AC electricity to the desired voltage level, and/or to DC if the load is, for example, a battery.

Throughout the various energy conversion stages from wind to the application of electricity, there are losses associated with each component. The term η_{wind} is the efficiency of the wind turbine system and it is defined as the ratio of output electricity to the energy in the wind. It is expressed in equation A.2, and it takes into account the energy lost from the wind up until the electricity output of the turbine system. The Betz limit is the maximum efficiency that a wind turbine can have, but the aforementioned components reduce the value further.

$$\eta_{wind} = \frac{E_{out}}{E_{in}} = \frac{E_{W_{out}}}{0.5\rho AU^2} \quad (\text{A.2})$$

Typical efficiencies of wind turbines range from 40% to 50% [77, 78].

The capacity factor of the turbine is also of importance, since it defines the ratio between the annual generated energy over the energy it is capable of generating, if it were working at maximum capacity every hour of the year. This is different from the efficiency, but determines how intermittent the energy source is. A typical value for utility scale is 37% according to [79], although this is very site specific. Offshore wind turbines have higher capacity factors than onshore wind turbines: in 2018 the average capacity factor of onshore and offshore wind installations was 22% and 37% respectively [80].

The *Windleaf*, which is selected for this model, is a micro-turbine manufactured by WindChallenge in Rotterdam. It is rated at 700 W. The annual generation capability stated on the website is 900 kWh per year, thus the capacity factor is found to be 14.6%, although this is subject to the location, thus it could be lower or higher. However this is the conservative value given by the manufacturer. [81]

B

ELECTROLYZER OVERVIEW

GREENHYDROGEN : *HyProvide P1* [61]

GreenHydrogen is a Danish company which specializes in electrolyzers and hydrogen solutions for renewable energy applications and on-site use. They offer alkaline and PEM electrolyzers. While their alkaline A30-A90 series is suited for MW scale applications, a small scale PEM option is also offered: the P1.

The P1 output ranges from 1 - 4 Nm³/h and the input power requirement is 5.5 kW/Nm³. This is equivalent to 0.08988 kg_{H₂}/h [82]. The data on the website is given for the 1 Nm³/h model version. The output pressure of the hydrogen is 50 bar. In some system designs this is high enough not to require additional compression and hence removing the need for additional energy.

The electrolyzer is claimed to have low capital investments, operational costs, and maintenance requirements. It is also modular therefore the system can start small and grow if needed.

AREVA: *H₂GEN* [83]

A French company which, other than their nuclear and renewable energy specializations, they also have a branch dedicated to hydrogen production. Their PEM electrolyzers are offered in output capacities from 5 to 120 Nm³/h. Considering the smallest model which produces 5 Nm³/h, this corresponds to 440 g_{H₂}/h and to 10 canisters per hour. For the preliminary case study design, this capacity is quite large, and this will be explained in the following chapter. For such a large production, the hydrogen would have to be redirected to another end user, otherwise the electrolyzer will be underutilized. Therefore sizes larger than 5 Nm³/h are not considered. The output pressure of this electrolyzer system is 35 barg, which is lower than the GreenHydrogen model.

Based on the specifications, the water input is tap water which means the electrolyzer system has a water purifier included, removing the need of an external purifier. The purification works with integrated reverse osmosis and electro deionisation.

The stack power consumption is given as 4.4 kWh/Nm³, while the system power consumption is given as 5.7 kWh/Nm³. The electrolyzer and its control system come fully inte-

grated in an outdoor unit. The stack efficiency is over 80% and the overall system efficiency is over 70%. Areva states that the device is "environmentally friendly, reliable, free from potassium hydroxide, and cost efficient."

NEL/PROTON: *H-Series, S-Series* [84–86]

NEL is one of the oldest electrolyzer manufacturers with a breadth of experience and world leading achievements throughout history, such as the first small scale electrolyzer plant in 1927 in Norway. The two most attractive models for this application are the S-Series and the H-series PEM electrolyzers.

The H-series electrolyzers have production capacities ranging from 2, 4, or 6 Nm³/h. The hydrogen output pressure is 15 bar, with an option of 30 bar offered. The S-Series is a smaller range of electrolyzers. The two models, S20 and S40, produce 0.52 and 1.05 Nm³/h respectively. This is equivalent to 1.14 and 2.27 kg/day at an output pressure of 13.8 bar.

Both of these models are containerized, compact, low maintenance and can be installed within hours. They also have a relatively low water consumption rate as compared to the other electrolyzers mentioned, but a lower efficiency.

Proton onSite has been mentioned in various sources throughout literature, but the models they produce are the same as the ones by NEL. In 2017, NEL acquired Proton On-Site, and added world-leading PEM electrolysis to their existing portfolio. NEL claims to be the worlds largest electrolyzer company.

HYDROGENICS: *HyLYZER* [87]

Hydrogenics is a Canada-based company which specializes in hydrogen production and applications. The HyLYZER is offered in two sizes: 1 or 2 Nm³/h. It is a simple, easily installable, compact system. The electrolyzers operate automatically by sensing the pressure at the output. These models are meant to be installed inside. Optional components to the electrolysis system are a water treatment system and a storage tank. The output pressure ranges from null to 7.9 barg.

ITM POWER: *HPAC*[88]

This Sheffield (UK) based company offers two units, the HPAC 10 & HPAC 40. The output pressure is 15 barg, and produce 0.7 and 2.8 Nm³/h respectively. The HPAC10 is uses 220/230 V AC, whereas the HPAC 40 requires a 415 V 3 ϕ connection. These units are recommended for indoor installations.

C

WATER PURIFICATION ADDITIONAL CONTENT

The option of buying readily purified water was also examined, to compare the prices per unit liter bought, as opposed to the price per unit liter purified. This option is more complex in that an external party would be involved and required to visit the site. The prices reported in [89] range between $\sim 13 - 18\$/L$.

The driver of the water delivery truck is not likely to drive a hydrogen truck, therefore this option is also not the most sustainable, since there are emissions in the water delivery. Hence, the option of on-site purification was chosen, for simplicity and independence of the system.

PURIFICATION METHODS

Demineralization refers to the process by which dissolved mineral solids found in the water are removed. The "contaminants" in water are minerals which have dissociated into (charged) ions, as well as non-charged organic contaminants such as bacteria and viruses. It may require multiple water treatment processes, such as ion exchange, distillation, and/or reverse osmosis.

Minerals in water usually dissociate into ions, positively charged ions are cations while negatively charged ions are called anions. Each of these ion groups are attracted to oppositely charged ions, or counter-ions. *Ion exchange* (IX) resins are plastic beads with a specific ionic functional group which, when placed in contact with ions in water have the effect of exchanging ions by switching them for less objectionable ions. For example, cations in water are exchanged with H^+ , while anions are replaced with OH^- , leaving pure H_2O as the result. Ion exchange demineralization offers water of high purity, and at a lower cost than distillation, but it may not be as pure as the ASTM type II specification. [90]

In [90] it is stated that ion exchange can reduce the number of dissolved solids to under 10 mg/L and reduce the electrical conductivity to under 2 mS/L , which is at least three orders of magnitude more than what the specification of water for electrolysis. Therefore

more rigorous and higher purity methods are required, such as distillation or reverse osmosis.

Distillation is the process by which water is evaporated, moved to a different chamber, and then re-condensed without the contaminants.

Osmosis is when a solution of low concentration permeates through a porous membrane into a solution of higher concentration. *Reverse osmosis* applies pressure to the higher concentration solution. The osmotic pressure is a pressure level that the osmosis process exerts in attempting to bring the concentrations to an equilibrium. In reverse osmosis, a pressure higher than the osmotic pressure in the higher concentration chamber forces the lower concentration through the membrane. The membrane allows water to flow through, but blocks ions, bacteria, and larger particles. Thus, the ions and contaminants do not pass through the membrane, purifying the water. The process can remove 98% of the salt content, and over 99% of particles and bacteria. [91, 92]

D

MORE MAPS OF MUNICIPALITIES

Distance from NB to Neighbourhoods

- 0 - 0.5 km
- 0.5 - 1 km
- 1 - 1.5 km
- 1.5 - 2 km
- 2 - 2.5 km
- 2.5 - 3 km
- 3 - 3.5 km
- 3.5 - 4 km
- > 4 km

— NB (in 25 municipalities)

□ Municipal Boundaries

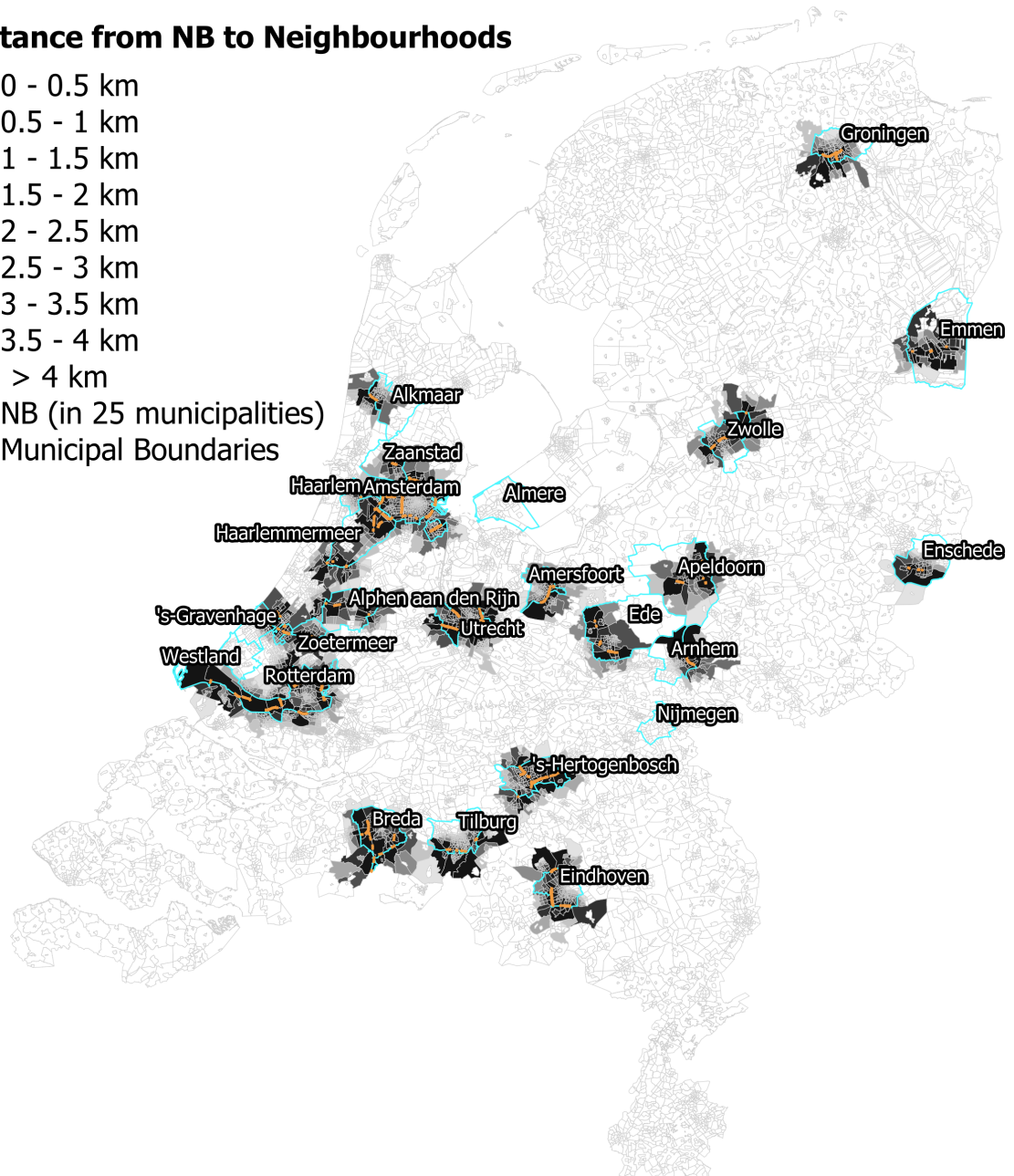


Figure D.1: Neighbourhood proximity to NBs in top 25 municipalities

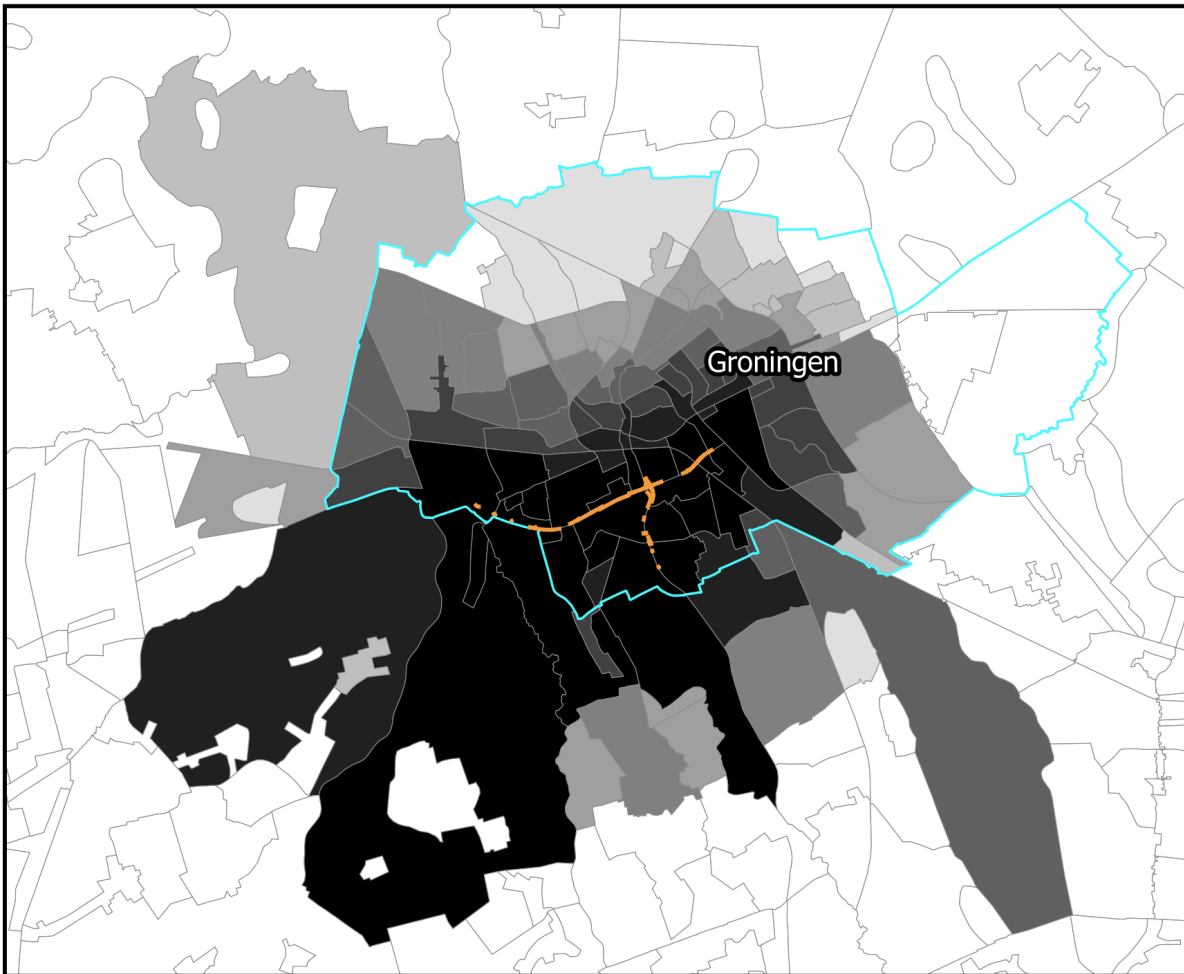


Figure D.2: Groningen

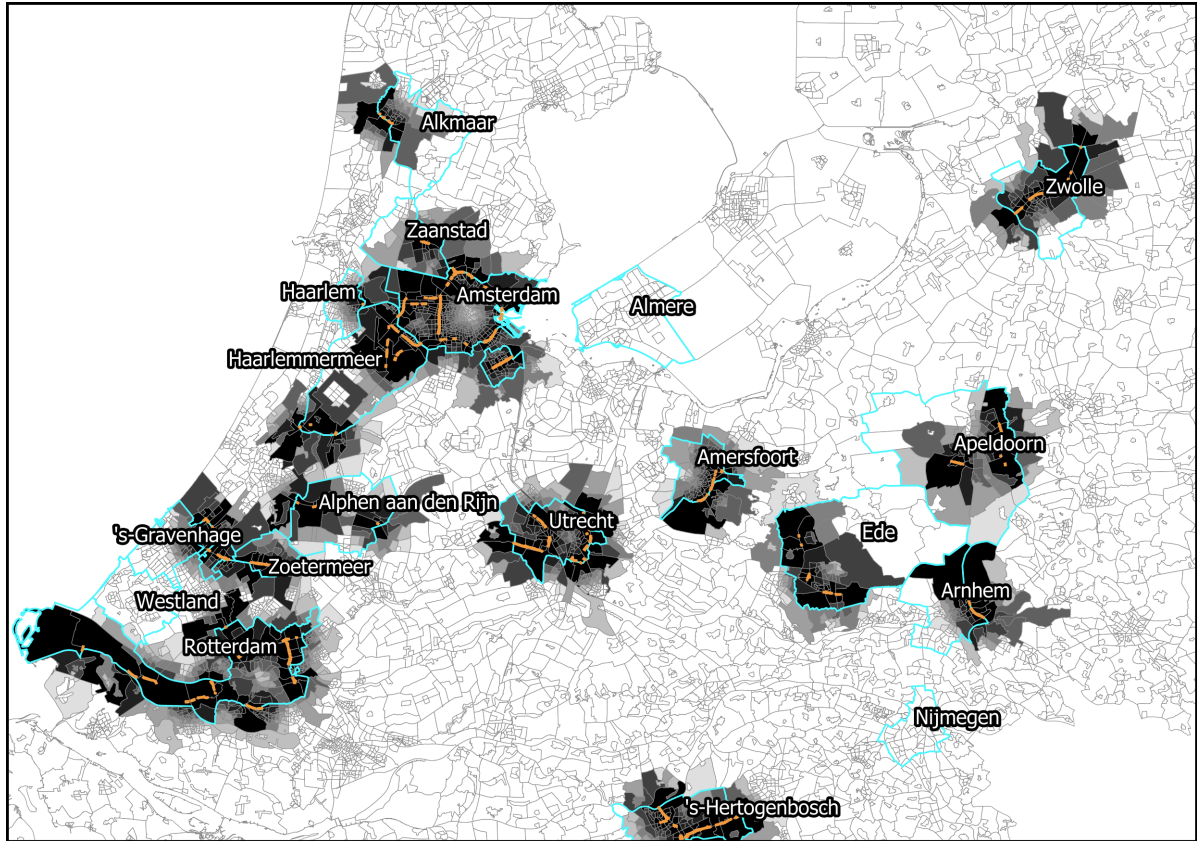


Figure D.3: Cluster of Municipalities

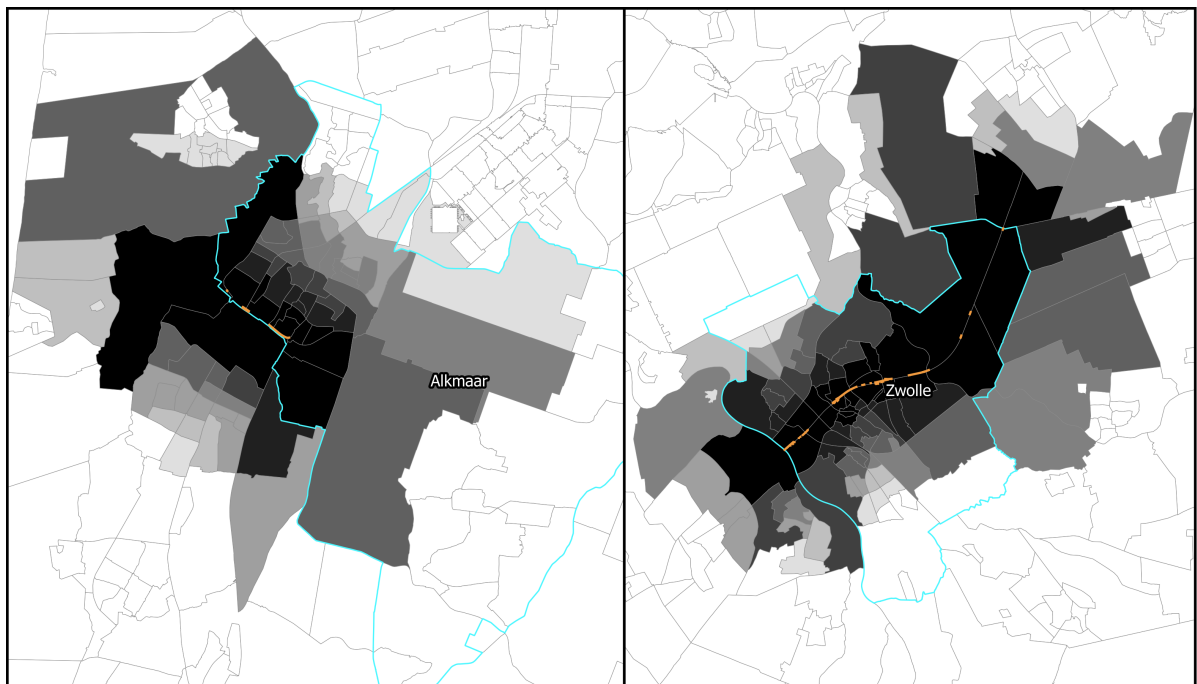


Figure D.4: Alkmaar and Zwolle

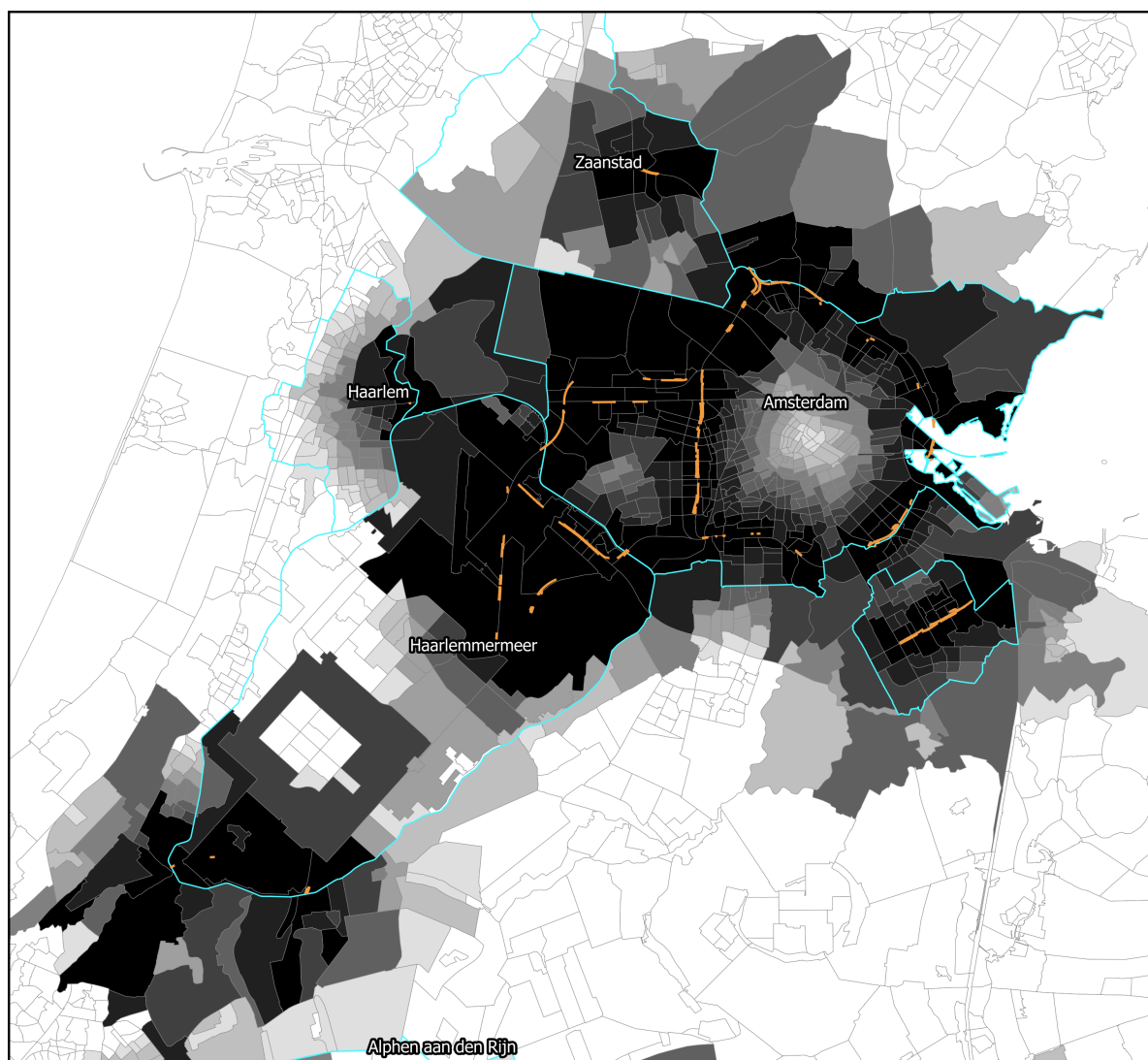


Figure D.5: Amsterdam, Haarlem, Zaanstad and Haarlemmermeer

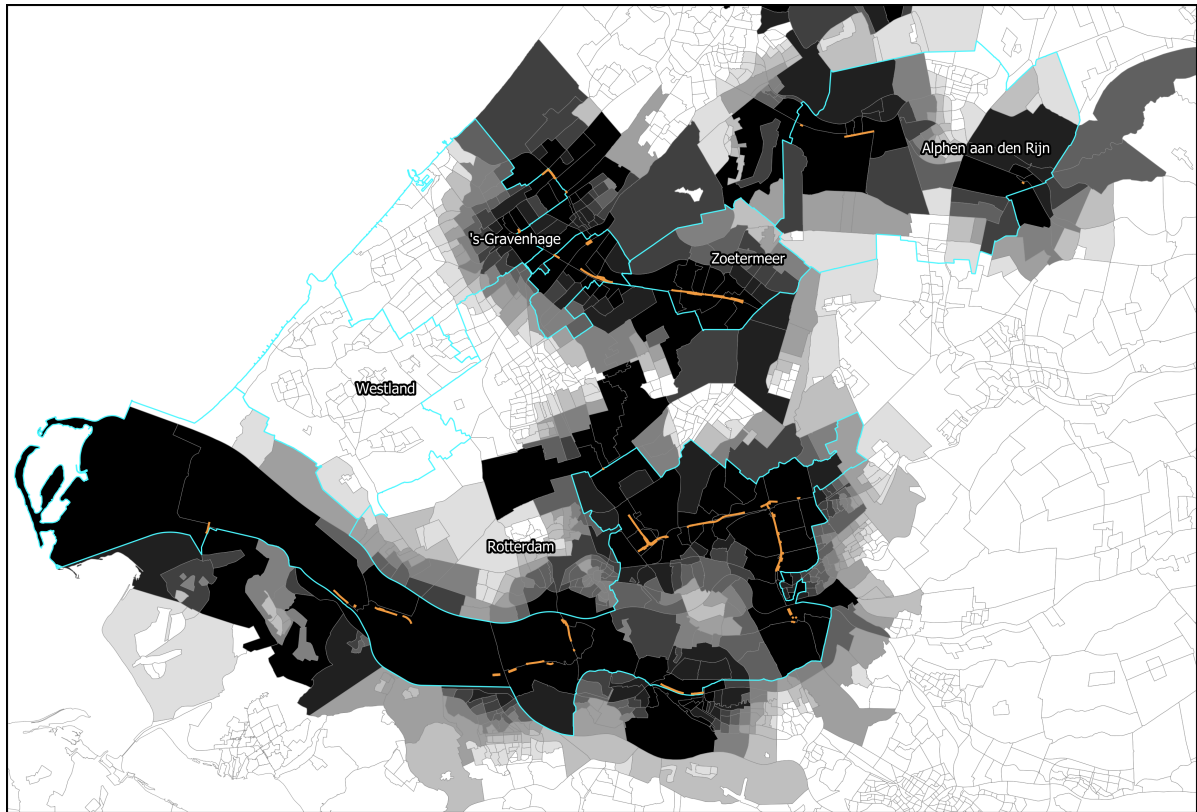


Figure D.6: Den Haag, Rotterdam, Zoetermeer, and Alphen aan den Rijn

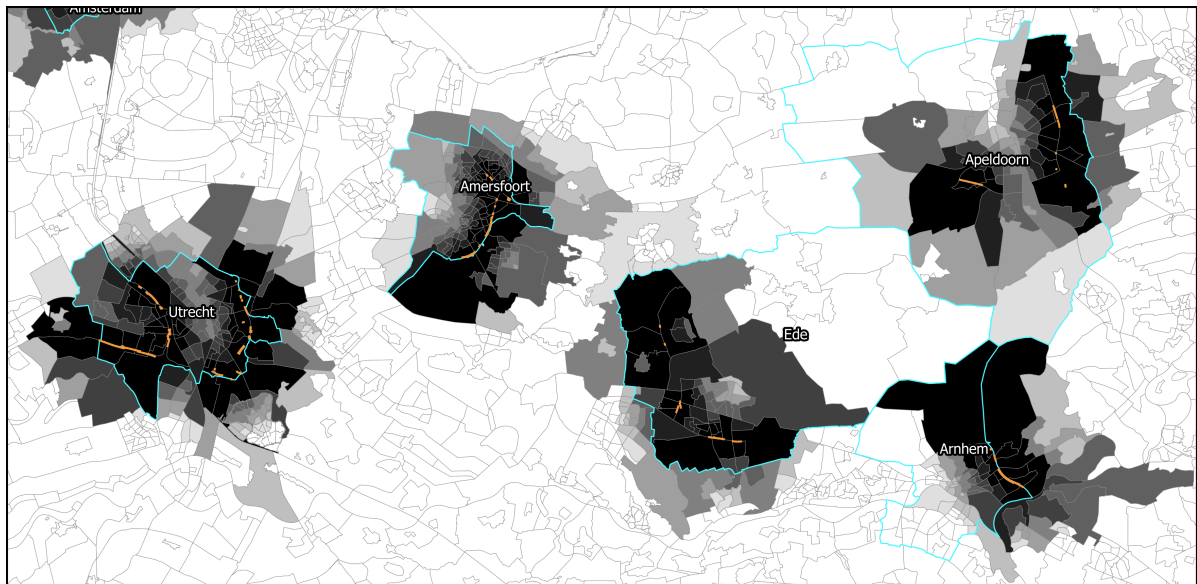


Figure D.7: Utrecht, Amersfoort, Ede, Arnhem and Apeldoorn

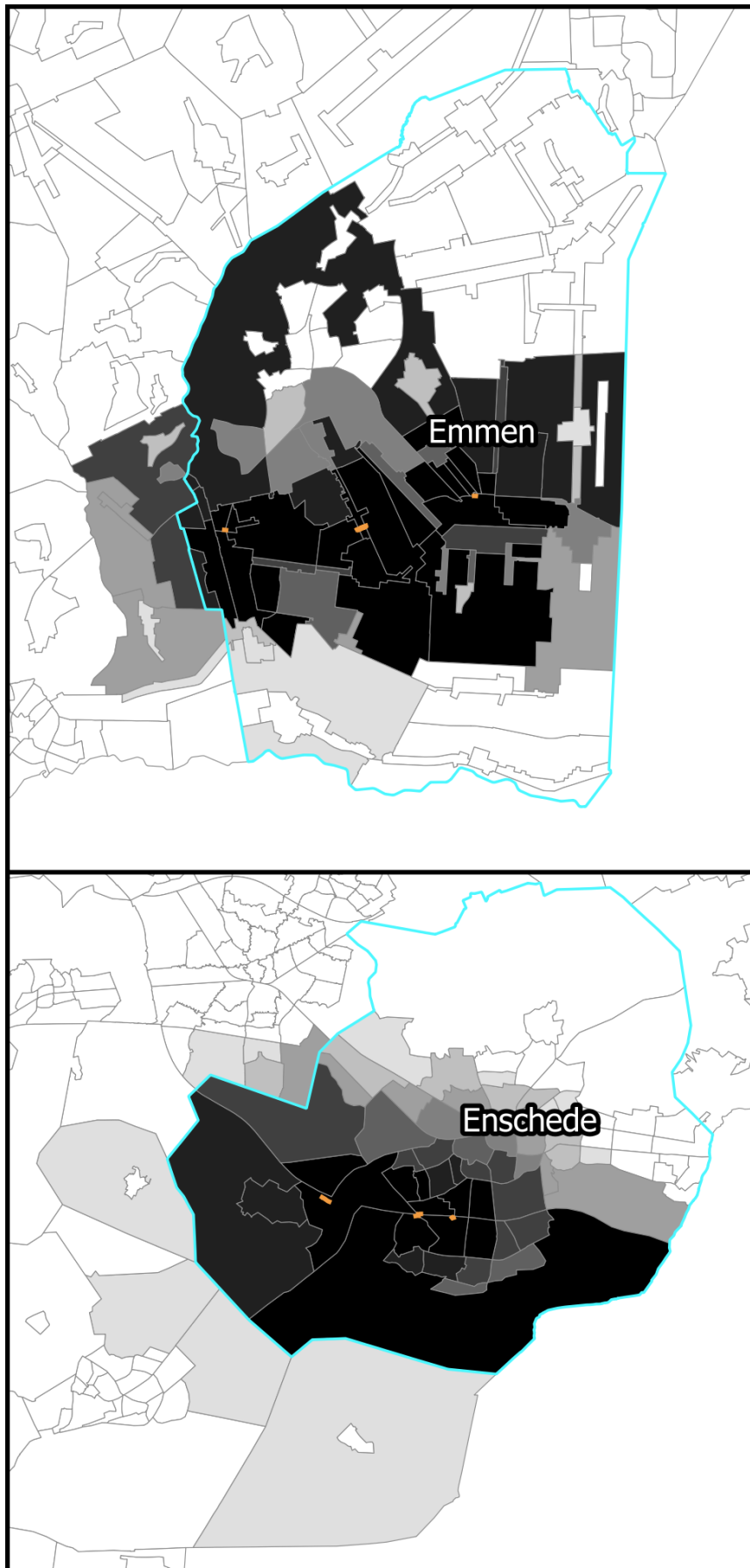


Figure D.8: Emmen and Enschede

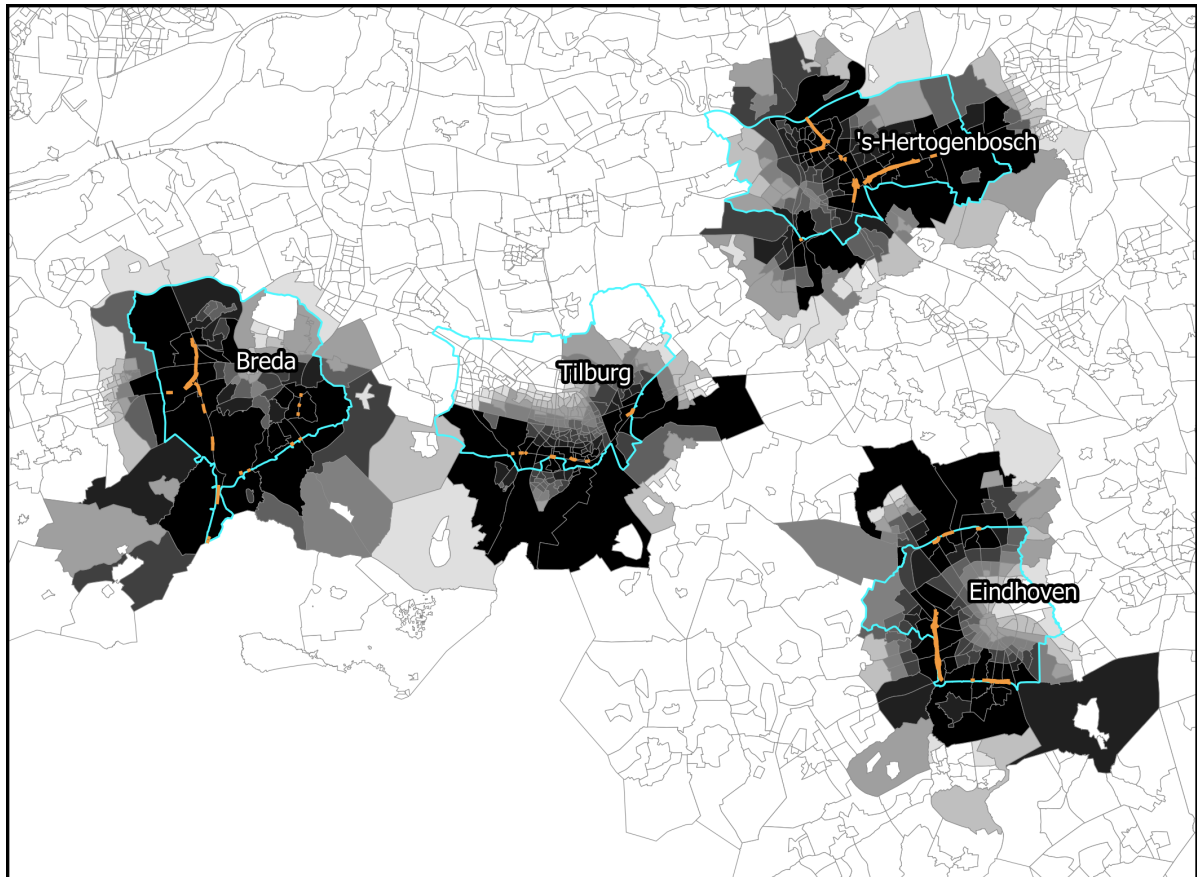
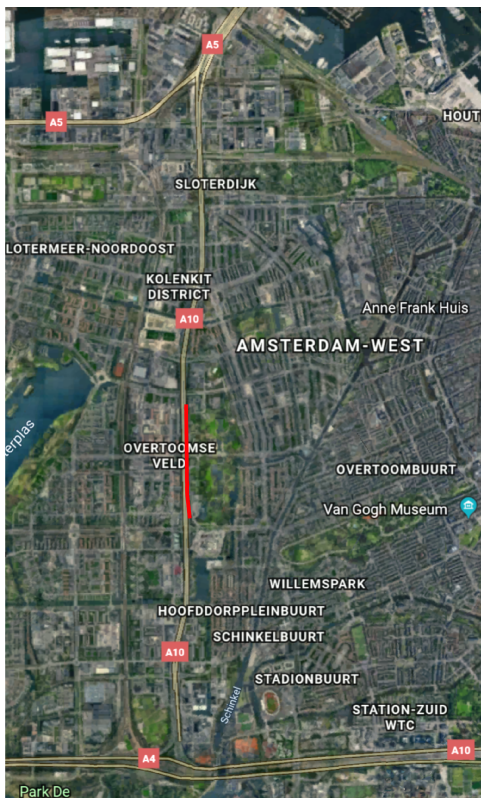


Figure D.9: Tilburg, Breda, 's-Hertogenbosch and Eindhoven

E

CASE STUDY DETAILED INFORMATION

Provided here are extra details of the locations of each case study.



(a) Noise barrier along A10 in Amsterdam West



(b) Noise barrier along A10 in Amsterdam South East/Diemen

Figure E.1: Details of Amsterdam Noise Barrier Locations



Figure E.2: Delft and Rotterdam Noord Noise Barriers



Figure E.3: Noise barrier along N470 in Delft

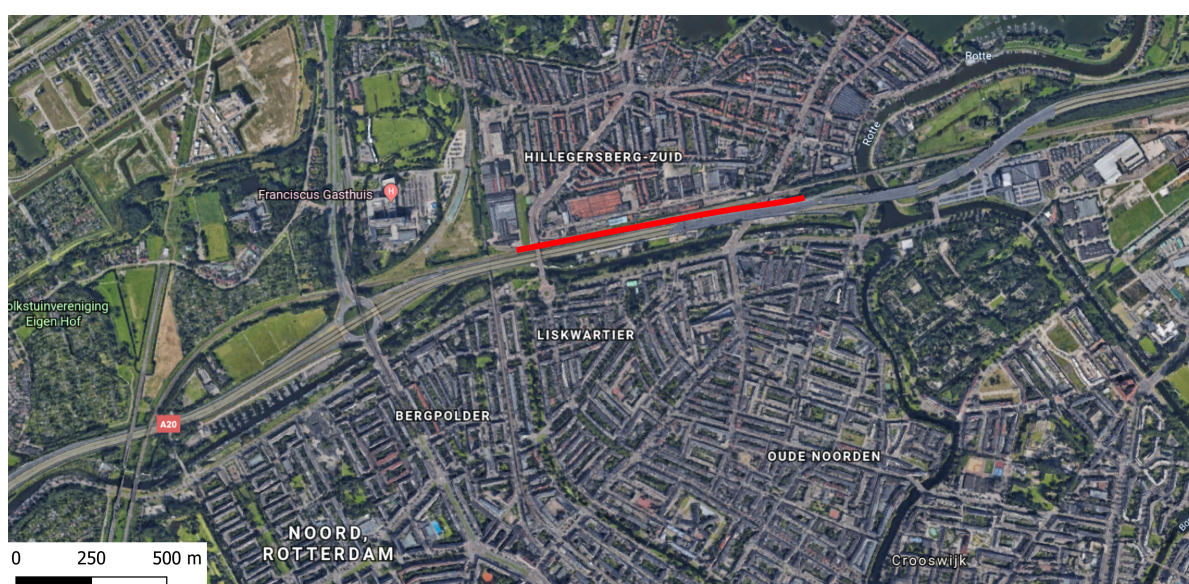


Figure E.4: Noise barrier along A20 in North Rotterdam

F

COST LITERATURE REVIEW NOTES

PV systems are classified in terms of installed capacity. According to NREL [10] a *residential* system is from 3 - 10 kW installed capacity, a *commercial* system is between 10 kW and 2 MW and anything higher than a 2 MW system is referred to as *utility scale*. The classification of systems is important because the cost of each differs significantly, with larger systems typically having lower costs per unit of installed capacity. This is a results of more shared costs such as the inverters. The PV system designed in this study is classified as a commercial scale system.

The cost of modules is generally given in per unit watt peak installed prices. Some examples of module costs are summarized in table F.1, along with the size of the system they were part of, the total cost of the modules, and the cost per unit watt. The unit of cost per Watt is useful because it is scalable (as long as the system size classification is the same).

Manufacturer	Rating	Price [€]	€/W	
Module Price Index		-	0.26	[71]
NREL PV System Cost Breakdown	200 kW _p	-	0.31 ¹	[10]
Canadian Solar Panel	275 W _p	105	0.38	[93]
Tata Solar Panel	265 W _p	107	0.40 ²	[94]
Boviet Solar Panel	270 W _p	115	0.43	[95]

Table F.1: Only Module Cost Survey

RECENT PRICE TRENDS & FACTORS

It should be noted that as the popularity and implementation of PV systems increases, the cost of the modules (and system components) decreases. The cost reduction is contributed to the technological advances and improvements in the design and production methods as well as the increased competition within the industry. Figure F.1 shows the price of PV

¹Prices given in U.S. Dollars, converted at a rate of 0.9 EUR/USD

²Prices given in Indian Rupees, converted at a rate of 0.013 EUR/RS

modules over the past 8 years [9]. This is also confirmed by [10], which has mentioned a price decrease in commercial systems of 65% from 2010 to 2017. Lower hardware costs, namely modules and inverters, contributed 82% of the overall decrease however higher module efficiencies were also a contributing factor.

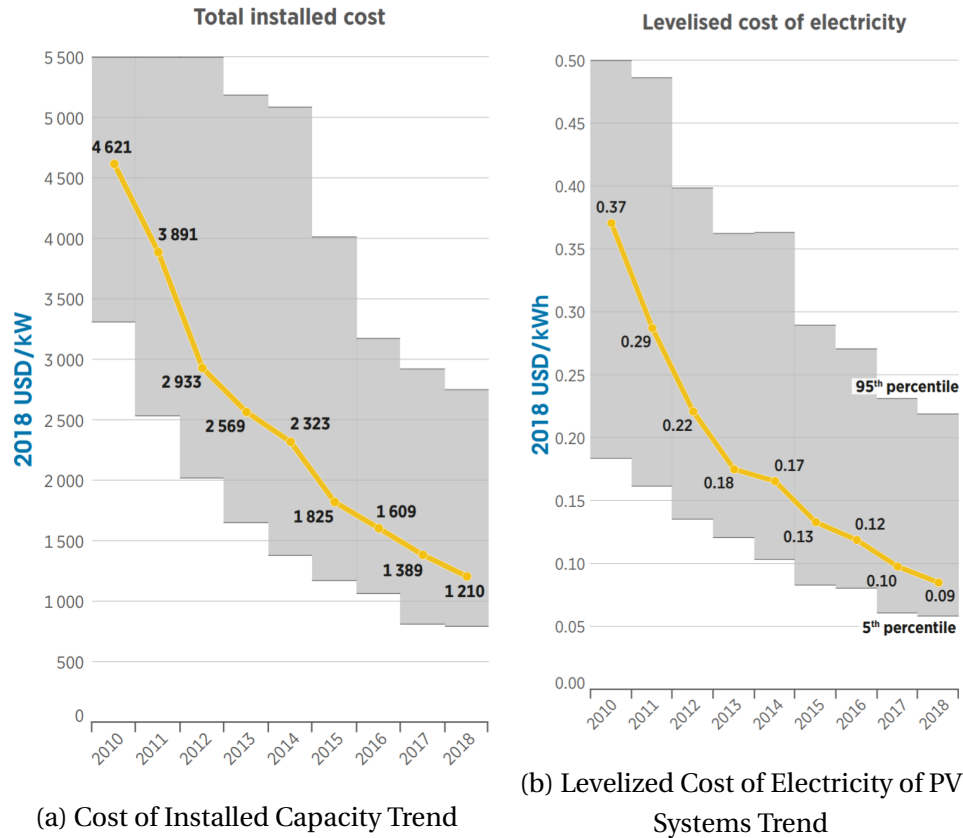


Figure E.1: [9]

There are various initiatives and incentives put into place in order to accelerate the affordability of solar electricity. One such initiative aiming to reduce the price of solar electricity so much that it becomes competitive with conventional fossil fuel sourced electricity is the SunShot [96]. In the US [97] states that the effective reduction in system cost through the Investment Tax Credit (ITC) incentive is about 30%. This value is also mentioned in a report published by the National Renewable Energy Laboratory [96], but it is assumed that it goes down to 26% by 2020. The SunShot goal for costs is 6, 7, and 9 cents/kWh in the utility, residential and commercial sectors without subsidies. The cost per W of the systems mentioned by [96] are 6.2\$/W, 3.1 \$/W, and 1.6 \$/W for the residential sector; 5.0\$/W, 2.2\$/W, and 1.3\$/W for the commercial sector; 4.1\$/W, 1.8\$/W, and 1.1\$/W for the utility sector for the years 2010, 2015 and 2020 respectively.

The cost of photovoltaic systems has decreased drastically in recent years. This is partly due to incentives, but also due to a mass production in solar panels, an increase in expertise of production and installation, social pressures to increase renewable energy generations and political agreements and goals which need to be met leading to subsidies and

governmental support for solar energy. Markets have been flooded with solar photovoltaic technology, much of it coming from China which has had enormous impact in the field of photovoltaic systems. Basic economics state that as the quantity of a product or service increases, the cheaper it becomes. Naturally, the price drop is more complex than this, but it is definitely an economic concept which has been proven in basic terms.

COST BREAKDOWN OF PV SYSTEMS

Commercial systems cost 1.85 $\$/W_{DC}$ in 2017 according to [10]. The breakdown of this cost is shown in figure E.2. The system costs are broken down as 47% to hardware costs, 35% to installation, and 18% to O&M by [98].

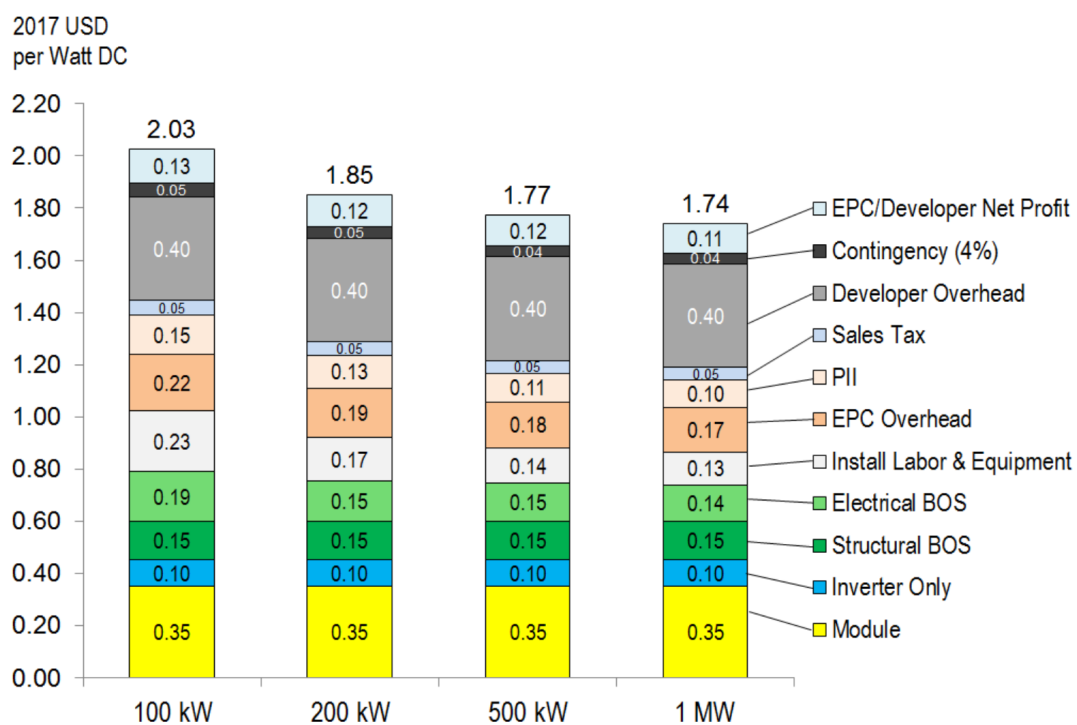


Figure E.2: Individual Component Cost out of total system cost for PV, 2017 [10]

G

GRID CONNECTION COSTS

Table G.1 shows the one-off connection fee categories that are payable to the grid operator depending on the capacity of the connection. The costs shown in the Cost column includes the connection to the grid and a 25 meter cable length. The additional cost per meter is shown in the "Cost per extra meter" column. The sum of these aforementioned costs are defined as $CAPEX_{Grid}$. The annual fee, payable to the grid operator for grid operation and maintenance services is shown in table G.2 and is defined as $OPEX_{Grid}$. It is also dependent on the connection capacity.

The costs shown in tables G.1 & G.2 are excluding VAT.

Connection Capacity	Cost [€]	Cost per extra meter [€/m]
3 x 80 A - 3 x 125 A	4.210	47,50
3 x 125 A - 3 x 175 kVA	5.330	50,00
175 kVA - 630 kVA	36.870	83,00
630 kVA - 1000 kVA	38.085	93,00
1000 kVA - 1750 kVA	46.700	96,00
1750 kVA - 3000 kVA	197.649	130,00
3000 kVA - 10000 kVA	270.000	152,00

Table G.1: One-off Grid Connection Costs [16]

It can be seen in both tables G.1 & G.2 that between 3-phase and 1-phase connections there is a substantial cost difference. Therefore, in the interest of maintaining reasonable $CAPEX_{Grid}$ and $OPEX_{Grid}$ system costs, the level of energy exchanged with the grid should optimally be below 175 kVA.

COST SPLITTING BETWEEN USERS

The 2 users of the grid connection are the Energy Wall and the electrolyzer system, denoted by the subscripts REN and H_2 respectively. The proportion of electricity sent to- or received from- the grid by users are not equal, therefore the connection cost is split between

Capacity Range	Connection Category	Annual Cost [€]
	LS	32,775
> 80 A - 175 kVA	Trafo MS/LS	78,00
> 175 kVA - 1,750 kVA	MS Distributie	712,00
> 1750 kVA - 3000 kVA	Trafo HS+TS/MS	1.505,00
> 3000 kVA - 10000 kVA	Trafo HS+TS/MS	7.767,00
> 10000 kVA	TS	130,00

Table G.2: Annual Grid Connection Costs, $OPEX_{Grid}$ [16]

its users. The cost is split and allocated depending on how much electricity is handled by the transformer for each user.

The total electricity handled by the transformer is E_G , the electricity sent to the grid from the Energy Wall is E_{REN2G} and the electricity sent from the grid to the electrolyzer is E_{G2H_2} .

$$E_G = E_{REN2G} + E_{G2H_2} [kWh] \quad (G.1)$$

The levelized cost of the grid connection LCG is defined as the cost of the connection C_{CON} per unit of energy exchanged with the grid E_G .

$$LCG = \frac{C_{CON}}{E_G} = \frac{C_{CON}}{E_{REN2G} + E_{G2H_2}} \left[\frac{\text{€}}{kWh} \right] \quad (G.2)$$

The levelized cost of grid connection is distributed by weight of how much energy is handled by the transformer. The cost is allocated to the corresponding user. It is split into LCG_{H_2} allocated to the hydrogen produced, and LCG_{REN} borne by the energy wall:

$$LCG = LCG_{H_2} + LCG_{REN} \left[\frac{\text{€}}{kWh} \right] \quad (G.3)$$

The cost allocated to the hydrogen production is part of the grid electricity cost.

$$LCG_{H_2} = LCG \times \frac{E_{G2H_2}}{E_G} \left[\frac{\text{€}}{kWh} \right]$$

$$LCG_{REN} = LCG \times \frac{E_{REN2G}}{E_G} \left[\frac{\text{€}}{kWh} \right]$$

The **final cost** of electricity that the electrolyzer pays for is defined as $LCOE_G$, expressed in equation 5.4. From the grid connection cost, only the cost associated with the electricity that is sent to the electrolyzer is considered, LCG_{H_2} . This is the only cost which trickles down to the cost for the user.

H

ADDITIONAL MATERIAL FOR SCOOTERS

Charging metal hydride canisters

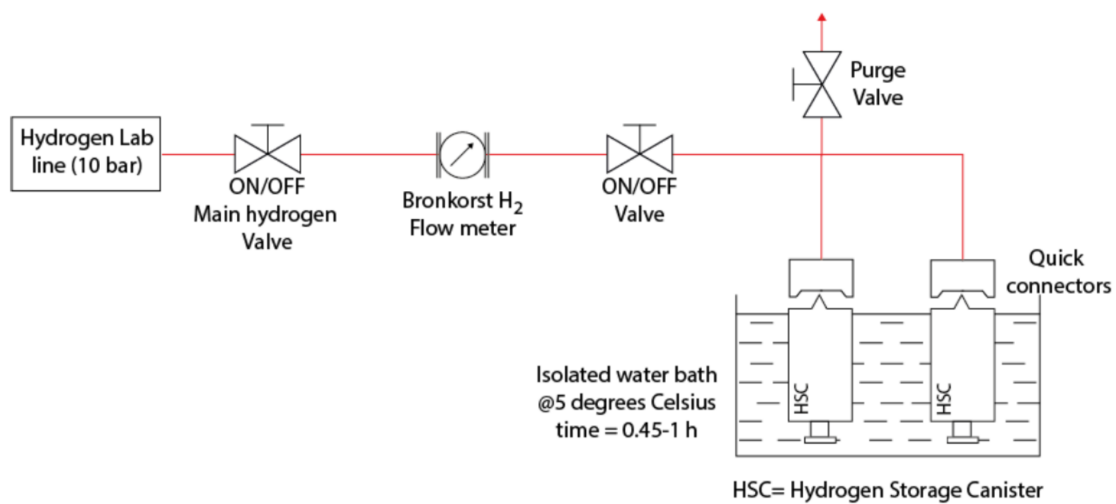


Figure H.1: Charging station diagram

I

BATTERY POWERED ELECTRIC SCOOTER REVIEW

In order to compare the hydrogen scooter model to current electric scooters which are similar in size. They are listed in terms of their engine size; the relevant information is given in table I.1.

Model	<i>GenZe 2.0e</i>	<i>MQi+ Sport</i>	<i>UQi</i>	<i>NQi Sport</i>	<i>AppScooter</i>	<i>Viva Light</i>
Manufacturer	Mahindra	Niu	Niu	Niu	Etergo	Gogoro
Engine Size [kW]	1.4	1.5	1.5	1.8	2	3
Charge Time [hrs]	3.5	7	3.5	7	2.3	Sharing
Battery Weight [kg]	13.5	8.3	5.2	10	8.5	9
Capacity [kWh]	1.6	2	1	1.74	1.155	1.3
Scooter Weight [kg]	105		58	95		71
Range/acu [km]	50	75-100	30-40	70	80	80
1 charge range [km]	50	100	35	70	240	85
Top Speed [km/h]	45	45	25 or 45	45	59	50
Cost [USD]	5750	3000	1900	2500	3400	1800

Table I.1: Battery Electric Scooter Selection Overview